Growth and retreat of the last British–Irish Ice Sheet, 31 000 to 15 000 years ago: the BRITICE-CHRONO reconstruction

CHRIS D. CLARK (iD), JEREMY C. ELY, RICHARD C. A. HINDMARSH, SARAH BRADLEY, ADAM IGNÉCZI, DEREK FABEL, COLM Ó COFAIGH, RICHARD C. CHIVERRELL, JAMES SCOURSE, SARA BENETTI, TOM BRADWELL, DAVID J. A. EVANS, DAVID H. ROBERTS (iD), MATT BURKE, S. LOUISE CALLARD, ALICIA MEDIALDEA (iD), MARGOT SAHER, DAVID SMALL, RACHEL K. SMEDLEY, EDWARD GASSON, LAUREN GREGOIRE, NIALL GANDY, ANNA L. C. HUGHES (iD), COLIN BALLANTYNE, MARK D. BATEMAN (iD), GRANT R. BIGG, JENNY DOOLE, DAYTON DOVE, GEOFF A. T. DULLER, GERAINT T. H. JENKINS, STEPHEN L. LIVINGSTONE (iD), STEPHEN MCCARRON (iD), STEVE MORETON, DAVID POLLARD, DANIEL PRAEG, HANS PETTER SEJRUP, KATRIEN J. J. VAN LANDEGHEM AND PETER WILSON

The BRITICE-CHRONO consortium of researchers undertook a dating programme to constrain the timing of advance, maximum extent and retreat of the British–Irish Ice Sheet between 31 000 and 15 000 years before present. The dating campaign across Ireland and Britain and their continental shelves, and across the North Sea included 1500 days of field investigation yielding 18 000 km of marine geophysical data, 377 cores of sea floor sediments, and geomorphological and stratigraphical information at 121 sites on land; generating 690 new geochronometric ages. These findings are reported in 28 publications including synthesis into eight transect reconstructions. Here we build ice sheet-wide reconstructions consistent with these findings and using retreat patterns and dates for the inter-transect areas. Two reconstructions are presented, a wholly empirical version and a version that combines modelling with the new empirical evidence. Palaeoglaciological maps of ice extent, thickness, velocity, and flow geometry at thousand-year timesteps are presented. The maximum ice volume of 1.8 m sea level equivalent occurred at 23 ka. A larger extent than previously defined is found and widespread advance of ice to the continental shelf break is confirmed during the last glacial. Asynchrony occurred in the timing of maximum extent and onset of retreat, ranging from 30 to 22 ka. The tipping point of deglaciation at 22 ka was triggered by ice stream retreat and saddle collapses. Analysis of retreat rates leads us to accept our hypothesis that the marine-influenced sectors collapsed rapidly. First order controls on ice-sheet demise were glacio-isostatic loading triggering retreat of marine sectors, aided by glaciological instabilities and then climate warming finished off the smaller, terrestrial ice sheet. Overprinted on this signal were second order controls arising from variations in trough topographies and with sector-scale ice geometric readjustments arising from dispositions in the geography of the landscape. These second order controls produced a stepped deglaciation. The retreat of the British–Irish Ice Sheet is now the world's most well-constrained and a valuable data-rich environment for improving ice-sheet modelling.

Chris D. Clark (c.clark@sheffield.ac.uk), Jeremy C. Ely, Sarah Bradley, Adam Ignéczi, Mark D. Bateman, Grant R. Bigg, Jenny Doole and Stephen L. Livingstone, Department of Geography, University of Sheffield, Winter St., Sheffield S10 2TN, UK; Richard C. A. Hindmarsh, British Antarctic Survey, Madingley Road, Cambridge CB3 0ET, Cambridgeshire, UK; Derek Fabel and Steve Moreton, Scottish Universities Environmental Research Centre (SUERC), University of Glasgow, Rankine Avenue, Glasgow G75 0QF, UK; Colm Ó Cofaigh, David J. A. Evans, David H. Roberts and David Small, Department of Geography, University of Durham, South Road Durham, Durham DH1 3LE, UK; Richard Chiverrell and Rachel Smedley, Department of Geography and Planning, University of Liverpool, Roxby Building University of Liverpool, Liverpool, Merseyside L69 7ZT, UK; James Scourse and Edward Gasson, University of Exeter, College of Life and Environmental Sciences, Penryn Campus, Penryn, Cornwall TR10 9EZ, UK; Sara Benetti and Peter Wilson, School of Geography and Environmental Sciences, Ulster University, Cromore Road, Coleraine, Londonderry BT52 1SA, UK; Tom Bradwell, Biological and Environmental Sciences, University of Stirling, Stirling FK9 4LA, UK; Matt Burke, Scottish Environment Protection Agency, Inverdee House, Baxter Street, Aberdeen AB11 9QA, UK; S. Louise Callard, Department of Geography, Newcastle University upon Tyne, Newcastle NE1 7RU, UK; Alicia Medialdea, CENIEH (Centro Nacional de Investigación sobre la Evolución Humana), P. Sierra de Atapuerca 3, 09002 Burgos, Spain; Margot Saher and Katrien van Landeghem, School of Ocean Sciences, Bangor University, Askew St, Menai Bridge LL59 5AB, UK; Lauren Gregoire and Niall Gandy, School of Earth and Environment, University of Leeds, Woodhouse, Leeds LS2 9JT, UK; Anna L.C. Hughes, Department of Geography, Manchester University, Oxford Road, Manchester M13 9PL, UK; Colin Ballantyne, School of Geography & Sustainable Development, University of St. Andrews, North Street, Fife KY15 5UF, UK; Dayton Dove, British Geological Survey, Edinburgh Office, Lyell Centre Research Avenue South, Edinburgh EH1 441P, UK; Geoff A. T. Duller and Geraint T. H. Jenkins, Department of Geography and Earth Sciences, Aberystwyth University, Llandinam Building, Aberystwyth, Ceredigion SY23 3DB, UK; Stephen McCarron, Department of Geography, Maynooth University, Rhetoric House, South Campus Maynooth, Maynooth, Ireland; David Pollard, College of Earth and Mineral Sciences, Penn State University, University Park, PA 16802, USA; Daniel Praeg, Géoazur, UMR7329 CNRS, Valbonne, France; Hans Petter Sejrup, Department of Earth Science, University of Bergen, P.O. Box 7803, Bergen N-5020, Norway; received 9th December 2021, accepted 17th May 2022.

At times during the last glacial period, Marine Isotope Stage 2: *c*. 29–12 ka, Britain, Ireland and the adjacent continental shelf were almost completely covered by a kilometres thick ice sheet. Over much of the 20th century, landform and sedimentary evidence of glaciation was interpreted to reconstruct an ice sheet covering around 70% of terrestrial Ireland and Britain and with the maximum extent not extending much beyond the present-day coastline (e.g. Bowen *et al*. 1986). Whether ice extended eastwards across the North Sea to be confluent with the Scandinavian Ice Sheet was the subject of much debate. With new techniques and based on data collected by ship-borne marine geophysics and coring, this 'small-ice' model was overturned by discoveries that the ice sheet extended in many places to near, or at, the edge of the continental shelf and covered most of the North Sea between Britain and Scandinavia (Sejrup *et al*. 2005; Bradwell *et al*. 2008b; Scourse *et al*. 2009; Clark *et al*. 2012). This view doubled the size of the ice sheet and demonstrated that it must have been heavily marine-influenced, given its extensive marine-terminating margins, with large sectors grounded below sea level. Published evidence of the glacial landform distribution and pattern (e.g. moraines and flow indicators) were combined with new mapping of the glacial geomorphology of the sea floor to produce a map of ice-marginal retreat (Fig. 1) for the whole of the British Isles (Clark *et al*. 2012). Published reports of geochronometric ages that constrain ice-sheet margins were scrutinized to build a database (Hughes *et al*. 2011; >800 ages). By combining the information on timing with the retreat pattern, a palaeoglaciological reconstruction of the shrinking ice sheet was built in a series of maps depicting the changes in ice-margin positions and flow geometry from 27 to 15 ka (Clark *et al*. 2012). A major limitation in this work however, was the lack of direct dating control for the maximum ice extents along the north and west continental shelf edge, in the North Sea and with no time control on ice-marginal recession until it back-stepped onshore. It could not be ruled out for example, whether the evidence of former ice margins on the continental shelf (summarized in Fig. 1) were from a more extensive previous glaciation(s).

In this paper, we continue the endeavour of Quaternary scientists to improve reconstructions of palaeo ice sheets and to learn about their climate interactions, but we were also specifically motivated by the requirements of the ice-sheet modelling community. On a warming Earth, ice sheets are shrinking and glaciologists are using numerical ice-sheet models to make forecasts of the rate of ice mass loss in Antarctica and Greenland, and the consequences for sea level rise over the coming centuries (Golledge 2020). To help improve the robustness of such forecasts and motivated by the quote below we formed a consortium of researchers called BRITICE-CHRONO.

> We highlight that developing a demonstrable skill in ice-sheet projection is hampered by a lack of data and observations for verification and testing. This is particularly acute for the marine ice-sheet instability. Improved geological histories of ice-sheet changes and the forcing that caused them could greatly assist in building such a skill.
>
> IPCC Workshop on Sea Level Rise and Ice Sheet instabilities. Malaysia, 21–24 June 2010 (IPCC 2010).

Given the above, the BRITICE-CHRONO project focussed on developing knowledge of the former British–Irish Ice Sheet by collecting hundreds of new geochronometric ages to constrain retreat across the marine–terrestrial transition. This was so that the ice sheet can be used as a data-rich environment to improve ice-sheet modelling approaches by having robust test data. That large parts of the British–Irish Ice Sheet (BIIS) were marine-based and drained by ice streams, and that its bed topography had many reverse slopes, overdeepenings and troughs, makes it a useful (but not direct) analogue for the West Antarctic Ice Sheet. The fjord topography of Scotland, with extended outlet glaciers and ice streams purging interior ice, provides a useful analogue for much of the Greenland Ice Sheet.

In this paper we first outline the scope of the BRITICE-CHRONO project and its achievements in improving the constraints and robustness of information about ice-sheet retreat. We then show how we used the new and existing legacy ages to build a margin isochrone reconstruction of the growth and retreat of the ice sheet at 1000-year timesteps from 31 to 15 ka, incorporating assessment of the likely errors. To produce an optimized reconstruction that includes ice physics, glacio-isostatic adjustment and sea level change we then used the empirical assessment of ice margin isochrones (and their errors) with a new procedure for combining empirical data with modelling. This optimized palaeoglaciological model reconstruction is presented in a series of palaeo-geographical and palaeoglaciological maps at 1-ka timesteps. Ice volume changes through time are plotted and compared with potential climate and sea level drivers of change. The new data are then used to test the following hypotheses:

- Hypothesis 1: that the marine-influenced sectors collapsed rapidly (<1000 years) and that once onshore the ice sheet stabilized and retreated more slowly. This hypothesis is consistent with the theoretical view on unstable marine-influenced ice sheets (Schoof 2007); we test if such behaviour actually occurred. An alternate view is that widespread purging of ice by fast flow happened while marine-margins retreated slowly, thereby dynamically thinning interior (land-based) ice, and preconditioning the ice sheet to more rapid retreat once it was terrestrially-based. This hypothesis is relevant to the Greenland Ice Sheet, because uncertainty exists as to the wider mass balance significance of
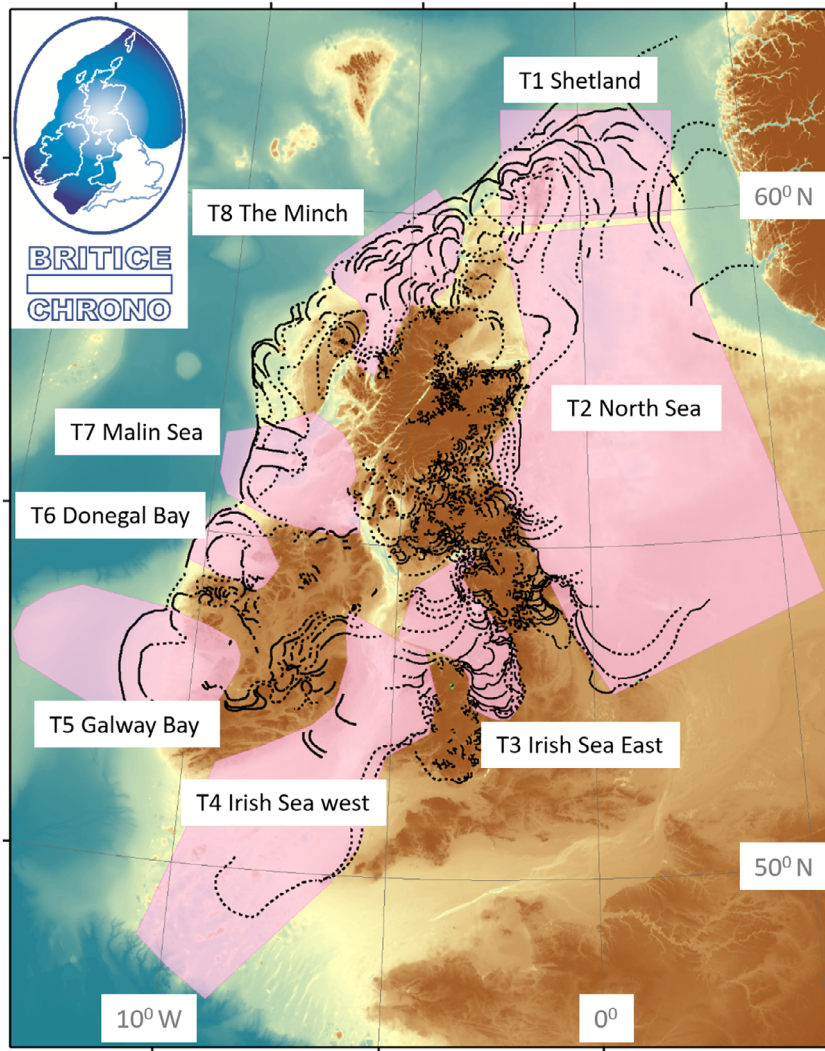
Fig. 1. The retreat pattern (black lines) for the British–Irish Ice Sheet (from Clark *et al.* 2012) was used as a sampling template for BRITICE-CHRONO's eight transects, as shown, capturing the marine to terrestrial transition. Onshore fieldwork and offshore geophysical cruises to sample material for dating were organized within these key transects.

'dynamic-thinning' (Choi *et al.* 2021), and how mass balance will be affected when marine-influenced sectors are lost.

- Hypothesis 2: that the main ice catchments draining the ice sheet retreated synchronously in response to external climatic and sea level controls. This might be expected if external drivers (e.g. warming or sea level rise) outweigh the local controls on ice retreat, for instance related to different water depths, adverse or normal bed slopes, differing tidal ranges and the presence or absence of buttressing ice shelves. However, we expect that such local factors might influence or modify retreat rates, and the extent to which this happens is vital for attaching significance, for example, to observed retreat rates in Antarctica. How cautious should we be in regarding observed retreat

rates at a specific place as being representative of the wider ice-sheet system? Are ice streams merely slaves to mass balance, or do they profoundly alter the course of deglaciation?

In the discussion we address mismatches between the empirical and model reconstructions; discuss key aspects of the ice sheet's evolution; and document and analyse variations in the pace of ice margin retreat and overall ice volume change. We then explore possible climatic, sea level, and dynamic controls on the retreat of the ice sheet, including instability, before summarizing and concluding. Finally we use lessons learnt from this palaeo record of ice-sheet change to suggest important issues for the monitoring and prediction of existing ice sheets and forecasts by ice-sheet modelling.

BRITICE-CHRONO project; constraining rates and style of marine-influenced ice-sheet decay

Here we outline aspects of the BRITICE-CHRONO project regarding its scope, methods and published work so far, as this underpins all the data used for analysis and testing of hypotheses in this paper. The project harnessed the expertise of over 50 palaeo-glaciologists, covering expertise in terrestrial and marine geology and geomorphology, geochronometric dating techniques and the modelling of ice sheets, oceans, and glacio-isostatic adjustment. The project ran from 2012 to 2018. Its aim was to conduct a systematic and directed campaign to collect and date material to constrain the timing and rates of change of the marine-influenced sectors of the BIIS. The retreat pattern (Fig. 1) formed the basis for a systematic sampling scheme and, given the focus on retreat rates from marine-calving to terrestrial-melting margins (hypothesis 1), our sampling was organized via a series of transects from the continental shelf edge to a short distance (~30 km) onshore. Eight transects (Fig. 1) were required to cover the key areas and to test our second hypothesis in relation to the synchrony, or otherwise, of the various sectors. Further details about the BRITICE-CHRONO project are described in Clark *et al.* (2021).

The growth and decay of the ice sheet broadly covers MIS 2, a glacial stage known regionally as the Late Devensian (32.0–11.7 ka): equivalent to the Late Midlandian of Ireland; Late Weichselian of NW Europe; and Late Wisconsinan of North America. More specifically, the main cold episode within the Late Devensian is known as the Dimlington Stadial (Rose 2008; 31–14.7 ka), which exactly covers our time scale of interest, and comprises Greenland Stadials 5–2. We ceased analysis at 15 ka because our focus was on the main ice sheet and its marine to terrestrial transition, rather than its later shrinking back to upland ice masses.

Acquiring samples for dating

Ages to constrain former ice-margin positions in time were derived using radiocarbon assay of organics, optically stimulated luminescence (OSL) of quartz sand grains, and surface exposure dating of both boulders and bedrock using terrestrial cosmogenic nuclides (TCN) ^{10}Be and ^{36}Cl. In marine settings, carbonate microfossils and bivalves were extracted from sediment horizons stratigraphically above or below subglacial diamictons (tills) – found in our seabed cores – and were subjected to accelerator mass spectrometry (AMS) ^{14}C dating. Ages derived by such means provided minimum or maximum ages (respectively) on ice presence.

Samples were collected on two research cruises aboard NERC's RRS *James Cook*: Cruise JC106, Celtic and Irish Seas, and Irish and Scottish continental shelf, 17th July – 24th August 2014; and Cruise JC123, North Sea,

Shetland and northern Scottish continental shelf, 3rd July – 2nd August 2015. To help find optimum sites for seabed coring we accessed archived or recently available marine seismic and high resolution bathymetric data. During the cruises, each planned transect was re-assessed using onboard geophysical and multibeam investigations in order to verify or change previous interpretations, fine tune core locations and add new ones. The geophysical tools used to identify coring targets were an EM710 multibeam echo sounder system that provided a swath of bathymetric data from which landforms could be identified, and a Kongsberg SBP-120 acoustic sub-bottom profiler revealing shallow sedimentary layers and structures. Coring used a British Geological Survey 6-m-long vibrocorer system and NMFSS 9–15 m piston corer. Core analysis was performed onboard with all whole cores run through a Geotek multi-sensor core logger (from the University of Leicester) to measure magnetic susceptibility, bulk density and p-wave velocity. Cores were then split and logged with information on sedimentary structures, colour, grain size, sorting, and bedding contacts, and any macrofaunal content was extracted and recorded. Measurement of sediment shear strength (in kPa) was recorded using a hand-held Torvane. These techniques helped define the depositional and glaciological contexts of the sediments. Selected samples of marine carbonate (typically single or broken valves of shells) were collected for submission for radiocarbon dating.

For terrestrial sites, surface exposure dating was applied to boulders (erratics and ice-transported boulders) and bedrock found on or near moraines using terrestrial cosmogenic nuclides (TCN) ^{10}Be and ^{36}Cl. Care was taken to only collect samples from above the marine limit, based on publications and field observations. Potential boulders for sampling for TCN dating were searched on high-resolution satellite images and aerial photographs, prior to fieldwork. At each sampling location five or more samples were collected. Most of the measured samples were from the tops of glacially transported boulders ($n = 152$), glacially abraded or plucked bedrock ($n = 22$), including eight bedrock/erratic pairs, and one sample was collected from the underside of a large granite boulder to confirm it had been flipped (Smedley *et al.* 2017b). This sample is not included in the samples used for the glacial reconstruction because the apparent exposure age (235 ± 15 ka) is much older than the age range of the reconstruction. Samples were collected using hammer and chisel, and powered saws and angle grinders with diamond cutting wheels. Sample thickness was recorded in the field and verified prior to sample processing. Calculated sample thickness corrections assume a sample density of 2.6 g cm^{-3} except for samples where the density was independently determined. Sample locations and elevations were recorded using handheld GPS. Positions and elevations were checked against Google Earth imagery

and Ordnance Survey topographic maps. Topographic and local shielding angles were measured with compass and clinometer and shielding factors were calculated according to Dunne *et al*. (1999).

We also targeted quartz sands found in association with ice-marginal landforms, for example from outwash sediment proximal to moraines, and derived age estimates by optically stimulated luminescence (OSL). This was mostly conducted from terrestrial sites but we developed a procedure for extracting OSL samples from seabed cores so that we could investigate the age of terrestrially-deposited glacial outwash sands now in the southern North Sea that became submerged during the postglacial marine transgression (e.g. Dogger Bank). Potential targets for investigation on land came from our knowledge of existing sites from publications, mostly quarries and coastal sections for OSL sampling. For important locations without outcrops, we deployed ground penetrating radar to find suitable sedimentary horizons and extracted samples with a Dando Terrier Rig operating in either percussive or rotary drill modes. On occasion, we used a JCB backhoe digger to access suitable samples.

A unified geochronological approach

Given the high number of dates derived on the project and the existence of a large legacy database from publications, a geochronology team (across the three techniques) handled all ages centrally. They archived and processed ages and associated information into two databases (BRITICE-CHRONO master spreadsheet; and the legacy database, BRITICE-database v3). This was important to ensure that all ages used in analyses and reported in publications were consistent, for example, with regard to calibrations and reservoir effects.

For marine radiocarbon ages, the effect of organisms consuming carbon in the water that is older than that consumed by organisms on land can lead to marine radiocarbon ages appearing many hundreds of years too old and requiring a correction often called delta R or ΔR. This marine reservoir effect is well known (Ascough *et al*. 2005), and is a problem with no perfect solution. We developed and adopted the following protocol in order to apply a consistent method that best reflects the circumstances of this study. Radiocarbon reservoir ages in the North Atlantic and adjacent shelf seas have varied both in space and time since the Last Glacial Maximum (LGM). The main controls on reservoir age are, in the deep ocean, the extent of air–sea exchange mediated by convective sinking that ventilates the deep ocean. When the Atlantic meridional overturning circulation is shallow to intermediate in depth, or breaks down completely, the reservoir ages derived from benthic carriers such as benthic foraminifera and molluscs can be very large, contrasting with much reduced reservoir ages when the circulation is vigorous, as at present. As a result, different

water-masses are characterized by contrasting reservoir ages based on their precursor sources e.g. the North Atlantic Current has surface waters with ages close to the modelled mean surface ocean value of 400 years (ΔR) whereas the East Greenland Current has ΔR = +300 years (total reservoir age of ~700 years) (Wanamaker *et al*. 2012). Estimated values of ΔR have undergone some changes in more recent publications (Heaton *et al*. 2020; Reimer *et al*. 2020), but these came too late in our workflow to be included. An assessment of the likely impact of the changes is discussed later on. In shelf–sea settings the reservoir ages are controlled by shelf hydrodynamics rather than deep ocean circulation. In extensive, shallow, well mixed settings, ventilation to the seabed results in ΔR close to 0, whereas settings that stratify have bottom waters with elevated reservoir ages. In glaciated margins the issue is complicated by meltwater entering the marine system that may have been in freshwater reservoirs (e.g. glacier ice) for many thousands of years. The ΔR reservoir ages can be constrained in two ways: (i) in deep sea settings by paired dating of planktonic and benthic foraminifera from the same levels within deep sea sediment cores (the smaller the difference the greater the amount of overturning); or (ii) in both deep and shallow water settings by dating of marine carriers associated with tephra layers of known age.

Some knowledge exists for variation in ΔR for the British Isles. During the Younger Dryas, dating of marine carriers from marine cores adjacent to the British–Irish shelf (St Kilda Basin) associated with the known age Vedde Ash indicates ΔR of +300 years (Austin *et al*. 1995). This is explained by the reduction in overturning that was the primary mechanism forcing the YD event. During Heinrich events, however, ΔR is documented to have been as high as +1000 or +2000 years in the deep North Atlantic (Voelker *et al*. 2000; Waelbroeck *et al*. 2001; Peck *et al*. 2006; Singarayer *et al*. 2008). Based on these data it is possible to propose ΔR values for specific time intervals for the NE Atlantic margin:

　　30–25 cal. ka BP: +300 years.
　　25–23 cal. ka BP: +700 years (Heinrich 2).
　　23–17 cal. ka BP: +300 years.
　　17–15 cal. ka BP: +700 years (Henrich 1).
　　15–12.9 cal. ka BP: 0 years.
　　12.9–11.7 cal. ka BP: +300 years (Younger Dryas).
　　11.7 cal. ka BP to present: 0 years.

To avoid applying these different corrections across space and time, and thereby introducing step changes in the timing, we chose to report all marine radiocarbon ages in the B–C master spreadsheet as three ages corresponding to ΔR = 0, ΔR = +300 and ΔR = +700. The default position reported in our papers is to use the ΔR = 0 correction but the other values may be referred to as appropriate in the interpretation and

discussion, especially where nearby constraining ages exist. However, our pragmatic solution to the reservoir problem is to treat all ages and uncertainties together (radiocarbon, OSL and TCN) along our individual transects, modelled using a Bayesian approach (see later). By incorporating uncertainty of the reservoir effect (we enter each radiocarbon age three times, according to the different values of ΔR per age) the modelling in comparison with other nearby ages and the spatial prior sequence acts as a sensitivity test to identify which combinations generate the highest probability solution.

Radiocarbon ages across all BRITICE-CHRONO publications, including this paper, use INTCAL13 (Reimer *et al.* 2013) for calibration. Subsequent to completing our analysis, a new version of the calibration scheme has been published, INTCAL20 (Heaton *et al.* 2020; Reimer *et al.* 2020). We have not performed any recalibrations to this revised scheme in order to maintain consistency across all BRITICE-CHRONO publications. Whilst differences in the new scheme for atmospheric carbon are very slight (<50 years) the main concern regards the change in age for marine samples arising from the reservoir effect, where Heaton *et al.* (2020) indicate that the offset has increased by mostly around 400 years from INTCAL13 to INTCAL20. However, the new marine corrections are only considered valid for the 'global ocean' (south of 50°N; Heaton *et al.* 2020). The BIIS is further north, terminating in the more complex 'polar ocean' where these marine corrections do not apply. Therefore, our approach above holds in light of the new calibration curve of Heaton *et al.* (2020).

It is known that biogenic carbonate background samples show apparent ages that are younger than mineral carbonate backgrounds (e.g. Nadeau *et al.* 2001). Therefore, we obtained background samples of marine shells (whole shell and shell fragments) and mixed planktic foraminifera from similar locations and sedimentological contexts to the unknown age samples to determine a BRITICE-CHRONO-specific biogenic carbonate background value. All the background samples are known to be more than 80 000 years in age. Three samples of shells (samples A–C) were recovered from the base of a 50-m-long marine sediment core (BH89/10) recovered from the Central Celtic Sea below the depth interpreted as base Weichselian by the British Geological Survey. The precise age of the samples has not been determined but they are expected to be late Middle Pleistocene shallow marine sediments. Three samples (samples D–F) were collected from terrestrial exposures of glaciomarine sediments from Warren House Gill, Durham and have been dated lithologically and by optically stimulated luminescence to MIS 8–12 (Davies *et al.* 2012). Samples A–F were large enough for repeated measurements to be made. Additionally, three samples of mixed foraminifera from the same sediment core horizon as samples A–C were picked. The for-

aminifera samples were only large enough for a single measurement to be made on each sample. The measured percent modern carbon (pmc) of the background marine shell samples (0.30±0.09, $n = 21$) and foraminifera (0.30 ±0.06, $n = 3$) were higher than both the mean of the project specific ISC measurements (0.13±0.06, $n = 25$) and the NERC Radiocarbon Facility's (NRCF) long term average value for Iceland Spar Calcite (0.17±0.08, $n = 192$). The key time period of interest for the BRITICE-CHRONO project is 13–31 ka. Applying the new biogenic carbonate background to the radiocarbon measurements of the unknown age samples makes ages between 40 and 100 years older for that time period. Applying an inappropriate background correction therefore represents a potential source of error equal to 1σ–2σ of the measurement error and could complicate the interpretation of results and prevent correlation between radiocarbon measurements and ages derived from other chronological techniques.

Rock samples for cosmogenic dating were processed at the SUERC Cosmogenic Nuclide Laboratory (^{10}Be $n = 84$) and at the NERC Cosmogenic Isotope Analysis Facility (NERC-CIAF Awards 9139.1013 and 9155.1014; ^{10}Be $n = 82$; ^{36}Cl $n = 8$). Both laboratories are housed at SUERC and regularly check chemistry reproducibility. Samples were processed together with a full chemistry of procedural blanks. The nuclide ratios ^{10}Be/^{9}Be, ^{36}Cl/^{35}Cl and ^{36}Cl/^{37}Cl were measured using the 5MV pelletron at the SUERC AMS Laboratory (Xu *et al.* 2010) and normalized to NIST SRM4325 with a nominal ^{10}Be/^{9}Be ratio of 2.79×10^{-11} (Nishiizumi *et al.* 2007) and Z93-0005 (PRIME Lab, Purdue) with a nominal ^{36}Cl/Cl ratio of 1.29×10^{-2}. Cosmogenic nuclide concentrations include a blank correction of 0.7–17% for ^{10}Be and 1–5% for ^{36}Cl. The uncertainties in the cosmogenic nuclide concentrations include the AMS counting statistics and scatter uncertainties from sample, procedural blank, and standards measurements.

Calculation of a surface exposure age requires a production rate calibration data set and a scaling method. We used two different calibration data sets and the time independent Lal (1991)/Stone (2000) scaling method in two different online calculators. At the time BRITICE-CHRONO produced its first publications surface exposure ages were derived using CRONUS-Earth online calculators (Developmental version; Wrapper script 2.3, Main calculator 2.1, constants 2.2.1, muons 1.1; Balco *et al.* 2008). Since these early publications this calculator changed name to 'The online calculators formerly known as the CRONUS-Earth online calculator' (http://hess.ess. washington.edu/) and the version has progressed to Version 3. Two other online calculators became available, CRONUScalc v2.0 (http://cronus.cosmogenicnuclides. rocks/2.0/; Marrero *et al.* 2016), and the Cosmic Ray Exposure Program (https://crep.otelo.univ-lorraine.fr/#/; Martin *et al.* 2017). For a given production rate calibration data set and scaling method, the different calculators

and versions produce results that are statistically indistinguishable. In an attempt to maintain a consistent approach authors of all BRITICE-CHRONO publications were asked to use the same BC-Chronology database with surface exposure ages calculated using the originally adopted CRONUS-Earth online calculators v. 2.3 as well as CRONUScalc v2.0. The latter was used because it allows calculation of ^{10}Be as well as ^{36}Cl surface exposure ages. We assumed an erosion rate of 1 mm ka^{-1}. Adoption of different erosion rates ($\leq$3 mm ka^{-1}) has very little effect on mean ages of samples (<1.5% difference). The two production rate calibration data sets used are the global calibration data set of Borchers *et al*. (2016) as implemented in CRONUScalc v2.0, and a local Scottish ^{10}Be calibration data set used to produce the Loch Lomond Production Rate (LLPR; Fabel *et al*. 2012). The main difference in the results based on the global and the LLPR production rate calibration data sets is the better precision in the external uncertainties derived from the LLPR calibration.

Luminescence dating of sediments provides a measure of the period of time that has elapsed since the last exposure of mineral grains to daylight, and in many environmental settings this corresponds to the last transport and deposition of the sediment (Rhodes 2011). The extent of exposure to daylight at the time of deposition is likely to be very variable for sediments associated with different parts of the glacial sedimentary system (Fuchs & Owen 2008) and a critical part of our approach was to address this potential challenge, addressed in four primary ways. First, the wealth of existing literature on the sedimentary record of the BIIS was used to select for dating those sites that contained facies most likely to be suitable for luminescence dating while also constraining the ice margin position, such as ice-marginal sediments and glaciofluvial outwash. Secondly, the sampling strategy was designed so that wherever possible multiple samples were collected from an individual site, or collection of sites in close proximity to each other, in such a way that there was good stratigraphical or geomorphological control on the relative age of the samples, thus providing a strong prior for subsequent Bayesian analysis. Thirdly, the OSL signal from quartz was selected for dating. Many studies have shown that this quartz OSL signal is the most rapid to bleach compared with other luminescence signals from quartz, or luminescence signals from other minerals (e.g. Colarossi *et al*. 2015), and thus there is the greatest likelihood that the signal was reset at deposition. Fourthly, for each sample that was dated multiple replicate analyses were undertaken to assess whether all grains had had their quartz OSL signal reset at deposition, or if only a proportion of the grains were reset (Duller 2006, 2008a). Replicate analyses were either undertaken on small aliquots containing only 10–20 grains of quartz (e.g. Bateman *et al*. 2018) or on single grains (e.g. Smedley *et al*. 2017a). A minimum of 50

small aliquots were analysed for each sample, or where single grains were used a minimum of 1000 were measured. In situations where quartz sensitivity was low the number of analyses was increased, for single grains as many as 11 700 per sample were needed in some cases (e.g. Roberts *et al*. 2020). In cases where the signal from only a proportion of the grains had been reset, statistical models were used to identify that population and ages calculated using results from those grains.

Measurements of OSL for BRITICE-CHRONO were undertaken at two laboratories, one in Aberystwyth and the other in Sheffield. The approach taken to determining the two parts of the age equation (equivalent dose and dose rate, see Duller (2008b) for an introduction to luminescence methods) are described here. The same approach to dose rate determination was used at both laboratories. The radionuclide content (K, U and Th) of each sediment was assessed by inductively-coupled plasma mass spectrometry (ICP-MS) at the same analytical laboratory (SGS laboratories, Canada), using a lithium metaborate flux method prior to digestion to ensure that resistate minerals, which often contain a significant proportion of the U and Th, were fully digested (cf. Bailey *et al*. 2003). Where possible, the gamma dose rate was measured *in situ* by portable gamma spectrometry, but in the small proportion of cases where this was not possible it was calculated using the U, Th and K values from ICP-MS. All dose rate calculations were undertaken using DRAC (Durcan *et al*. 2015) with the conversion factors of Guérin *et al*. (2011). Luminescence measurements used a combination of small aliquot and single grain measurements of the OSL signal to determine the equivalent dose. Consistency between the two laboratories was ensured by use of the same primary material for beta source calibration (Hansen *et al*. 2015), and assessed by a number of intercomparisons using samples of a range of complexities. The simplest material was from a beach ridge in Denmark that had been the target of an international laboratory intercomparison (Murray *et al*. 2015). The two BRITICE-CHRONO laboratories obtained identical values for the equivalent dose (D_e) of 4.7±0.1 Gy (Aberystwyth) and 4.7±0.2 Gy (Sheffield). In Data S1 we compare single grain data from analyses for two BRITICE-CHRONO samples where measurements were replicated in both laboratories, and even for sediments where the degree of resetting of the OSL signal at deposition varied from one grain to another. These challenging circumstances required the application of complex statistical models, and the two sets of measurements gave results that easily overlapped within statistical uncertainties, illustrating the consistency of the ages obtained from the two laboratories (see Data S1).

There have been some areas of the BIIS studied by BRITICE-CHRONO that have proven challenging for OSL methods. In parts of western Ireland the dominance of limestones making up the bedrock of the source areas

for glacial sediments meant that extracting sufficient quartz grains for luminescence analysis was sometimes difficult (Roberts *et al.* 2020). In some sectors, such as the terrestrial lobe to the east of the Welsh mountains (Transect 3) and parts of the Malin Sea and the Minch (Transects 7 and 8) incomplete resetting of the OSL signal seemed to be more common than elsewhere, and whilst it was often possible to obtain ages, their uncertainties were sometimes large. Subsequently, samples from these areas have been explored using other luminescence methods, such as single grain measurements of feldspars (Smedley *et al.* 2019) and luminescence dating of cobbles (Jenkins *et al.* 2018; Chiverrell *et al.* 2021). However, in general the measurement of the OSL signal from quartz for small aliquots and single grains has been successful across large parts of the BIIS and provided 156 ages to anchor key stages in the dynamic record of the ice sheet.

As part of the BRITICE project (that preceded BRITICE-CHRONO) all known ages (numbering 1189) reported in the scientific literature relating to the BIIS were compiled into a database (Hughes *et al.* 2011: the BRITICE database v1; Hughes *et al.* 2016: the BRITICE database v2). The ages were taken at face value in a previous reconstruction of the ice sheet (Clark *et al.* 2012) even though many should really have been 'retired', because of outdated technology or lack of reliability, or are lacking in sufficient supporting details. The geochronology team on BRITICE-CHRONO revisited these legacy databases, updating them to include more recently published ages, and devised and then applied a quality assurance procedure to filter out less reliable ages. This was a difficult task with some possible contention (regarding which ages do and do not get retired), and so for full transparency the criteria for assessing ages across TCN, OSL and ^{14}C have been reported in Small *et al.* (2017a, b), including the traffic light system (green, amber, red) that was devised. The revised quality-assured legacy database is presented in that publication. The number of ages reduced from 1189 to 507 by age filtering those that fell outside the time scale relevant to this project. Specific criteria were applied to each dating technique (and green, amber, red categories) to make an objective assessment of the likelihood that an age is influenced by the technique-specific sources of geological uncertainty. Brought together the definitions of quality assurance are:

Green; Ages considered reliable and should be included in analysis. Any conflicts with new data will need to be specifically addressed.
Amber; Ages available for inclusion in analysis. Their reliability remains open to re-assessment pending new data.
Red; Ages available for comparison with constructed retreat histories. Inclusion in analysis is dependent on new and supporting evidence. (i.e. retired unless new supporting information becomes available).

Excluded; Assessed but judged not to be accepted into the screened database. This is usually because the data are outwith the remit (i.e. age filtered or there is insufficient information to make an assessment).

Ideally, at a particular site, numerous replicating ages will exist that robustly define a relevant geological event (deglaciation), although this is often not the case. By grouping ages into sites, the quality assurance procedures found only 45 sites (23 TCN, 16 ^{14}C, 6 OSL) received the highest (green) quality assurance rating and are considered well dated. A further 53 sites (19 TCN, 31 ^{14}C, 3 OSL) are constrained by ages with amber quality assurance rating. The assessment of ages yielded a significant reduction in the amount considered suitable for synthesis in comparison to the number used in the previous reconstruction (e.g. Clark *et al.* 2012). This increase in caution regarding which ages should be used is judged to be appropriate given that a main aim of BRITICE-CHRONO is to provide robust geochronological data on ice retreat for testing and improving ice-sheet models.

For the first time in the context of reconstructing ice sheet-scale dynamics, we adopted a Bayesian age sequence modelling approach to the existing filtered legacy ages and our newly generated geochronological database. This method provides a basis for quantitatively identifying ages that may be suspect (outliers) and thereby reasonably ruled out. Importantly for our now large database, it also offered a method for integrating across our three dating techniques (Rhodes *et al.* 2003) and incorporating the marine reservoir uncertainties. Its third advantage is that for ages that are closely spaced and with overlapping error bars, it permits a narrowing of the probability age range, thereby increasing precision. Bayesian age sequence modelling has been routinely applied to sets of closely spaced, stratigraphically-related samples (e.g. ^{14}C ages for lake sediment cores), and the relationships identified used to narrow age uncertainty (Bronk Ramsey 2009). In the context of ice-sheet retreat, rather than applying the Bayesian approach to stratigraphically defined depth (as per lake sediment example) we applied it spatially to retreating ice margin sequences along our transects. This approach was pioneered and is described in Chiverrell *et al.* (2013) to plot the advance and retreat phases of the Irish Sea Ice Stream using existing legacy ages.

The BRITICE-CHRONO dating results

The BRITICE-CHRONO team conducted >1500 person-days of field data collection (terrestrial and marine) including sampling from 28 islands (e.g. Foula and Scilly Rock) and acquiring 18 000 line-kilometres of marine geophysical data. Sampling for dating was spread across 914 sites (Fig. 2) with samples totalling ~15 tonnes of sand, mud and rock. After laboratory analyses the
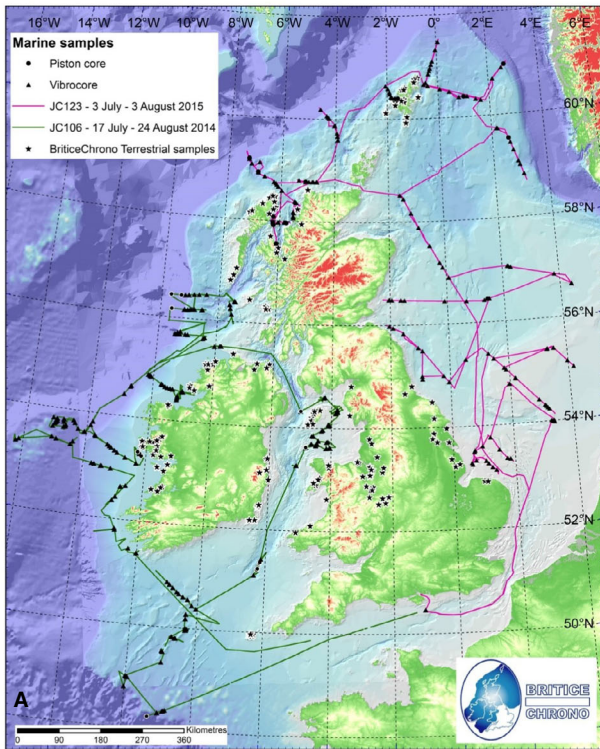
LEGACY AGES:

| | Green | | Amber | | Red | | | |
	Sites	Ages	Sites	Ages	Sites	Ages	Removed by age filter	All Ages
14C	16	55	31	96	-	254	281	686
OSL	6	22	3	7	-	16	61	106
TCN	23	104	19	37	-	91	165	397
Totals	**45**	**181**	**53**	**140**	**-**	**361**	**507**	**1189**

BRITICE-CHRONO AGES:

| | Green | | Amber | | Red | | | |
	Sites	Ages	Sites	Ages	Sites	Ages	Removed by age filter	All Ages
14C	50	103	42	51	-	19	165	338
OSL	38	80	2	2	-	29	51	162
TCN	24	77	23	54	-	43	16	190
Totals	**112**	**260**	**67**	**107**		**91**	**232**	**690**
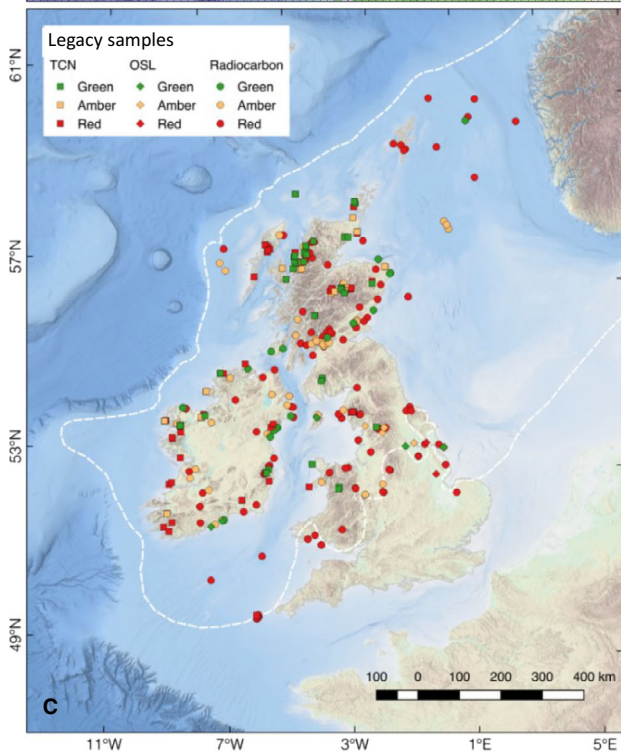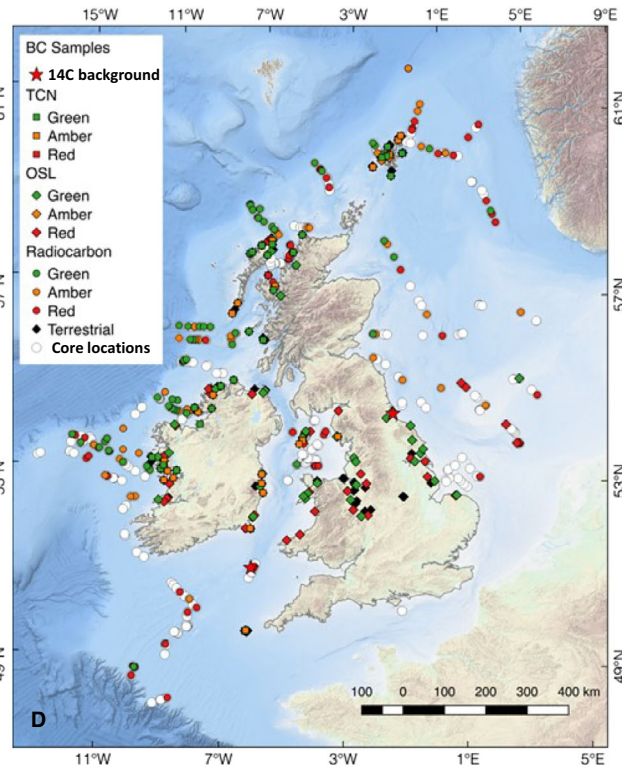
Fig. 2. A. Distribution of the BRITICE-CHRONO samples collected for dating, spread across 914 sites. Seabed samples were collected by vibro and piston corers from two research cruises in 2014 (green) and 2015 (purple). Terrestrial samples (asterisks) were collected for the immediately onshore zones of each transect in order to capture the pace of the ice margin retreat once it back-stepped onshore. B. Summary table and maps of age constraints from the (C) Legacy archive and (D) BRITICE-CHRONO databases. See text for details of the red, amber and green quality designators. The full Legacy database is available in Small *et al.* (2017b) and the BRITICE-CHRONO database in Data S2, this paper.

project generated 690 new ages: 338 radiocarbon; 190 TCN; 162 OSL. These were subjected to the same quality assurance procedures described earlier, decreasing the number to 458 (173 ^{14}C, 111 OSL, 174 TCN) by age filtering those that fell outside the time scale relevant to this project. Grouping ages into sites yielded 112 sites rated as green (50 ^{14}C, 38 OSL, 24 TCN) and 67 sites designated as amber (42 ^{14}C, 2 OSL, 23 TCN). Figure 2 summarizes the ages available for use in reconstructing the ice sheet. Ages are recorded in the BRITICE-CHRONO master spreadsheet (Data S2). The database includes: transect number; sample codes; site names and location; grid references and latitude, longitude; notes on stratigraphical and depositional contexts; uncalibrated and calibrated ages, quality assurance colour-coding (green, amber, red); the final ages we used and their uncertainty envelopes; and further comments. More specific information per dating type is also included, such as moisture content for OSL, boulder lithology for TCN, and sample type for radiocarbon dating (e.g. foraminifera, single valve *Mya truncata*). The full descriptions of the sedimentological, stratigraphical and interpreted glaciological contexts are described in a series of BRITICE-CHRONO papers (see below) and a column in the database identifies which ages are reported in which papers. Figure 2 summarizes the legacy and new BRITICE-CHRONO ages displaying their spatial spread and tabulating the red, amber and green quality designators. Some 367 ages (green and amber) are available for constraining ice-sheet extent and timing.

Overview of the BRITICE-CHRONO findings per transect

The new ages and their stratigraphical and glaciological contexts are reported in a series of 23 publications, which include local to regional reconstructions of the glacial history (Peters *et al.* 2016; Sejrup *et al.* 2016; Evans *et al.* 2017, 2018a, b; Small *et al.* 2017a, 2018; Smedley *et al.* 2017a, b; Arosio *et al.* 2018; Bateman *et al.* 2018; Callard *et al.* 2018, 2020; Chiverrell *et al.* 2018; Lockhart *et al.* 2018; Roberts *et al.* 2018, 2019, 2020; Bradwell *et al.* 2019; Ó Cofaigh *et al.* 2019; Scourse *et al.* 2019; Wilson *et al.* 2019; Tarlati *et al.* 2020). Additionally, each transect team summarized their publications and findings into an overview reconstruction per transect, plotting the withdrawal of ice margins across the seabed and the marine–terrestrial transition. It was important to incorporate the marine and terrestrial evidence in this way to produce a combined synthesis, rather than leaving marine and terrestrial findings separate as is frequent in the wider literature. There is a single story to tell. These benchmark publications are reported in a special issue of *Journal of Quaternary Science* (BRITICE-CHRONO reconstructions of the last British-Irish Ice Sheet, 2021; Benetti *et al.* 2021; Bradwell *et al.* 2021a, b; Chiverrell *et al.* 2021; Evans

et al. 2021; Ó Cofaigh *et al.* 2021; Scourse *et al.* 2021), each documenting ice-marginal positions, flow geometry and geochronological constraints as the ice margin withdrew. These results on the pacing of ice withdrawal were used to interpret the main controls that drove and modulated ice-sheet retreat. Regarding Hypothesis 2 (see earlier; synchrony or not of different sectors) it is important to note that each transect team reconstructed and interpreted their results prior to and independent of the ice-sheet reconstruction that is built and reported in this paper. This was deliberate in order to minimize the potential for interpretative biases leaking into reconstructions regarding synchroneity, or not, between transects. We now summarize some of the main findings from the BRITICE-CHRONO publications.

Transect 1, Shetland and adjacent continental shelf areas. – Bradwell *et al.* (2021a) report new mapping and analysis for a large study area (100 000 km^2) covering the northernmost sector of the ice sheet, including the main islands of Shetland, the outlying islands and surrounding sea floor. The stratigraphical and interpreted glaciological contexts of the 71 new ages are described. A synoptic sector-wide reconstruction combines onshore and offshore evidence with Bayesian chronosequence modelling. Ice masses are reconstructed, varying in size between local upland ice caps and a large ice dome over the entire Orkney–Shetland Platform which remained glaciologically distinct from the ice sheet over mainland Scotland. At its maximum extent (26–25 ka) the ice dome, connected to ice grounded over the North Sea Basin, underwent a dramatic reduction in size until 23 ka, and lost its confluence with Fennoscandian-sourced ice. The Shetland Ice Cap dynamically readjusted to this new geometry with asymmetric re-growth followed by a rapid collapse between 19 and 18 ka in response to the opening of a large marine embayment to the east. Final deglaciation occurred between 17 and 15 ka probably through disintegration into several small ice centres on mainland Shetland, Foula and the now-submerged continental shelf (e.g. Pobie Bank). Changing ice mass configurations and ice-marginal oscillations are interpreted as having high sensitivity to the marine influences on calving and from ice-flow geometry fluctuations from coalescence with and separation from adjacent ice masses.

Transect 2, North Sea. – This is the largest of the 'transects' (Fig. 1), in reality a large box with cruised transect lines within it and with ice retreat in multiple directions rather than along a simple retreat corridor. The results are reported in a series of papers. Prior to, and in preparation for the BRITICE-CHRONO cruise in the North Sea, new mapping and interpretation of glacial landforms was conducted using existing bathymetric and shallow seismic data from which a reconstruction of ice-flow geometry, ice divides and retreat behaviour was

assembled (Sejrup *et al*. 2016). This suggested a dramatic collapse and reorganization of North Sea ice, triggered by loss of mechanical buttressing as the grounding line of the Norwegian Channel Ice Stream (NCIS) withdrew. On the east coast of England, Evans *et al*. (2017) described the stratigraphy and provided the first direct chronological constraints on Glacial Lake Pickering, which was impounded by North Sea ice pressing up against the topography of eastern England. Further south along the coast, Bateman *et al*. (2018) reported on new mapping of glacial geomorphology in the Humber Gap. This permitted estimation of the western maximum inshore extent and thickness of North Sea ice. OSL ages constrained the timing of this maximum extent and the subsequent punctuated withdrawal and re-advances responsible for the emplacement of the Skipsea and Withernsea tills and the damming of ice dammed lakes. At North Cave, on the edge of the Yorkshire Wolds, Evans *et al*. (2018a) reported the sedimentology and stratigraphy of a fan deposit at the eastern edge of the basin occupied by Glacial Lake Humber. OSL and radiocarbon ages revealed that sedimentation and emplacement of the (fluvioperiglacial) fan occurred in MIS 3 (49–37 ka). The low altitude of the fan demonstrates that relative sea level was lower at this time when Glacial Lake Humber did not exist suggesting that North Sea ice had yet to advance far enough south to block the Humber Gap. This mid-Devensian fan is interpreted as deriving from sediment transport from snow-melt in a periglacial environment.

Chronological control on ice margins across the southern North Sea has for many decades been weak, usually using extrapolations of ages from adjacent onshore regions and drawing lines connecting evidence in eastern England to Denmark's Main Stationary Line, and by stratigraphical correlation of lithologically similar tills (e.g. Bolders Bank Formation). From marine geophysical surveys on the BRITICE-CHRONO cruise (JC123 2015) and core samples collected for OSL and radiocarbon dating, Roberts *et al*. (2018) provided the first direct dating control of ice margins in the southern North Sea. Landforms and sediment packages described and interpreted from bathymetric and shallow acoustic survey lines, along with radiocarbon and OSL ages were used to build a reconstruction of ice advance and retreat. The area was terrestrial at this time owing to lower relative sea level. As ice advanced southwards it impounded Glacial Lake Dogger on its southern margin, and ice then advanced into the lake and subsequently retreated. Stresses imparted by the ice are interpreted to have glaciotectonically thrust and folded the proglacial lake sediments generating the relief of what is now Dogger Bank. The dating control indicates advance at sometime between 30 and 25 ka and retreat by 23 ka. To the west, in the lower elevations between the east coast of England and the recently generated Dogger Bank, a lobe of ice advanced to the Bolders Bank limit to impinge on

what is now the North Norfolk coast. This offshore record is consistent with the new findings reported above at North Cave (Dove *et al*. 2017; Evans *et al*. 2018a).

At the southernmost limit, North Sea ice penetrated some tens of kilometres onshore in Lincolnshire and North Norfolk. This has been known from morainic deposits and till sheets, grounding line fans in glacial lakes, and from glaciotectonic landforms (e.g. Straw 1979; Pawley *et al*. 2008). Multiple ice limits have been postulated with the view that they were reached more than once and spanning numerous glaciations (see Evans *et al*. 2018b for an overview), but there was no direct chronological control to tie down specific limits or test the hypothesis of multiple glaciations. This situation is rectified in Evans *et al*. (2018b), which used OSL ages and sediment–landform associations (including use of borehole information and ground penetrating radar and excavations by JCB digger) to fix onshore ice limits in time. Ice is reconstructed as reaching the Garrett Hill Moraine in North Norfolk around 21.5 ka, dating this limit as MIS 2. Immediately south of here, at the Stiffkey Moraine, which was previously thought to be from an older glaciation (between MIS 2 and 12) is confirmed by OSL ages. It is of MIS 6 age (141 and 165 ka) indicating an extensive ice sheet at this time. In Lincolnshire the maximum extent of penetration by North Sea ice during MIS 2 was attained at 19.5 ka, represented by the Marsh Tills and the Stickney and Horkstow Moraine.

Withdrawing from its southern limits on Norfolk, the ice lobe retreated as a terrestrially terminating margin until around 200 km north, offshore County Durham and Northumberland. Here, geophysical data collected on the BRITICE-CHRONO cruise revealed a spectacular bed imprint comprising a mixture of soft and hard-bedded landforms, including mega-scale glacial lineations and streamlined drift and bedrock, and subglacial meltwater channels all radiating to a large grounding zone wedge (Roberts *et al*. 2019). Taking into account the depositional contexts interpreted from sediment in seabed cores, along with acoustic facies from sub-bottom profiler and seismic data, the ice lobe is reconstructed as representing the transition from a terrestrial piedmont-style margin to a marine-terminating margin with a grounding line. Onshore OSL ages, and radiocarbon ages on foraminifera extracted from glaciomarine sediments constrain the switch from terrestrial to marine conditions between 19.9 and 16.5 ka, as the North Sea became inundated. In the transect overview paper, Evans *et al*. (2021) used the two Bayesian transects to analyse 68 new and 37 legacy ages to build a reconstruction of ice margin extent and retreat. The reconstruction incorporates the maximum extent and timing of British ice, the location and timing of British and Scandinavian ice uncoupling, and assesses the main controls on flow dynamics and the pattern of retreat, including the effects of marine inundation.

Transect 3, Irish Sea east. – In common with the southern margin of the North Sea, ice withdrew from a land-based setting back into the marine environment; from Cheshire and Shropshire back into the eastern Irish Sea. At its maximum, the ice lobe reached as far south as the Wolverhampton Line near Birmingham and impounded a series of ice dammed lakes as it retreated northwards across a shallow adverse slope. The margin left behind a rich record of ice-marginal landforms, sands, gravels and lake deposits, reported in Chiverrell *et al.* (2021); this paper sets out the stratigraphical context of the new OSL ages. The chronological work combined single grain and small aliquot OSL measurements of quartz, and cobble-based OSL of feldspars (see Jenkins *et al.* 2018 for methods) in outwash gravels. These ages were integrated with published ages in a Bayesian age sequence model of the retreating ice margin from its maximum limit at around 26 ka, with ice margins passing northwards through Shropshire and Cheshire between 25 and 22 ka. For the offshore region, information from geophysical data and seabed cores collected on the BRITICE-CHRONO cruise (JC105, 2014) were combined with information from terrestrial fieldwork and sampling on adjacent landmasses, notably the Isle of Man and the Cumbrian and Welsh coasts. New OSL and TCN ages are reported in Chiverrell *et al.* (2018) and were combined with existing published ages in a Bayesian age sequence model of ice margin retreat from the coast of North Wales (around 21 ka) to the Isle of Man (20 ka) and northwards to the Southern Uplands of Scotland (15 ka). For the first time, age constraints are provided for the Scottish Re-advance (19.2–18.2 ka), which suggests it was a regional event across the Isle of Man and Cumbrian lowlands and not linked with Heinrich Event 1. The retreat sequence northwards from Liverpool across Lancashire (between 21–17 ka) to Cumbria is reported in Chiverrell *et al.* (2016) demonstrating slow rates of retreat relative to adjacent regions. Overall, the pace and timing of retreat were found to be primarily driven by climate warming but mediated by ice piracy from the adjacent Irish Sea Ice Stream. Local topographic factors were influential in modulating retreat in relation to the reconstructed ice dammed lakes. As ice withdrew northwards into the Irish Sea, ice from the Welsh uplands expanded to fill the vacated space.

Transect 4, Irish Sea west. – Interacting with ice dynamics on Transect 3, this transect covers the mid and distal portions of the Irish Sea Ice Stream. New ages were used to track variations in grounding line retreat rate as the ice stream withdrew through a narrowing and shallowing of its trough. On the west (Irish) bank of the ice stream, Small *et al.* (2018) built a retreat reconstruction demonstrating that changes in trough cross-sectional geometry exerted a control on the pace of retreat, and that pinning of the margin in a constriction led to dynamic thinning,

preconditioning subsequent rapid retreat. On the east (Welsh) bank of the ice stream (Llŷn Peninsula), Smedley *et al.* (2017a) applied OSL ages to a detailed geomorphological record of ice margins, which yielded a high-resolution chronology over 3000 years and 123 km of retreat. In general, faster retreat rates were found with greater trough depths and wider calving margins and with centennial-scale ice-marginal oscillations not matching with climate forcing. At the southernmost terrestrial extent, new ages acquired on the Isles of Scilly (Smedley *et al.* 2017b) resolved a longstanding uncertainty demonstrating that last glacial ice reached this far south. Lockhart *et al.* (2018) investigated the controversial megaridges that exist down the central trunk of the ice stream bed: are they glacigenic bedforms produced by the ice stream or do they arise from tidal currents? They concluded that both scenarios were appropriate, where tidally induced sediments mantled a partially eroded subglacial topography, which acted as anchors for sediment storage. A surprising and important finding was that the maximum extent of the Irish Sea Ice Stream is 150 km farther south than hitherto reconstructed, as far as the continental shelf break in the Celtic Sea, as first proposed by Praeg *et al.* (2015). This was confirmed by results presented by Scourse *et al.* (2019) who also show, using new ages, that the timing of advance was between 27 and 24 ka.

Combining the dating results from Transects 3 and 4, Scourse *et al.* (2021) built a Bayesian chronosequence extending from the Celtic Sea to southern Scotland and recording ice margin retreat over 800 km and 10 000 years. The pace of retreat varied widely in relation to bed topography, and a short-lived purging of mass propagating down the ice stream is suggested by Scourse *et al.* (2021) to have enabled the margin to advance as far as the shelf break at 25.5 ka. Increased outflow along the ice stream is thought to have stolen ice from the accumulation area feeding ice to the English Midlands in an act of catchment piracy.

Transect 5, Galway Bay. – Peters *et al.* (2016) and Callard *et al.* (2020) use our new radiocarbon ages and investigations of sea floor geomorphology and geology to reconstruct the timing of maximum extent on this part of the continental shelf, west of Ireland, and constrain timing of retreat back across the shelf. Significant surprises here are that ice grounded on the sea floor of the Porcupine Bank, extending the ice sheet much further west than previously thought, with evidence of a long stillstand in retreat at a huge grounding zone complex at a mid-shelf position. Roberts *et al.* (2020) plot the timing of ice margin withdrawal from the inner shelf and across the marine to terrestrial transition linking it to the terrestrial evidence of ice margin position and changes in ice-flow dynamics (flowsets; Greenwood & Clark 2009). The complete sequence of retreat from Porcupine Bank to the modern-day coast is reconstructed using Bayesian age

sequence modelling in the transect overview paper (Ó Cofaigh *et al.* 2021). Ice was grounded on the outer shelf at 27 ka and retreat had started by 26 ka, reaching a mid-shelf pause at 24 ka where it built the large grounding zone wedge. The pause was due to shallower water depths and sedimentary build-up of the grounding zone wedge subsequently stabilizing the margin. Over the whole time range, early oscillatory retreat from the outer shelf was followed by slow episodic retreat, which decelerated further as the ice margin became pinned on the Aran islands before becoming terrestrially-based at 17 ka. Onset of retreat is thought to be due to glacio-isostatically induced high relative sea levels promoting increased calving.

Transect 6, Donegal Bay. – To the northwest of Ireland, Ó Cofaigh *et al.* (2019) report findings of sea floor geomorphology and geology and our new dating constraints for the ice flowing out from Donegal Bay to the shelf edge. Ice reached the continental shelf edge after 26 ka and commenced retreat prior to 25 ka, building the Donegal Bay Moraine in a mid-shelf position, formed during a stillstand and re-advance between 20 and 18 ka. By 17–16 ka, Benetti *et al.* (2021) show that the ice margin back-stepped onto land. A key conclusion is that sea level rise initiated deglaciation from the shelf edge due to local glacio-isostatic crustal depression. Onshore in NW Ireland, the mountains of Donegal nourished an ice dome within the Irish Ice Sheet and that contributed ice both westwards into the Donegal Bay ice flow and northwards into an ice stream flowing across the Malin Sea. Wilson *et al.* (2019) report geochronological data that demonstrate marked contrasts in the timing and rate of deglaciation of this ice dome, showing asymmetry between the northern (22–21 ka) and southern (18 ka) sectors and reflecting the different timing of retreat by the adjacent ice lobes and streams.

Transect 7, Malin Sea. – The Barra Fan Ice Stream drained ice from much of western Scotland and northwest Ireland and is shown by Callard *et al.* (2018) to have reached the continental shelf edge in the Malin Sea around 27 ka and with most of the area of the Malin Shelf deglaciated as early as 20 ka. Two deep troughs with reverse bed slopes were interpreted as having accelerated retreat of the ice stream. In common with Transect 6, the early onset of retreat, prior to climate warming, is suggested to have been due to local glacio-isostatic loading promoting increased iceberg calving. On land, new dating by cosmogenic exposure methods constrains ice surface thinning in the trunk of the Hebrides Ice Stream at 21 ka and demonstrates that ice margins retreated back onto land around 17 ka (Small *et al.* 2017a). Analysis of glacially derived sediments in the Donegal-Barra Fan at the mouth of these ice streams permitted Tarlati *et al.* (2020) to reconstruct the latest presence of ice-sheet activity on the continental shelf to 17 ka, consistent with

findings reported above. They were also able to show restoration to cold water conditions and some iceberg activity during the Younger Dryas (12.7 ka), although the source of icebergs remains unknown. In Benetti *et al.* (2021) Bayesian age sequence modelling of all legacy and BRITICE-CHRONO ages was used to synthesize ice retreat across and between the Donegal Bay and Malin Sea sectors, finding much faster retreat in the Malin Sea Ice Stream (~20 m a^{-1}) compared to Donegal Bay (~2–6 m a^{-1}). Differences in retreat rates and timing are interpreted to be due to variability in topographic controls including the location of pinning points.

Transect 8, the Minch. – The Minch Ice Stream flowed northwards along a topographic trough and across the continental shelf, evacuating ice from the NW sector of the Scottish Ice Sheet. Using sea floor evidence of grounding zone wedges along with new timing constraints from the adjacent landmasses, Bradwell *et al.* (2019) demonstrated that retreat of the ice stream's grounding line was episodic. The low-angled flat-topped morphology of some of the grounding zone wedges permitted identification and reconstruction of ice shelf evolution associated with retreat of the grounding line. A step change in the retreat rate arose from loss of the ice stream's buttressing ice shelf, with such loss thought to be controlled by the trough shape and bed strength imparted by the underlying geology. This marine-sector loss hastened the demise of the ice stream and dynamically affected surface elevation and flow configuration of the wider ice sheet. In the transect overview publication, Bradwell *et al.* (2021b) synthesize the above with new age assessments from the sea floor to build a reconstruction of the advance and retreat for the Minch Ice Stream encompassed within the wider NW sector of the Scottish Ice Sheet, including the adjacent Hebridean Islands. Ice was already advancing into the Minch around 32–31 ka and reached the edge of the continental shelf by 30 ka, perhaps only fleetingly, and by 29 ka was already in retreat. By 28–27 ka the ice-sheet margin had receded to the mid-shelf, exposing the island of North Rona and the adjacent shelf. Present-day land areas in northern Lewis (Outer Hebrides) were exposed by 26 ka, during the LGM global sea level minimum. The rate of ice-sheet retreat slowed at 24 to 23 ka once the ice stream terminus had withdrawn from the shelf into the topographic confinement of the Minch. At around 20–19 ka, a phase of rapid frontal retreat ensued – interpreted as one or more collapse events – with the loss of the buttressing ice shelf. This ice stream retreat left a separate ice cap on the northern Outer Hebrides, with final disappearance of ice on Lewis by 16–15 ka, by which time the ice margin had back-stepped onto mainland Scotland.

Method of ice sheet-wide reconstruction

In order to build an ice sheet-wide reconstruction of the growth and retreat of the ice sheet, we did not merely join

up (interpolate) palaeo-ice margins between those identified on the transects, nor did we approach the problem by adjusting the previous ice sheet-wide reconstruction (Clark *et al.* 2012) using the new ages. Rather, we started again from the basic ingredients of landform and sedimentary information about the pattern of retreat and using all quality-controlled legacy ages and new BRITICE-CHRONO ages. Given the large number of ages and the topographic complexity of the British Isles (not a flat circle), with multiple uplands yielding ice centres that likely merged and separated through time, the task of reconstruction was large; naïve thoughts of more ages making it easier were unfounded! The ice sheet was reconstructed covering the growth and decay between 31 000 and 15 000 years, yielding palaeoglaciological maps at 1000-year time intervals. First, we assembled an entirely empirically based reconstruction by drawing ice margins that best satisfied the pattern and timing evidence, and expressing spatial uncertainty in margin position (see later). This is the equivalent method used in many previous reconstructions of for example, the Laurentide (Dyke & Prest 1987), British–Irish (Clark *et al.* 2012) and Fennoscandian ice sheets (Stroeven *et al.* 2016) but with the additional specification of including spatial uncertainties in margin positions at the set timeslices, similar to the approach used in Hughes *et al.* (2016) for the Eurasian Ice Sheet complex. Although rarely stated, such approaches require judicious drawing of ice margins across areas with little or no evidence. This task of interpolation is qualitative and heuristic, guided by expertise and prior knowledge of typical ice margin geometries, for example making lobate shapes and accounting for bed topographic variation. Our second approach was to produce a model reconstruction, a numerical ice-sheet model that works well replicating existing ice sheets (Bueler & Brown 2009; Winkelmann *et al.* 2011) was applied to the BIIS and forced (see later) to reasonably match its spatial extent at each timeslice. This approach has the large advantage of providing some confidence that the reconstructed geometry is physically plausible. Additionally, our choice of model (see later) permitted incorporation of the effects of (local to global) glacio-isostatic adjustment, ice streams, grounding lines and ice shelves. The method also produces a 3D rather than map-plane reconstruction from which ice volumes can be calculated. For completeness and given that both the empirical and model reconstructions could be useful for further research we present both cases and explain the methods below.

Method of empirical reconstruction

To build the reconstruction of palaeo-ice sheet margins we assessed tens of thousands of pieces of information, assembled in time and space to produce maps of spatially continuous palaeo-margins at 1000-year (isochrones) time intervals. Evidence used included the position of landforms such as moraines, grounding zone wedges and lateral meltwater channels, the extent of glacigenic sediments, and the position in space and time of geochronological constraints including their stratigraphical context, relationship to nearby landforms and their error range in timing. Given such volumes of data, it was not possible to build up the reconstruction using familiarity with site names and ages and building simple maps. Rather, the task first required considerable data reduction and generalization whilst retaining the key constraining information. This was performed in a series of thematic layers and associated tables managed in a GIS (ArcGIS) and in which all interpretations of ice sheet-wide ice margins were built. We used the BRITICE V2 (Clark *et al.* 2018) GIS database of glacial landforms comprising 170 000 features, along with hundreds of elements of new mapping of ice-marginal features from the eight BRITICE-CHRONO transects (Benetti *et al.* 2021; Bradwell *et al.* 2021a, b; Chiverrell *et al.* 2021; Evans *et al.* 2021; Ó Cofaigh *et al.* 2021; Scourse *et al.* 2021). These new data were used to adjust and refine the overall pattern of retreat presented in the Clark *et al.* (2012) ice-sheet reconstruction, but ignoring its timing. This first-order pattern of retreat was overlain on a rendition of on- and off-shore topography, providing a spatial template to guide the drawing of ice margin isochrones.

Geochronological constraints were added to the GIS as dated points, retaining their error ranges. Their stratigraphical context was interpreted and then reduced to one of the following categories:

1 Ice advance constraint, which may derive from dated material (e.g. shells) incorporated within till (ice advance must post-date the youngest given age), or dated material from a unit stratigraphically below and close to a till unit. These provide maximum and tight age constraints on ice advance; ice likely advanced over the site after but close (*c*. 10–100 years) to the given age.

2 Ice retreat constraint, dated material from units stratigraphically above and close to a till (e.g. ^{14}C age on shell in proximal glaciomarine deposits lying centimetres above a till horizon). These provide a minimum and tight age constraint on ice retreat; ice must have retreated prior to the stated age but presumed to be close to its age (10–100 years).

3 Margin age constraint, dated material with a strong association with landform evidence of an ice margin (e.g. OSL age of outwash sands in front of a moraine or cosmogenic age estimate of a boulder on a moraine). These provide a tight age constraint on the position of a palaeo-ice margin.

4 Ice free constraint, dated material recording ice free conditions (e.g. animal bones in caves, or organic sediments in a non-glacial unit) but its connection to evidence of ice cover (till or moraine) is lacking. The

constraint is that the site had to be ice free at this time, but the ice margin may have advanced or withdrawn many thousands of years prior to the stated age and it is therefore only a loose constraint, perhaps 1000s of years.

All ages were assigned to these categories as a means of data reduction without losing the key stratigraphical contexts. In practice and for cases where numerous ages exist at a site, or at nearby sites (~10s km), comparisons between them sometimes led to the realization that ages originally assigned as tight minimum ages on ice retreat were better relegated to being (loose) ice free constraints. Consider for example a ^{14}C age on a shell extracted from a core of glaciomarine sediments a short distance (10 cm) above a till. The shell was chosen for sampling thinking it would be a tight minimum age constraint (10–100 years) on ice retreat, and this would be the starting presumption. But if nearby ages did not fit this timing then such ages were sometimes demoted to being a loose age constraint (e.g. an ice free age constraint) bearing in mind that they are only ever minimum age constraints (ice could have withdrawn much earlier). Perhaps in this example, 10 cm was too large a distance above the till unit given that the (unknown) sedimentation rate might have been slow. The elapse of time might have been thousands of years rather than decades.

Two geochronological databases were used: those derived from the published literature – called the Legacy Database – and the newly acquired ages in the BRITICE-CHRONO database (Data S2). Both databases were subjected to stringent quality control procedures (see earlier and Small *et al.* 2017b) in order to distinguish those ages that can be regarded as providing robust constraints (e.g. five ages at a site showing strong statistical replication) from those that are less so and are worth considering for retirement from any interpretation (e.g. using a now-obsolete measurement technique). Dating constraints on ice margin position were used as outlined above (advance or retreat constraints; margin or ice free), and paying attention to their quality control flags, using the green and amber categories. Occasionally, ages categorized as red were used if they could easily be incorporated without requiring large or radical changes to the reconstruction.

The first task was to build ice sheet-wide margins per timeslice to produce what we term the Optimum Isochrons. These represent the ice margin position that we favour based on the pattern and timing data. The margins were hand-digitized into the GIS. To aid this process the retreat pattern map was used in combination with the ages of dated sites (rounded to nearest hundred years), which were colour-coded into the four categories (e.g. ice retreat constraint) essential for guiding the context of constraint (maximum, minimum, advance, retreat, etc). The positioning of margins was based entirely on the pattern and timing data sets held in the GIS, with any published accounts regarding fluctuations of ice margins ignored. Ice margins were drawn to reflect their likely position with consideration to the surrounding landform and dating evidence and were not merely 'snapped' to a moraine position at a date. In cases of contradiction between ages, the simplest case was selected. Ice-marginal dynamics may have been more complicated in reality but we chose the most parsimonious solution that satisfied the data. A frustration in this process is that not enough of the time–space 'jigsaw puzzle' is available everywhere to yield a single unequivocal outcome. This mostly arose when nearby (100 km) ages conflicted in places where the precise direction of retreat is ambiguous, such as over parts of the North Sea or in locations where the ice sheet likely spilt into component ice caps over uplands. In such cases we were guided by the Bayesian-defined ice margins per transect, because this modelling process made choices regarding which outlier ages could be ignored. Where relevant, and if not contradicting the wider reconstruction, adjustments to the isochrones were made to bring the margins from the two methods (ice sheet-wide vs. transect based) into broad consistency. When reconstructing a particular timeslice, due attention was paid to its preceding and succeeding timeslices to ensure consistency. In the absence of information otherwise (i.e. in blanker areas without morainal landforms or ages) margins were either simply kept in place or drawn with monotonic and steady retreat between the timesteps.

Whilst the Optimum Isochrons incorporate some soft knowledge in their reconstruction and thereby represent the preferred case, two further sets of isochrones were reconstructed, one reflecting the largest ice extent possible and another for the smallest ice extent possible without contradicting age constraints. This was to: (i) relax the precision implied by a single optimum line on a map, by widening the reconstruction to be consistent with alternative scenarios in places where limited data permit these; (ii) account for variations in timing using the full uncertainty range in reported ages; and (iii) provide a means of spatially representing uncertainty in the timing of margin positions in order to aid comparisons with numerical ice-sheet modelling experiments. For each timeslice, working clockwise around the ice-sheet perimeter, the optimum position was advanced and shrunk as far as it could go without contradicting an age constraint to build the Big and Small Ice Isochrones. For places with numerous age controls, this distance might be only tens of kilometres but in other areas the distance might be much greater until the next age constraint is encountered. For the Big Ice reconstruction, margins were plotted being sure not to exceed the known maximum footprint of the ice sheet. These tasks were iterative between timesteps, and importantly for the Small Ice extents, once plotted for the whole time period they required adjusting to ensure that at some point during glaciation the known maximum limits were

reached, and permitted this to be at different times at different sectors around the perimeter. The task of Big and Small Ice reconstructions is complicated by the need to know which end of the dating error bar to use, depending on whether the margin was retreating or advancing (see Fig. 3) and whether plotting Small or Big Ice isochrons. In building reconstructions, age conflicts inevitably occurred, with the first recourse being to attempt to include all ages by adjusting ice margin geometries accordingly, sometimes by varying retreat directions or using consideration of ice thinning expos- ing higher ground first, for example. Where this was not appropriate, because the pattern of retreat was well known, then an age was demoted and not included. This was easily justified when a particular was found to disagree with numerous other ages nearby (10s of kilometres).

The vexed problem of re-advances

From observations of change in existing ice sheets and from theoretical considerations, we know that ice mar- gins and grounding lines can respond to changes in mass balance, changes in basal slipperiness or ice shelf buttressing, for example, on time scales of years to a century. Such variations are therefore likely to have

occurred during retreat of the BIIS, but they remain below our resolution and precision in dating. The worth of our approach in fact is that we can document change over the century and many thousand year time scales, which is arguably the main, first order, signal of retreat, but of course we will have missed shorter term (<100 year) oscillations. However, larger and longer term re-advances (>100 years) are included in our reconstruction. They may have been climatically driven or have arisen from internal glaciological instabilities, and some may have been substantial in space (tens of kilometres) and time (hundreds of years). These are part of our remit, but there is a problem in robustly defining them and also in relating them to the prior literature on re-advances. Over many decades of investigation, numer- ous advances of ice margins indicated by sedimentary and landform records have been proposed and named. A complication here is that prior to the wide availability of geochronometric dating, such advances were often assigned (speculatively correlated) to known climate signals of warming-cooling, originally the fourfold glaciations (Penck & Bruckner 1909), then to the more variable and spiky oxygen isotope ratios within glacial cycles and more recently to ice and ocean core records of Heinrich Events and Dansgaard-Oeschger cycles. With often little or no dating control on the re-advances, and
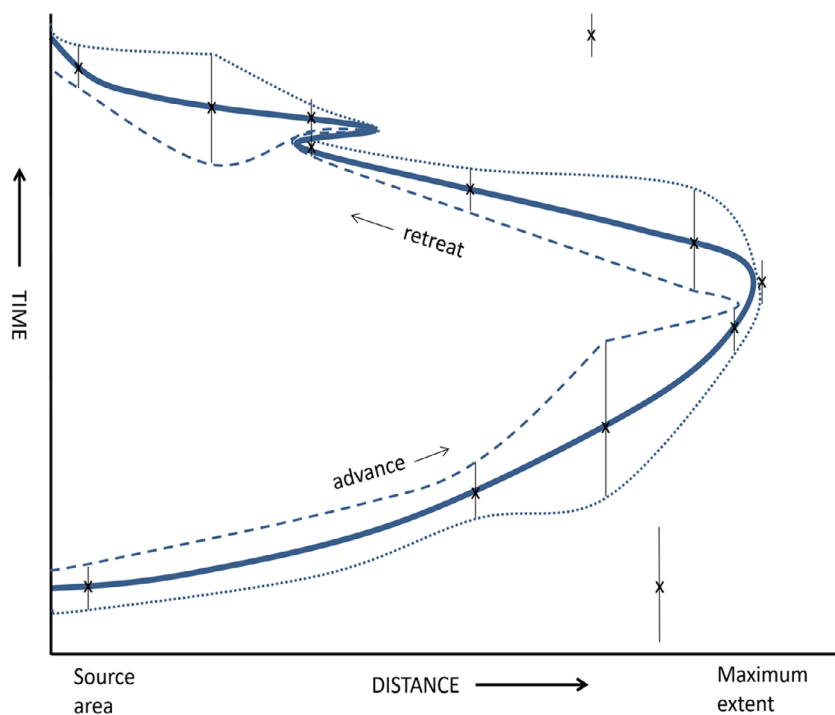

Fig. 3. Schematic time-distance diagram illustrating how ages were used differently according to whether they constrain advancing or retreating margins and whether used to plot the Optimum Isochrons (solid line) or Small Ice (dashed) or Big Ice (dotted) Isochrons. This is relevant because ages are typically quoted as a median age with an error bar (e.g. 23.7 ka ±218 years) and we permitted them to take values in this range (e.g. 23.5– 23.9) as follows: Optimum Isochrons used the median value, the Big Ice Isochrons the oldest end of the error bar during advance but the youngest end during retreat, and the Small Ice Isochrons using the opposite (youngest during advance and oldest during retreat). Interpretations of ice advance, retreat or re-advance for dated sites are deduced from their stratigraphical or geomorphological contexts and relationships.

minimal assessment of their spatial scale (metres or kilometres re-advance, how much of the ice-sheet perimeter?) this was considered the sensible thing to do to make sense of glacial variations and link them to climate drivers. The British Isles have a rich record of such putative re-advances. These are variously named, such as the Drumlin Re-advance in Ireland (Synge 1952), the Wester Ross Re-advance in Scotland (Robinson & Ballantyne 1979) and re-advances in the Killard Point Stadial (McCabe *et al.* 2005), across the ice sheet, and with many more reported over the years. With varying degrees of robustness, sometimes with good dating control through to none, these have often been linked to variations in climate. Given our large campaign on collecting new dates, the approach of BRITICE-CHRONO has been to retain the analysis of data (landforms, sediments and dates) and their interpretation entirely separate from climate signals, and only to make the comparisons after we have built our reconstructions of margin variation through time. In this manner we aim to have built independent observations from which it is possible to ask how the climate drivers influence ice-sheet variations. It is only now that we have enough ages that this more robust route can be taken, a privilege that the earlier investigations in the literature did not have. In this publication we do not uncritically build proposed re-advances from the literature into our reconstruction, but limit ourselves to reporting re-advances only when observations with chronological control require that they exist. We only plotted them at these places and with no presumption that they represent sector-wide behaviour, and took a minimalist approach in only plotting the distance of withdrawal and then re-advance that is required to satisfy the data. This means that some re-advances previously interpreted as reflecting major climate-influenced oscillations (e.g. McCabe *et al.* 2005) appear in our reconstruction as localized margin shifts of the order of hundreds of metres to a few kilometres. Some may find this lack of connection to previously proposed and named re-advances controversial.

Method of model reconstruction

Ice-sheet models are usually run completely independent of the empirical evidence of ice-sheet extent, timing and flow dynamics and are driven by climate and sea level proxies, with Boulton & Hagdorn (2006), Hubbard *et al.* (2009) and Patton *et al.* (2017) being relatively recent examples covering the BIIS. The resulting simulations can stand as reconstructions, and are often compared with the empirical record after models have been run, as a form of validation (e.g. Ely *et al.* 2019). This approach of keeping models and data separate is particularly useful for exploring specific scientific questions, such as: does the formulation of physics in the ice-sheet model allow it to correctly predict where the main

ice streams turn up (e.g. Gandy *et al.* 2019)? This approach is less useful, however, for producing 'the best' reconstruction of ice-sheet history. This is because model simulations rarely match well with the evidence base, mainly we suspect because the climate drivers are insufficiently known (Stokes *et al.* 2015), or because improvements to the model physics are required. The usual challenge therefore is to pick which, of many model simulations, best match the evidence or to find ways of varying the climate inputs to attempt a better matching. Alternatively, data and models can be combined in 'data-calibrated' approaches (e.g. Tarasov *et al.* 2012). We pioneer a new data-calibration approach deliberately combining an ice-sheet model with our extensive data constraints on the ice sheet. This is so we can use the physical aspects of modelling, climate and sea level forcing to build an optimal reconstruction of the ice sheet through time that matches well with the evidence. This model reconstruction has the advantage of a numerical consideration of ice physics, and plots its own ice extents roughly matching those defined in the empirical record, but varying from them as the flow physics requires. Ice-flow variables, such as direction, velocity and thickness, can be derived from the model physics, rather than from an interpretation of the evidence. This approach therefore should stand as a state of the art model reconstruction; a simulation of the glacial history. In short, the approach is to model the ice-sheet-shelf system at discrete 1-ka timeslices with the modelled ice extent forced toward the empirically defined margins and using sea level records and loading/isostasy to constrain the thickness.

We expect that the ice sheet is rarely in steady state equilibrium with its drivers, with time delays in ice-sheet response lagging earlier climate events. It is for this reason that time-dependent dynamical ice-sheet modelling is appropriate, but such models are difficult to force to fit to the empirical data and their formulation has not been designed with this in mind. We take a two-step approach to this challenge by first using a static ice-sheet model (i.e. assumed to be in balance at each timestep) to get the approximate ice extent and thickness correct (i.e. matching with empirical evidence). We then use these static 3D ice-sheet simulations to guide a more dynamic ice-sheet model. In this manner, a sophisticated dynamical ice-sheet model with complex physics is nudged to conform to the empirical evidence base. The novelty here is that we use methods to nudge the model to get it close to what is empirically known, but let the physics and dynamics in the model depart from this where they need to.

First, we used a model of ice flow to build physically simplified static ice sheets to match the reconstructed optimum margin isochrones. These were produced using the Gowan ICESHEET 1.0 model, which builds an ice-sheet surface (Gowan *et al.* 2016). This approach has a minimum of inputs and essentially fits the typical parabolic surface profile of an ice sheet to the identified

empirical margin positions. It does this by assuming steady state conditions at each timeslice (no imbalances) and that ice-sheet spreading is by perfectly plastic flow behaviour (Nye 1952; Reeh 1982; Fisher *et al*. 1985). The only inputs are ice extent, basal topography and a map of basal shear stresses. ICESHEET 1.0 has been shown to reasonably capture estimates of ice thicknesses across modern ice sheets (Gowan *et al*. 2016). Note that there are no climate inputs or dynamics in this model, nor ice streams nor ice shelves. The model was run for the 17 timeslices (31–15 ka). For convenience we call these our plastic ice sheets (Fig. 4). Because the method required a basal shear stress map across the domain, we created one based on the distribution of known palaeo-ice streams (set as 20 kPa), soft sediment (25 kPa) and exposed bedrock (130 kPa), with refinements using the type of landforms present. Areas of drumlins for example have a shear stress value that was 'slippier' (60 kPa) than those without. This map has a strong control on the resulting ice-sheet thickness and so values were varied from more slippy to sticky to build a range of ice-sheet reconstructions from thin to thicker, respectively. Additional to this uncertainty on basal slippiness we added different scenarios on the style and duration of coalescence between British and Scandinavian ice over the North Sea to reflect our lack of confidence here. These varied from two lobes that briefly kissed and then separated, with an overall reconstruction of thin ice, to a thicker ice model where the coalescence persisted for long enough for a major ice divide (~1500 m) to grow over what is now the North Sea.

Next, in order to determine which of the above plastic model scenarios (four were made) was the best approximation of the actual ice sheet we compared their mass loading of the lithosphere with relative sea level records.
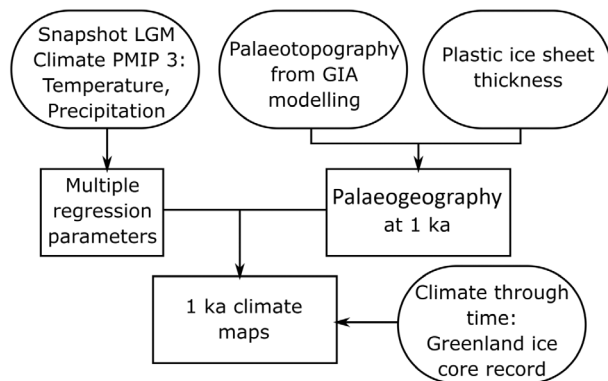

Fig. 4. Approach for building bespoke regional climate fields of temperature and precipitation for driving a dynamical ice-sheet model of the British–Irish Ice Sheet. Fields of temperature and precipitation from climate modelling of the LGM are adapted to better reflect the known BRITICE-CHRONO palaeogeographical reconstruction of the area, including the ice-sheet palaeotopography, and are scaled to vary over the 1-ka timesteps using the Greenland ice-core records (see main text for further explanation).

The logic here is that the best plastic ice-sheet scenario is that which is consistent with both local relative sea level constraints and wider assessments of global glacio-isostatic adjustment and ice-sheet variation elsewhere (e.g. changes in size of the Laurentide Ice Sheet). For these reasons the comparison of the plastic model scenarios to sea level constraints were conducted by glacio-isostatically modelling the effect of mass loading (35 to 0 ka) across the Northern Hemisphere (e.g. Bradley *et al*. 2011). This required us to also build plastic ice-sheet model reconstructions for the Scandinavian and Barents Sea ice sheets fitted to the ice extents of DATED (Hughes *et al*. 2016). An important by-product of this GIA modelling is that it allowed us to produce palaeotopographies of the ice-sheet bed at each 1-ka timeslice, plotted as isostatically depressed DEMs upon which we then ran dynamical ice-sheet model simulations.

The next step was to run the more complex dynamical ice-sheet model PISM (Parallel Ice Sheet Model; Bueler & Brown 2009; Winkelmann *et al*. 2011), suitably guided or nudged such that it achieves a rough match to the ice-sheet thicknesses per timeslice in the plastic ice-sheet simulations. The greater physical realism (e.g. it has ice streams) of this model and the property that it can be out of equilibrium means that it should yield a much improved reconstruction, and that will diverge from the oversimplified plastic reconstructions where it needs to. The PISM model is a hybrid shallow stress balance model, combining both the shallow-ice and shallow-shelf approximations (SIA and SSA, respectively). The SIA is used to solve ice flow in the slow-flowing interior of the ice sheet, where no sliding occurs. The SSA enables PISM to model flotation ice shelves, but can also be used as a sliding law to model ice stream flow (Bueler & Brown 2009). We use a pseudo-plastic sliding law (Schoof 2006), with sliding occurring when the basal shear stress exerted by the ice exceeds the basal yield stress. Whilst various methods were attempted to determine basal yield stress, the most successful at replicating the pattern of reconstructed ice streaming was to directly input the map of values used in the plastic ice-flow modelling. We also considered marine ice-sheet physics following the PISM-PIK approach (Winkelmann *et al*. 2011); this means that stresses at the ice shelf front were considered and grounding-line position was parameterized at a sub-grid scale (Gladstone *et al*. 2010). Given uncertainty in the position of ice shelves, a simple thickness-based calving model was used. Furthermore, our experiments used the sub-shelf melt parameterization of Martin *et al*. (2011), which has a melt factor rate parameter, which we tuned to the extent of the grounding line we reconstructed.

Typically, a dynamic ice-sheet model is driven by a field of climate parameters that vary over the time-span of the model run, and ideally we want to run the model under the actual climate for the area, but this is of course

insufficiently known. We therefore developed a bespoke regional climate field to drive the modelling adapted from the mean temperature and precipitation fields of the PMIP 3 LGM global climate model experiments (Braconnot *et al*. 2011), and varied through time using the Greenland ice-core record. Our approach is summarized in Fig. 4. A difficulty is that the boundary conditions for the PMIP simulations included an LGM ice sheet that differs in extent, elevation and temporal resolution from our BRITICE-CHRONO reconstruction. This is a problem because the temperature and precipitation fields exist at the elevation of the ice sheet used and if we used these fields in our own ice-sheet modelling it would attempt to recreate the PMIP ice-sheet extent and topography. To prevent this problem we sought statistical relationships in the PMIP data between climate and ice-sheet geographical position and elevation and then used these relationships to derive a more appropriate climate field for our BRITICE-CHRONO ice-sheet extent and elevation. This was achieved using multiple regression to derive latitudinal, longitudinal and topographic relationships between climate variables. Multiple regressions have been successfully used to drive ice-sheet models previously (Hubbard *et al*. 2009; Patton *et al*. 2017), but these studies have perturbed modern climate data, rather than the LGM climate that we adapt from. Bespoke temperature and precipitation fields to drive our dynamic modelling were derived using the multiple regression fields applied to our palaeogeography of the domain (plastic ice-sheet thicknesses on GIA-modelled topography), yielding climate maps. To do this for all timesteps, rather than just at the LGM, each 1-ka climate reconstruction field was offset by the Greenland Ice Sheet temperature record (Dansgaard *et al*. 1993; Seguinot *et al*. 2018), assuming 7.3% reduction in precipitation per degree Kelvin of temperature reduction (Huybrechts 2002). Rather than linearly interpolating through time between these 1-ka climate fields, a glacial index approach was used (Niu *et al*. 2017), whereby the climate state at a point in time is scaled between the nearest two 1-ka climate fields according to the ice-core oxygen isotope record. Temperature and precipitation were converted into surface mass balance using a positive degree-day method (Calov & Greve 2005).

The approach described so far effectively nudges the PISM simulations toward the target ice extent and elevations in the plastic model simulations. This approach however, could not achieve a sufficient match to the empirical evidence in a few selected places and timings, and this motivated us to develop and apply a further nudge. The philosophy here is that the dynamical model is mostly doing a good job of simulation but that in some places it needs adjusting. So a mechanism was devised that essentially melted more ice from a lobe that advanced too far beyond that in the empirical reconstruction. In these cases the climatic mass balance was adjusted to produce an ice thickness of zero beyond the empirical reconstruction. The rate at which this adjustment occurs was defined by a user-input parameter. We found that too small values of this parameter led to a modelled ice sheet that was too large. Conversely, large values introduced model artefacts arising from overfitting to the detail of the empirically defined margin. It was decided not to overuse this nudge even though some places remained stubbornly difficult to match even with this approach, from which we might learn something about the modelling or the underlying empirical data (see Discussion). Philosophically we are comfortable making such nudges because there are large unknowns in climate drivers and basal friction and yet the ice sheet's pattern and timing of retreat is now very well constrained. To reiterate, our aim is to achieve a physically plausible ice-sheet reconstruction of appropriate extent, thickness and flow geometry.

The model was initially run at 5-km horizontal resolution, with alterations to sub-shelf melt, calving, thicknesses and the mass balance adjustment factor made iteratively to tune the model to the empirical reconstruction. The final model reconstruction was run on a 2.5-km horizontal grid, with 101 vertical layers in the ice, spaced so that they are concentrated at the ice base (vertical resolution is 10 m at the base of the ice, and 69 m at the ice surface). To capture the interaction between the BIIS and Fennoscandian Ice Sheet (FIS), the model domain extended east beyond the British Isles, to cover Norway, Denmark and southern Sweden.

Results

Here we present both the empirical reconstruction and model reconstruction of the ice sheet's growth and decay along with the rise and fall in land and sea floor palaeotopographies. We then proceed to discuss these findings and use them to test the hypotheses outlined earlier.

Empirical reconstruction of ice-sheet extent

The empirical reconstruction of ice extent is presented in Fig. 5 and in Data S3. Due to the large volume of data, it is not practical to document how each landform, sediment facies and age was used to build the reconstruction. However, we provide a narrative here of some of the main underpinning published constraints and with reference to the BRITICE-CHRONO ages (e.g. T8SUAI0) indicating the transect and sample number to help find them in the dating master spreadsheet in Data S2. Ice limits were drawn to link the available landform evidence with the geochronological constraints as expressed conceptually in time–space in Fig. 3, and spatially as reported in fig. 16 of Clark *et al*. (2012). The comments below, grouped into timeslices, therefore explain key choices made on where to draw the minimum, maximum and optimum ice limits,

and noting how we dealt with areas of no data, and should be helpful for anyone wishing to build or refine a new reconstruction. If this is not your task we suggest skipping this section and moving to the glaciological interpretations that arise from the preferred model reconstruction, which is where the evolution of the ice sheet is portrayed and discussed.

Pre 31 ka. – The BIIS began in the uplands and northerly latitudes of Scotland. A number of advance ages suggest that between 38–31 ka ice cover in Scotland was minimal. These are Reindeer Cave, Assynt, where antlers indicate ice free conditions (Lawson 1984), glacifluvial sediments beneath till at Toddlehills, Aberdeenshire (Gemmell *et al.* 2007), organic samples below a late Devensian till at Balglass Burn, central Scotland (Brown *et al.* 2007), woolly rhinoceros remains at Wilderness Pit, Bishopbriggs (Jacobi *et al.* 2009), reindeer antler and other organic remains at Sourlie (Jardine *et al.* 1988), lake detritus and organic deposits beneath a Late Devensian till at Tolsta Head, NE Lewis (von Weymarn & Edwards 1973; Whittington & Hall 2002), an aeolian sand unit between two tills at Garrabost, E Lewis (T8GABB02); shells beneath glacial deposits at Peicir, NW Lewis (Sutherland & Walker 1984) and glaciotectonized sand below a Late Devensian till at Suainebost Sands, also in NW Lewis (T8SUAI01, T8SUAI02, T8SUAI03). An ice free period in the Mid-Devensian (*c.* 38–32 ka) for parts of Scotland is consistent with numerical modelling results (Boulton & Hagdorn 2006; Hubbard *et al.* 2009; Patton *et al.* 2017), which indicate that the climate in Britain at this time was not conducive to extensive glaciation. It is also consistent with evidence from ice-rafted debris (Scourse *et al.* 2009).

31 ka. – Geochronological evidence for ice margin positions prior to 31 ka is patchy and has large uncertainties. We therefore start our reconstruction at 31 ka. The number of constraints at this time are still few, so we consider ice nourishment on high ground, guided by independent numerical model simulations (Hubbard *et al.* 2009; Patton *et al.* 2013b). In our optimum reconstruction we depict three centres of ice accumulation: central Scotland, Northern Ireland and Shetland. Glacigenic deposits on the continental slope indicate glaciation of the Minch at 30 ka (JC123-036PC). The advance of ice in this region at 31 ka is constrained by organics underlying glacial sediments at Tolsta Head, Lewis (Whittington & Hall 2002). Within uncertainty,

this age could either be ice free or ice covered at 31 ka. To satisfy this advance age and the evidence for shelf-edge glaciation at 30 ka, we place the extent of ice in this region just beyond the site of this age. Further north, glacigenic deposits on the West Shetland continental shelf break, beyond Otter Bank, suggest shelf-edge glaciation at approximately 30 ka (JC123-052VC). We therefore depict an ice margin advancing to this position. In Central Scotland, advance ages suggest that the margin is nearby or beyond Balglass Burn (Brown *et al.* 2007) and Wilderness Pit, Bishopbriggs (Jacobi *et al.* 2009). There is a lack of ages elsewhere constraining the build-up of ice at this time, notably in Northern Ireland and Shetland.

Our maximum extent reconstruction considers the presence of glacigenic debris on the upper continental slope (Sula Sgeir Fan, 036PC and Rona wedge, 052PC) adjacent to former ice stream tracks to indicate shelf-edge glaciation. Similarly, we take glacigenic material originating from Shetland in the Faroe-Shetland Channel to indicate shelf-edge glaciation north of Shetland (Becker *et al.* 2018). A lack of Norwegian material, and ages on ice advance within the NCIS, indicate that the BIIS was not confluent with the (FIS) at this time (Becker *et al.* 2018; Morén *et al.* 2018). Advance ages found in the Witch Ground Basin (Graham *et al.* 2010) and the Fladen Deep (Sejrup *et al.* 1994, reinterpreted in Sejrup *et al.* 2016) limit the extent of glaciation of the North Sea. In Northern Ireland, advance ages from the Ards Peninsula, County Down (Hill & Prior 1968) limit ice cover in the Irish Sea. A series of ages and sedimentological evidence that indicate the advance of the Irish Sea Ice Stream before a re-advance of mainland Irish ice constrain the extent of glaciation in southern Ireland during this time (Ó Cofaigh & Evans 2007). An advance age in Galway Bay (JC106-191VC) limits ice advance west of Ireland. Ice extent is limited in the Malin Sea by an advance age (JC106-116VC), and IRD evidence on the Barra-Donegal fan suggests that ice was not at or near the continental shelf until 27 ka (Scourse *et al.* 2009). Elsewhere, a lack of time constraints mean that we place the maximum ice-sheet margin at the limit of glacial material.

In our minimum extent reconstruction we consider the presence of glacigenic debris on the upper continental slope near the Minch (JC123-036PC) and Otter Bank (JC123-052VC) to require sediment delivery to the continental shelf break. We therefore place the ice-sheet margin halfway across the continental shelf at this time. In the Minch, minimum ice extent is limited by advance

Fig. 5. The empirical ice-sheet reconstruction at 26, 24, 21, 20, 17 and 15 thousand years ago. The optimum ice limits (white with blue boundary) represent the favoured interpretation of the underlying data incorporating all geological, geomorphological and glaciological soft knowledge. From these optimum positions, limits were advanced and shrunk as far they could go without contradicting an age constraint to build the maximum and minimum ice limits (see inset key). These define the uncertainty around the optimum position, with the true ice limit likely to lie within this zone. Note that changes in palaeotopography and coastline position are also reconstructed. The full 17 timeslices (31–15 ka) are available as a poster figure and slideshow in Data S3.
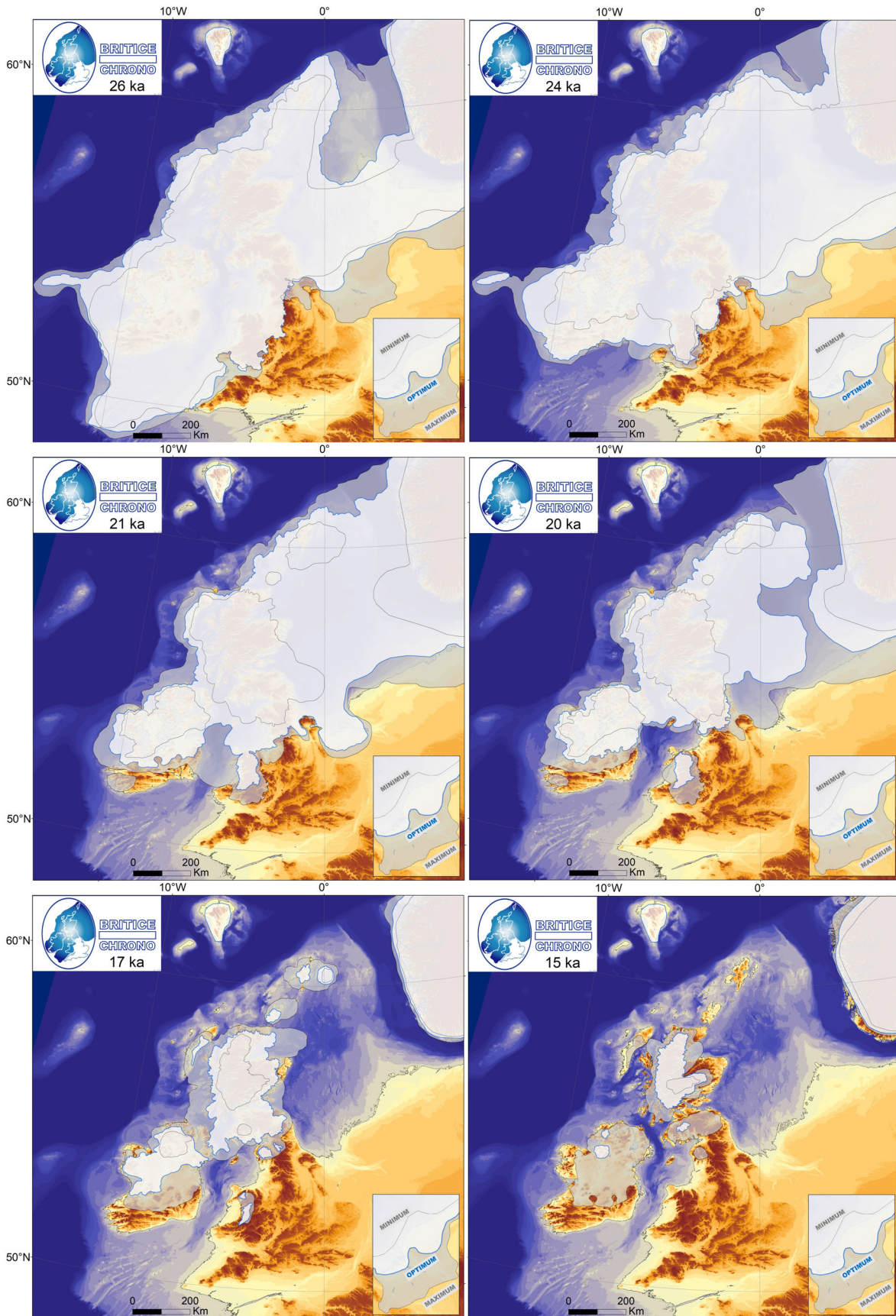
ages on Tolsta Head (Whittington & Hall 2002). The minimum extent of ice is also limited in central Scotland by ages at Wilderness Pit, Bishopbiggs (Jacobi *et al*. 2009) and Balglass Burn (Brown *et al*. 2007). In our minimum reconstruction ice masses are therefore limited to the high ground.

30 ka. – In the optimum reconstruction, we interpret glacigenic debris on the continental shelf break near the mouth of the Minch (JC123-036PC) and Otter Bank (JC123-052VC) to indicate shelf-break glaciation at this time. Geochronological ages no longer limit the advance of ice in these regions, such as at the Tolsta Head site, Lewis (Whittington & Hall 2002), at this time. The presence of ice-rafted debris from Shetland in the Faroe-Shetland Channel at 29 ka indicates that ice was advancing in this region (Becker *et al*. 2018). Ice advance likely occurred in Aberdeenshire, over the previously limiting ages reported by Gemmel *et al*. (2007). The advance of ice is limited south of the North Channel by ages on the Ards Peninsula, County Down (Hill & Prior 1968). Glacial lineations, erratic dispersal trains and glacially moulded bedrock indicate that ice from Britain advanced over northern and central Ireland (Greenwood & Clark 2009). There is a lack of geochronological constraint for this advance, but using inferences based on monotonic growth of the ice sheet we place this advance at 30 ka. In the Malin Sea and Hebrides, ice had yet to reach the continental shelf break (Scourse *et al*. 2009), but we advance the ice from its 31-ka position assuming monotonic growth and using the ice-flow pattern. In southwest Ireland, near County Kerry and County Cork, we depict a small ice cap due to the presence of well-developed cirques with low cirque floor altitudes (Barr *et al*. 2017) and with reference to numerical model experiments (Hubbard *et al*. 2009).

The maximum extent reconstruction conforms to the same constraints as at 31 ka, with two exceptions. In southwest Ireland we advance ice toward the limiting age in Galway Bay (JC106-191VC), but do not yet advance it onto the Porcupine Bank due to several limiting ages (JC106-158VC; JC106-167VC; JC106-177VC). In the Cheshire lowlands, ice could not have advanced over the site at Chelford (M. Bateman, pers. comm. reported in Hughes *et al*. 2016).

In the minimum extent reconstruction we depict ice at the continental shelf break in the Minch and Otter Bank regions. This is due to the presence of glacigenic debris on the continental shelf, indicating that the BIIS reached its maximum extent in this region at this time (JC123-036PC and JC123-052VC). Elsewhere we depict a slight advance of the ice, constrained by the same limiting ages as in 31 ka.

29 ka. – In the optimum reconstruction, ages recovered from cold water foraminifera on the Outer Minch shelf indicate the retreat of ice from the shelf break (JC123-

035PC). We assume a similar withdrawal of ice at Otter Bank, on the West Shetland shelf, but IRD evidence indicates that the BIIS was at the shelf break near Shetland (Becker *et al*. 2018). Ice from the Firth of Forth had yet to advance over the Fladen Ground Basin (Sejrup *et al*. 2016). In the southern portion of the North Sea, proglacial sediments deposited on a till (JC179VC) dated to 31.2±2.1 ka and overridden lake sediment that overlies a presumed MIS 2 till (150VC and 151VC), dated to 29.5±1.9 and 26.2±2.1 ka respectively, provide constraint on an early advance of ice. We assume growth of ice over high ground in northern England. In the North Channel, our reconstruction is limited in the Ards Peninsula, Northern Ireland, by an advance age (Hill & Prior 1968). For the rest of the Irish sector of the BIIS and the Kerry-Cork Ice Cap we assume monotonic advance. An absence of limiting ages for the rest of the offshore area from Ireland to the Minch means that we assume monotonic advance of the ice sheet between timeslices.

In the maximum reconstruction, ice advanced from its position at 30 ka in several regions. Using the oldest possible age, in the Cheshire lowlands, ice is no longer limited by the Chelford age (M. Bateman, pers. comm. reported in Hughes *et al*. 2016). We therefore reconstruct an ice sheet at the maximum extent. The advance age on the Ards Peninsula, County Down (Hill & Prior 1968) is no longer limiting. We therefore advance ice through the Irish Sea. But the BIIS has not yet advanced over the dated materials in southeast Ireland from Ó Cofaigh & Evans (2007). In the Bristol Channel, the maximum extent of glaciation is debated (Rolfe *et al*. 2012; Carr *et al*. 2017; Gibbard *et al*. 2017). Given this uncertainty, for this maximum reconstruction we therefore reconstruct an ice-sheet-filled Bristol Channel. Three ages limit shelf-edge glaciation along the western continental shelf. First, ice is limited in its position in Galway Bay by advance ages derived from foraminifera (JC106-190VC). Second, in Donegal Bay, shelf-edge glaciation is prohibited by advance ages derived from shells in diamict (JC106-112VC). Third, shell fragments within tills limit glacial advance in the Malin-Hebrides sector (JC123-125VC). We therefore use these sites as maximum positions for glaciation. Elsewhere, a lack of deglacial ages means that we place the maximum ice-sheet margin at the limit of known glacigenic material.

In the minimum reconstruction, ice-sheet retreat in the Minch occurred. Retreat ages derived from cosmogenic exposure dating suggest that Airgh na Goathie, Lewis, must have been ice covered at this time (T9AIR01), as well as Cape Wrath, NW Scotland (T8WRA01). The BIIS was at its maximum position across Shetland, so we reconstruct shelf-edge glaciation at this time. Ice cannot yet have advanced over Toddlehills, Aberdeenshire (Gemmell *et al*. 2007), or the Fladen Deep, North Sea (Sejrup *et al*. 2008), but we minimally reconstruct an

advancing ice sheet nearer to these locations at this time to reflect wider glaciation at a later stage. A lack of constraining data means that we do not place ice over Ireland and Wales in this minimum ice-sheet reconstruction.

28 ka. – In the optimum reconstruction, cosmogenic nuclide ages from North Rona indicate retreat of the Minch Ice Stream at this time (Everest *et al.* 2013). We assume that similar retreat occurs in the Otter Bank and Fair Isle regions. Radiocarbon ages from shells recovered from glaciomarine sediments on the shelf north of Shetland constrain retreat in this area (JC123-074VC and JC123-075VC). Ice was yet to advance over the Fladen Ground (Sejrup *et al.* 2016). Assuming that the 29-ka advance was short-lived, we place the isochrone at a mid-point in the southern North Sea. The advance ages from County Down (Hill & Prior 1968) are no longer limiting, so we depict an advancing ice sheet in the Irish Sea, consistent with Bayesian age sequence modelling (Chiverrell *et al.* 2013). In the absence of further constraints, we assume monotonic advance across the rest of Ireland, leading to a coalescence of the main Irish Ice Sheet and the Kerry-Cork Ice Cap, following the landform based reconstruction of Greenwood & Clark (2009). An advance age on the shelf between Galway Bay and Porcupine Bank limits the extent of ice in this western sector (JC106-190VC), leading us to propose a mid-shelf position in this sector. We assume monotonic advance in the Donegal Bay and Malin-Hebrides sector, but advance ages limit this to behind the continental shelf break (JC106-112VC and JC123-125VC). Based on the advance of more southerly marine sectors and the extent in the Minch, we place the maximum glaciation to the west of Lewis at this time, leaving St Kilda as an ice free region (after Ballantyne *et al.* 2017). Ice sheet-climate modelling suggests that conditions were favourable for a Welsh Ice Cap at this time (Patton *et al.* 2013a, b). Here we draw a small independent ice cap based upon the glaciation pattern and with influence from these numerical models.

In the maximum reconstruction, ice remains along the shelf break across the Minch and Otter Bank regions. We regard the ages at Foula to be nunataks, beyond the resolution of our reconstruction, at this time (Everest *et al.* 2013). North of Shetland, radiocarbon ages limit ice extent in this area (JC123-074VC and JC123-075VC). Ice cannot advance over the Fladen Ground (Sejrup *et al.* 2016). We depict a mid-shelf position of the NCIS, as evidence from IRD suggests that the NCIS had not reached the shelf break. Advance ages in southeast Ireland no longer limit ice extent here (Ó Cofaigh & Evans 2007), leading us to reconstruct a maximum ice sheet at the Celtic Sea shelf break. Advance ages limit our reconstruction on Porcupine Bank (158VC, 167VC, 177VC; Peters *et al.* 2016). Advance ages also limit the extent of ice in Donegal Bay (112VC) and onto the

Malin-Hebrides shelf break (125VC). Elsewhere, a lack of ice free ages means that we place the maximum ice-sheet margin at the limit of known glacigenic material.

In the minimum reconstruction, in accordance with the spatial rule and the optimum reconstruction, we depict an ice sheet at its maximum in the Lewis region. At this time, TCN ages on North Rona indicate that the Minch outer shelf was deglaciated (Everest *et al.* 2013), but ice-marginal ages on Lewis (Airigh na Goathie, T8AIR01) and Cape Wrath (T8WRA01) indicate that in the Minch the ice sheet was at least at a mid-shelf position. We depict a retreating minimum ice sheet in the Fair Isle and Otter Bank regions, but a marginal age west of Shetland (073VC) indicates ice still covered the shelf here. It is possible that ice advance may have taken place over Wester Rora (Gemmell *et al.* 2007), so we depict ice advance a few kilometres east of these ages. We slightly expand our ice sheet to cover the Ards Peninsula, County Down advance age (Hill & Prior 1968). A lack of constraints means that we use ice-sheet modelling results to reconstruct a plausible remainder of the margin to help us draw limits that reflect likely ice extents in relation to topography (Hubbard *et al.* 2009).

27 ka. – In the optimum reconstruction, we reconstruct monotonic retreat of the Minch Ice Stream and across the Fair Isle and Otter Bank regions, limited in the Minch region by the North Rona cosmogenic ages (Everest *et al.* 2013). Ice advance could not have yet taken place over the Witch Ground and Fladen basins (Sejrup *et al.* 2016). In the southern North Sea, ice-sheet advance is demarked by overridden glaciolacustrine sediments in the Dogger Bank region. We assume that this advance was coincident with a southerly coalescence of the BIIS and the FIS, with the FIS advancing through the Norwegian Channel. Given the proximity, we also reconstruct an advance to maximum extent in the Vale of York lobe during this time. In Cheshire, we also reconstruct an ice advance, but this is limited in extent by dated glacifluvial sands beneath a till (M. Bateman, pers. comm. in Hughes *et al.* 2016). The Welsh Ice Cap is assumed to have expanded at this time to coalesce with the BIIS in the Irish Sea and Cheshire lobe. In the southern Irish Sea and into the Celtic Sea, numerous ages and sediment provenance data from along the southern Irish coast constrain the advance of ice through the Irish Sea at this time (Ó Cofaigh & Evans 2007; Ó Cofaigh *et al.* 2012). On the west coast of Ireland, advance ages on the Porcupine Bank and outer Galway Bay Shelf lead us to reconstruct a grounded ice mass on the Porcupine Bank (JC106-158VC; JC106-191VC). We reconstruct this maximum extent as being coincident along the western continental shelf break through Donegal Bay and the Hebrides Ice Stream. This is supported by advance ages along the shelf break (JC106-112VC; JC106-115VC), later deglaciation ages inside of this limit (JC106-198VC; HC106-177VC; CE-08-018; JC106-

147VC), and IRD records (Scourse *et al.* 2009). We assume a retreated position of the ice sheet west of Lewis, in accordance with the reconstructed position in the Minch at this time.

In the maximum reconstruction, there are a few ages that prevent us from placing the ice sheet at its maximum extent. Ice did not advance over the Fladen Ground/ Witch Ground basins at this time (Sejrup *et al.* 2016). Shelf slope provenance data demonstrate that the NCIS was not at its maximum at this time (Becker *et al.* 2018). OSL ages also suggest an ice free enclave over Dogger-land (150VC). Elsewhere, we reconstruct an ice sheet at the maximum possible position, and given that we are aiming to document empirical uncertainty, we reconstruct an ice sheet at the maximum position in areas where the limit of ice during this time is contested (Rolfe *et al.* 2012; Ballantyne *et al.* 2017; Carr *et al.* 2017; Gibbard *et al.* 2017).

In the minimum reconstruction, the Minch Ice Stream has retreated beyond the northern tip of Lewis (T8AIR01–03), yet Cape Wrath is yet to deglaciate (T8WRA01). Radiocarbon ages from cold water for-aminifera, closely associated with glacial sediments, indicate that the west of Shetland remained glaciated until 23.8±0.3 ka (JC123-073VC). We therefore reconstruct ice cover across this site and assume ice cover was continuous between Shetland and mainland Scotland. Ice had yet to advance over the Fladen and Witch Ground Basins (Sejrup *et al.* 2016). Given the expansion of ice elsewhere at this time, we reconstruct an enlarged ice sheet in the southern North Sea, across northern Wales and through the Irish Sea. Several advance ages constrain 27 ka to be the maximum extent of ice across the western continental shelf from Ireland to the Hebrides (JC106-112VC; JC106-115VC; JC106-198VC; HC106-177VC; CE-08-018; JC106-147VC; JC106-158VC; JC106-191VC). Following our minimum reconstruction logic, a lack of constraints means that in this minimum reconstruction ice had retreated from the shelf west of Lewis.

26 ka. – In the optimum reconstruction, the Minch Ice Stream had retreated from its 27-ka position, to include an ice free region in northern Lewis (T8AIR01–03). A mid-shelf position along the Otter and Fair Isle regions is reconstructed, consistent with a deglaciated North Rona and later deglacial ages landward (T8WRA01–04; JC123-073VC). Ice is yet to advance over the Fladen Ground (Sejrup *et al.* 2016), but we continue to reconstruct coalescence between FIS and BIIS in the southern North Sea. In the Dogger Bank-Wash area, we reconstruct ice advance near to the Sandsend site, which was ice covered prior to 23.0 ka (Roberts *et al.* 2013a, b). Ice still dammed Lake Humber during this time and the Vale of Pickering was impounded by ice in our reconstruction. We reconstruct a small advance in the Cheshire lobe region. At this point, Bayesian age sequence modelling

suggests that ice reached its maximum extent in the Celtic Sea, with the presence of glacigenic sediments on the shelf break having been found (Praeg *et al.* 2015; Scourse *et al.* 2019; JC106-012VC). Mega-scale glacial lineations found in Liverpool Bay record part of the bed imprint of a phase of activity of the Irish Sea Ice Stream (Van Landeghem & Chiverrell 2020). A slight retreat of ice on the Porcupine Bank is reconstructed, due to the presence of ice free ages in the Slyne Trough (JC106-198VC); this may be the timing of ice-shelf formation and degrounding of ice through the Trough (Peters *et al.* 2016). A slight retreat of ice across the western Irish continental shelf is reconstructed, with retreat of the northern section of the Hebrides Ice Stream recorded by dated ice proximal sediments (JC106-147VC). Retreat west of Lewis also occurred at this time (Peacock *et al.* 1992).

In the maximum reconstruction, ice is at its maximum extent for the majority of the ice sheet. This includes the advance of ice over the Fladen Ground to glaciate the northern North Sea. The ice sheet was not at its maximum west of Lewis, due to the deglacial ages of Peacock *et al.* (1992). Ice had also retreated from the continental shelf north of Shetland (JC123-074VC; JC123-075VC). Postglacial sediments also indicate that ice retreated from the eastern edge of Dogger Bank (JC123-151VC). Elsewhere, we reconstruct an ice sheet at the maximum possible position.

In the minimum reconstruction, the Minch Ice Stream had retreated enough to uncover Ard Bheag Bhragar on Lewis (T8ABB01–04) and Cape Wrath (T8WRA01–04). The shelf immediately west of Shetland was yet to deglaciate (JC123-073VC), and we reconstruct an ice-covered Shetland and Orkney Isles. To account for the lake deposits in JC123-150VC and JC123-151VC on Dogger Bank, a confluence of the FIS and BIIS in the southern North Sea is reconstructed in order to impound a glacial lake. Our reconstruction includes a greater cover of ice over Wales, coinciding with the maximum extent of ice in the Celtic Sea. We reconstruct an ice sheet that has withdrawn from Porcupine Bank, consistent with dated ice proximal sediments in Slyne Trough (JC106-198VC; JC106-177VC). Further north, in Donegal Bay, the margin is constrained by dated foraminifera in two cores: JC106-103VC indicates ice free conditions at this time, whilst JC106-101VC indicates that ice is yet to have retreated from this area, leading us to reconstruct a mid-shelf position between the two cores. A retreated mid-shelf position is also reconstructed for the Hebrides-Malin Ice Stream (JC106-147VC).

25 ka. – In the optimum reconstruction, we assume monotonic retreat of the ice margins of the Minch, Fair Isle, Otter and Shetland sectors. The BIIS had not yet advanced over the Fladen Ground (Sejrup *et al.* 2016), but we assume advance of the NCIS at this time. In the southern North Sea we assume monotonic retreat. We

reconstruct an advance of ice in the Cheshire region, and a concurrent expansion of ice over Wales, where we reconstruct ice at its maximum limit. In the Celtic Sea, cosmogenic nuclide dating and optically stimulated luminescence dating on the Isles of Scilly indicate ice free conditions at this time (Smedley *et al.* 2017b). Further evidence for the BIIS retreating in this area is found in shell remains closely associated with glacial sediments found near the Celtic shelf edge (JC106-012VC). Sediments on Porcupine Bank indicate multiple re-advances at this time (JC106-167VC), with older deglacial ages further offshore (JC106-158VC), and thus we place the margin at a retreated overall position for this timeslice. In Donegal Bay, for the Hebrides-Malin Ice Stream and west of Lewis, we reconstruct monotonic retreat.

In the maximum reconstruction, the BIIS had retreated in the Minch region, as recorded by the retreat ages on the northern part of Lewis (T8AIR01–04), and on Rona (Everest *et al.* 2013). We reconstruct an expanded ice free sector west of Lewis to coincide with this, and the ages of Peacock *et al.* (1992). We reconstruct an ice free Dogger Bank, coincident with the timing of the Dogger Lake (JC123-150VC; JC123-151VC). The BIIS also retreated in the Celtic Sea (Smedley *et al.* 2017b and JC106-012VC). Elsewhere, we reconstruct an ice sheet at the maximum possible position.

In the minimum reconstruction, the Minch Ice Stream is pinned between the north of Lewis (T8ABB01–02) and Cape Wrath (T8WRA01–04), with mainland Lewis (T8BRA01–03; T8UB01–04; T8ISL01–02) and the Orkney Isles (Phillips *et al.* 2008) yet to deglaciate. Ice cover extends to Shetland (JC123-073VC), but ice is yet to cover the Fladen Basin (Sejrup *et al.* 2016). Confluence of the BIIS and the FIS is reconstructed, in order to dam the Dogger Lake (JC123-150VC; JC123-151VC). Lake Humber is also dammed to the north at this time (Murton *et al.* 2009). In Cheshire, we reconstruct an ice-sheet advance over Cherry Orchard Farm (T3COF3) and expand the neighbouring Welsh Ice Cap to its maximum extent. Under a minimum interpretation, numerous sites indicate an ice free Celtic Sea and southern Ireland (Ó Cofaigh *et al.* 2012; Smedley *et al.* 2017a; Scourse *et al.* 2019; JC106-045VC; T4WEXF03; T4CSP01), with the Irish Sea Ice Stream pinned between the Llyn Peninsula (T4NEF03; T4CEIF02) and Wicklow Mountains (T4WIK01–02). Deglaciation of the Porcupine Bank is indicated by dated foraminifera on the Galway Bay mid-shelf (JC106-190VC). In Donegal Bay, we reconstruct a slightly retreated ice sheet, behind dated ice proximal sediments (JC106-102VC), but covering later deposited sediments (JC106-101VC). Proglacial deposits (T7ALTB02) and cosmogenic ages at Malin Head (T7MH02–04) indicate that northwest Ireland was yet to deglaciate. We therefore reconstruct a Malin-Hebrides Ice Stream that covers Malin Head and two sites on the mid-shelf (JC106-154VC; JC106-151VC).

24 ka. – In the optimum reconstruction, the Minch Ice Stream had now retreated beyond northern Lewis (T8SKIG01–02) and Cape Wrath (T8WRA01–04). We assume monotonic retreat between northern Scotland and Shetland. The coalescence of the BIIS and FIS had now covered the Fladen Deep (Sejrup *et al.* 2016), and we reconstruct an advance of the Norwegian Channel Ice Stream (NCIS) limited in extent by advance ages in the Tampen region (Rokoengen *et al.* 1982). A minor advance in the southern North Sea is also reconstructed, to account for the depositional sequence north of Dogger Bank (JC123-155VC). We reconstruct ice advance through the Cheshire Lowlands, consistent with advance ages in the region (M. Bateman, pers. comm. in Hughes *et al.* 2016) and to account for later deglacial ages (T3BORR01–03; T3BRID01–04). Cosmogenic nuclide ages (Phillips *et al.* 1994) are consistent with radiocarbon ages (Hedges *et al.* 1994) which indicate a retreat of ice from southwest Wales. This, and evidence from southern Ireland (T4CSP01–03), constrain the position of the Irish Sea Ice Stream. Withdrawal of ice from southern Ireland at this time is consistent with the later southern Irish re-advance (Ó Cofaigh & Evans 2007; Ó Cofaigh *et al.* 2012). We also reconstruct a separate Kerry-Cork Ice Cap at this time, consistent with ice free ages in southern central Ireland (Woodman *et al.* 1997) and an early deglaciation of this region indicated from exposure dating of the interior (Barth *et al.* 2016). In the Porcupine Bank region, we reconstruct ice-shelf regrounding, consistent with the sedimentological record (Peters *et al.* 2016) and multiple ages that demonstrate that the Slyne Trough was ice free at this time (JC106-199VC; JC106-198VC). In Donegal Bay, we reconstruct a slightly retreated ice sheet, behind dated ice proximal sediments (JC106-102VC), but covering sediments interpreted to have been deposited at a later age (JC106-101VC). The ice margin in the Malin-Hebrides region is constrained by ice free ages from several cores (JC106-146VC; JC106-147VC), and later deglacial ages further inland (JC106-154VC; JC106-151VC).

In the maximum reconstruction, there is no change to ice extent in the Minch. At Otter Bank, we reconstruct ice retreat of ~15 km from the shelf edge (JC123-056VC). A similar magnitude of retreat is reconstructed on the continental shelf west of Shetland (JC123-073VC). There is no change to reconstructed ice extent west of Shetland, the NCIS, or southern North Sea. In Cheshire, we reconstruct a slight retreat of ice, consistent with Bayesian age sequence modelling (Chiverrell *et al.* 2021). Ice retreat in the Irish Sea is constrained by cosmogenic nuclide ages at Carnsore Point (T4CSP01). Porcupine Bank remains ice covered in this scenario. Ice retreat is reconstructed in Donegal Bay to the mid continental shelf (JC106-102VC).

In the minimum reconstruction, the ice in the Minch had retreated further, exposing Geireadha Mor, Lewis (T8GEI02). Ice retreat occurred west of Shetland (JC123-073VC). Ice advance occurred over the Fladen Deep (Sejrup *et al.* 2016), which we assume corresponds to a mid-shelf position of the NCIS. This corresponds to the deposition of Dogger Bank Lake sediments (JC123-150/151). No change in ice extent is reconstructed in the southern North Sea. A small ice retreat is reconstructed across the Pennines, which is mirrored in Cheshire (OSL ages from Bradleys Sand Pit; Chiverrell *et al.* 2021) and North Wales. There are few constraints west of Galway Bay, leaving us to assume a mid-shelf position, which covers marginal ages that are unlikely to have yet been exposed (JC106-180PC). In Donegal Bay, ice had retreated further (JC106-101VC), exposing the mid-shelf. Ice also retreated to expose Malin Head (T7MH02–03). We reconstruct a concurrent small retreat of the Hebrides Ice Stream, but ice had yet to retreat to the shore (JC106-151VC) and covered Mingulay (T7MIN02–07).

23 ka. – In the optimum reconstruction, we assume monotonic retreat from the Minch to western Shetland. North of Shetland, we reconstruct an ice advance (JC123-075VC; JC123-074VC). Though these ages record ice free conditions at 28.3 and 29.8 ka, respectively, we consider these to be loose constraints on ice advance and 23 ka to be the most glaciologically plausible time for ice advance in the area, as this is coincident with the NCIS reaching the shelf-break (Becker *et al.* 2018), and overriding the Tampen ridge (Rokoengen *et al.* 1982). In the southern North Sea, we reconstruct ice retreat over the glaciotectonically elevated protuberance of Dogger Bank (Roberts *et al.* 2018), whilst along the east coast of England, we depict a small advance toward Dimlington (Penny *et al.* 1969). We assume monotonic advance across Yorkshire and the Pennines. In Cheshire, Bayesian age sequence modelling places the margin to most likely be nearby the Wood Lane site (Shfd14033/14034; Chiverrell *et al.* 2021). We assume monotonic retreat of ice around Wales. In the Irish Sea, we reconstruct an ice limit further north that exposes the Screen Hills site. A series of ages also indicate retreat across southern Ireland (Woodman *et al.* 1997; Bowen *et al.* 2002; Ballantyne & Stone 2015). At this time, we also reconstruct a separation of the main ice sheet from the Kerry-Cork Ice Cap. This is supported by evidence from MacGillicuddy's Reeks of ice thinning in this region at this time (Barth *et al.* 2016). Concurrent with this separation, we place a minor advance on the south coast of Ireland, to explain advance ages from Ballycroneen Strand, County Cork, attributed to the expansion of inland ice (Ó Cofaigh *et al.* 2012). West of Galway Bay, ice retreated from the continental shelf break. Monotonic retreat is assumed along the west coast of Ireland, apart from Donegal Bay

where a mixture of offshore and onshore ages constrains the ice position. Ice proximal marine clays and silts indicate that ice is yet to leave the offshore region (JC106-099VC). Onshore, sites to the south of the bay were ice free at this time (McCabe *et al.* 2007a, b; Brockhill Quarry, Shf15013). On the continental shelf to the west of the Hebrides, two offshore sites record ice stream retreat (JC106-151VC; JC106-153VC). Monotonic retreat between timesteps is assumed to the west of the Outer Hebrides.

In the maximum reconstruction, the ice margin in the Minch retreated onshore in two locations – the north of Lewis at Port Na Skigersta (T8SKIG) and Cape Wrath (T8WRA01–04). There is no change at this time in the margin position near Shetland or in the Norwegian Channel Ice Stream. Similarly, the maximum reconstruction remains the same for the southern North Sea to Wales. In the Irish Sea, we reconstruct a small retreat of the ice stream margin, consistent with Bayesian age sequence modelling (Scourse *et al.* 2021). At this time, we also reconstruct the separation of the Cork-Kerry Ice Cap from the main ice sheet (Woodman *et al.* 1997; and Barth *et al.* 2016), as well as a re-advance on the southeast coast of Ireland (Ó Cofaigh *et al.* 2012). On the west coast of Ireland, the maximum limit had retreated from Porcupine Bank, due to nearby ice free ages that must be exposed in the subsequent timeslice (JC106-190VC). To the south of Donegal Bay, data indicate that ice must have been onshore (McCabe *et al.* 2007a, b), but in the centre of the bay we reconstruct an ice limit near to ice proximal laminated clays and silts (JC106-101VC). The southern portion of the Malin-Hebrides ice stream complex remains at the shelf break, but there is some retreat to the north (JC106-136VC; 139VC; 142VC). The ice position remains unchanged to the west of the Outer Hebrides.

In the minimum reconstruction, we assume monotonic retreat in the Minch region and west of Shetland. The NCIS is reconstructed to have reached its maximum extent at this time (Becker *et al.* 2018). In the southern North Sea, we reconstruct an advance of the lobe along the east of England (often called the 'North Sea Lobe'), impounding Glacial Lake Pickering, to anticipate that the maximum extent is reached in the subsequent timestep. In Cheshire and Wales we depict monotonic retreat, consistent with Bayesian age sequence modelling. In the Irish Sea, the reconstruction places the margin on Anglesey (McCarroll *et al.* 2010). In the absence of further evidence, monotonic retreat is assumed across southern Ireland. The ice margin remains the same in Donegal Bay. In the Malin Sea sector, ice retreated onshore, following the OSL and TCN ages from County Antrim (Shfd 15017; T7CAR). Toward the Hebrides, ice has retreated across a number of sites from the mid-shelf (JC106-149VC; 151VC; 154VC), but remains covering the Outer Hebrides (T7MIN; T7SGU; T8ISL; T8RUB).

22 ka. – In the optimum reconstruction, the Minch Ice Stream continued to retreat, exposing Geireadha Mor (T8GEI). Monotonic retreat is assumed along the Orkney–Otter Bank region. West of Shetland, we reconstruct a minor re-advance (JC123-073VC; Bradwell *et al.* 2019). We reconstruct ice retreat to the north of Shetland, uncovering the site of Ross (1997). Although not expressed in our reconstructed isochrones it could be that the ages of JC123-073VC and in Ross (1997) were part of a widespread re-advance north of Shetland. Monotonic retreat is assumed in the NCIS. In the southern North Sea, our optimum reconstruction places ice at its maximum extent, reaching Norfolk and Lincolnshire (after Evans *et al.* 2018a). The maximum extent of the York Lobe (Vale of York Ice Stream) is assumed to be contemporaneous. In Cheshire, our reconstruction continues to show ice retreat, using the position noted in the Bayesian age sequence model of Chiverrell *et al.* (2021). Monotonic retreat is assumed for the Welsh Ice Cap, which remains attached to the main ice sheet. In the Irish Sea, we reconstruct an ice stream that is beginning to bifurcate, based on sea floor geomorphology (Van Landeghem *et al.* 2009; Van Landeghem & Chiverrell 2020). Toward the east, retreat is recorded from OSL dating at Bryn-yr-Eryr (T4BRYN02) and at Anglesey (McCarroll *et al.* 2010). On the western side of the Irish Sea, numerous ages constrain retreat, the closest of which are the OSL ages of deltaic deposits at Ballyhorsey (T4BHOR02) and TCN dating of striated bedrock on the Hill of Howth, Dublin (T4HOH). This retreat is also consistent with TCN dating of a meltwater channel at Wicklow Head (T4WIK), an erratic at Bray Head (T4BRY), and the exposure of the Wicklow Mountains (Ballantyne *et al.* 2006). Monotonic retreat is assumed around much of the rest of Ireland, with no further direct constraints at this time. Near the Malin Sea, TCN dating at Bloody Foreland records ice retreat onshore at this time (Ballantyne *et al.* 2007), with ice stream retreat also recorded further east at Malin Head (Bowen *et al.* 2002) and Corvish (McCabe & Clark 2003). The Hebrides Ice Stream also continued to retreat, with its margin position constrained by TCN dating at Carnan Mor (T7CAR; Small *et al.* 2017a). Monotonic retreat is assumed for the remainder of the Outer Hebrides.

In the maximum reconstruction, the ice margin remains the same in the Minch and across the continental shelf of northwest Scotland. We depict a slight retreat toward north Shetland, constrained by the age in Ross (1997). The NCIS remained at the continental shelf break. There is no change in margin position in the southern North Sea, across Yorkshire and the Pennines. In Cheshire, we reconstruct a slight retreat of the Cheshire lobe, consistent with the upper age limits of Bayesian age sequence modelling (Chiverrell *et al.* 2021). In the Irish Sea, we reconstruct a slight retreat of ice, corresponding to the onshore emergence of the

Blackstairs Mountains (Ballantyne & Stone 2015). The Cork-Kerry ice cap is also reduced in size at this timeslice (Barth *et al.* 2016). On the continental shelf west of Galway Bay, we reconstruct ice retreat of approximately 30 km, uncovering dated ice proximal glaciomarine sediments (JC106-190VC). There is only a minor change in maximum position near Donegal Bay, uncovering OSL ages from a second onshore site at Glenulra Quarry (McCabe *et al.* 2007a, b; Shfd 15712). Three ages constrain retreat of the Malin-Hebrides sector (JC123-125VC; JC106-151VC; JC106-154VC). Due to these constraints, and to be glaciologically plausible, we also depict retreat of ice to the west of the Outer Hebrides.

In the minimum reconstruction, ice in the Minch is depicted to have retreated to uncover OSL samples from the site at Garrabost (T8GABB). Ice is also assumed to have retreated onshore in northern Scotland, but still covers the Orkney Isles (Phillips *et al.* 2008). This is the first timeslice in which separation of the BIIS and FIS over the North Sea occurs. This conforms to ages north of Shetland (Ross 1996), in the Witch Ground Basin (Sejrup *et al.* 1994) and in Aberdeenshire (Phillips *et al.* 2008). Note that these have amber and red quality ages according to the scheme of Small *et al.* (2017b). This is the timing of maximum extent in the southern North Sea, with ice extending to Norfolk and along the east coast of England (Evans *et al.* 2018a). For simplicity, we also interpret this to be the maximum extent of the Vale of York Lobe. The Welsh Ice Cap is reconstructed to be independent (Hedges *et al.* 1996; T4ABER), but still covering the interior high ground of Snowdonia (Glasser *et al.* 2012). In the Irish Sea, ice is reconstructed to have uncovered part of the Cumbrian coastline to conform with cosmogenic and OSL ages (T3BC; T3GUTT) and on the Isle of Man (Thomas *et al.* 2004; Thrasher *et al.* 2009; T3CREG). We reconstruct ice retreat across southern and central Ireland. The Cork-Kerry Ice Cap is presumed to have deglaciated into small mountain glaciers at this time (Barth *et al.* 2016). Ice is reconstructed to be on the Arran Islands in Galway Bay (T5IM). Ice is onshore in part of Donegal Bay, but the nearby high ground contains a number of sites that had yet to be exposed (Wilson *et al.* 2019). We depict retreat across the north coast of Northern Ireland (T7ROS; T7CAR; T7GLEN), but assume that the Scottish and Irish ice sheets remained attached. Monotonic retreat is assumed for the Hebrides Ice Stream. No change in margin position is reconstructed in the Outer Hebrides.

21 ka. – In the optimum reconstruction, we reconstruct monotonic retreat of the Minch Ice Stream, with Ard Bheag Bhragar to the west of Lewis exposed at this time (T8ABB). Monotonic retreat is assumed for the NW Scottish continental shelf. North of Shetland, we reconstruct a minor re-advance, consistent with Ross (1997). Monotonic retreat is assumed for the NCIS. In the southern North Sea and east of England, we reconstruct

retreat from the maximum position. The margin position is consistent with OSL dating (155VC; Thorestthorpe; North Ferriby; Sandsend; Bateman *et al.* 2018; Evans *et al.* 2018b). Glacial Lake Humber is presumed to be dammed at this time (Murton *et al.* 2009). In Cheshire, ice had retreated to near the present-day shoreline, exposing the site at Tremeirchion Caves (Rowlands 1971). We reconstruct monotonic retreat of the Welsh Ice Cap, depicting that attachment still occurred with the Irish Sea Glacier. The margin in the Irish Sea had retreated to a position constrained by the ages of McCarroll *et al.* (2010), which were ice free, and OSL ages at Aberogwen, which suggest ice cover persisted. The southern tip of the Isle of Man is now reconstructed to be ice free (T3CREG). A number of sites in eastern Ireland also record ice free conditions at the time, including TCN and OSL ages at the Hill of Howth and Howth Delta (T4HOH; T4HOW), TCN ages at Bray Head (T4BRY), Wicklow Head (T4WIK), and the Wicklow Mountains (Ballantyne *et al.* 2006). We reconstruct monotonic retreat across southern Ireland and a reduction in size of the Kerry-Cork Ice Cap. Ice to the west of Galway Bay is presumed to have been at a mid-shelf position at this time. Monotonic retreat is assumed for much of the west coast of Ireland. TCN ages at Bloody Foreland (Ballantyne *et al.* 2007), Malin Head (Bowen *et al.* 2002) and radiocarbon ages at Corvish (McCabe & Clark 2003) were uncovered at this time. The position of the Hebrides Ice Stream is constrained by TCN dating on Carnan Mor (T7CAR). Monotonic retreat is assumed for the remainder of the Outer Hebrides.

In the maximum reconstruction, the Minch Ice Stream has retreated off the northern tip of Lewis (T8GEI). There are no changes along the remainder of the northwest continental shelf or the NCIS. In the southern North Sea, ice must have retreated from its maximum position, with OSL ages registering exposure (JC123-155VC; Bateman *et al.* 2018). In Cheshire, we depict a slight ice retreat, conforming to the OSL ages at Wood Lane (Shfd14033). Ages also limit the southern margin of the Welsh Ice Cap (Phillips *et al.* 1994). In the Irish Sea, we reconstruct ice retreat, consistent with the maximum estimates of Bayesian age modelling (Scourse *et al.* 2021). Ice must also have exposed Slievenamon in southern Ireland (Ballantyne & Stone 2015). No other constraints exist for this maximum reconstruction across the rest of Ireland at this time. For the Hebrides Ice Stream we reconstruct retreat beyond a sea floor radiocarbon age (JC106-149VC). Elsewhere we keep the ice margin position the same.

In the minimum reconstruction, we reconstruct an ice limit covering the TCN age at Rainish (T8RAI01). Due to TCN ages at Morven (Phillips *et al.* 2008), we reconstruct a separation of the main Scottish Ice Sheet from a remnant ice cap over the Orkneys. Using the logic of a minimum reconstruction, we also depict a separate Shetland Ice Cap at this time, with the northern margin limited by a TCN age (Bradwell *et al.* 2021a). The

position of the lobe down the east coast of England is constrained by OSL ages at Seaham (Sea14; Roberts *et al.* 2019). In England, ice has retreated in the Stainmore Gap (Davies *et al.* 2019), and south of the Lake District (Telfer *et al.* 2009). We also reconstruct separation of Scottish and Irish ice at this time, due to a lack of constraints to the contrary. For the remainder of Scottish ice, retreat occurs in the Hebrides Ice Stream, but numerous sites are yet to be deglaciated along the Scottish coast (Peacock 2008; T7TMC) and Outer Hebrides (T7SGU; T8ISL; T8RUB). The separate Irish Ice Sheet is limited in extent by ages near Kilkeel (McCabe & Haynes 1996; McCabe & Clark 1998; Clark, Gibbard *et al.* 2004; McCabe *et al.* 2005), in Galway Bay (T5KSW; T5BH01; JC106-180PC), at Claddaghuff (T5CL), the Ox Mountains (Clark *et al.* 2009), Malin Beg (Ballantyne *et al.* 2007) and Poisoned Glen (T7PG).

20 ka. – In the optimum reconstruction, the Minch Ice Stream continued to retreat (T8GABB), and we presume monotonic retreat across the rest of the continental shelf toward Shetland. We reconstruct the splitting of the FIS and BIIS over the North Sea at this time. This timing is based on marine foraminifera found in the southern North Sea, which have been dated to 19.9 ka (JC123-137VC) and 19.6 ka (JC123-132VC), and is supported by ages from the Fladen Deep (Graham *et al.* 2010). Our interpretation follows that of Sejrup *et al.* (2016), that the ice sheets split apart either side of the Ling Bank channel, leading to a rapid drainage of the Dogger Lake (Hjelstuen *et al.* 2017). The margin in the southern North Sea retreats at this time away from the Lincolnshire and Norfolk coasts (JC123-132VC), exposing the site at Seaham (Sea14; Roberts *et al.* 2019). We presume this leads to a similar retreat of the York Lobe, and further west the ice margin position is constrained by the Norber Erratics in the Yorkshire Dales (Vincent *et al.* 2010). Ice had now retreated from the Cheshire Basin and Liverpool Bay (T3BRAD; T4ABER; T3BC02; T3GUTT), leaving an independent Welsh Ice Cap, where we presume monotonic retreat has occurred. In the Irish Sea, retreat had exposed the Isle of Man (Thomas *et al.* 2004; Thrasher *et al.* 2009; T3JURB; T3TURK; T3BAL), and with the margin position on the east coast of Ireland constrained by ice free ages at Kilkeel Steps (Clark, Gibbard *et al.* 2004, Clark, McCabe *et al.* 2004). Along the southern margin of the Irish Ice Sheet, we assume monotonic retreat. In Galway Bay, the ice margin has retreated to the Aran Islands (T5IM), with monotonic retreat assumed along the rest of the west of Ireland. On the Malin Sea coast, TCN ages from boulders indicate exposure at this time (T7ROS), whilst there is a small re-advance at Corvish (McCabe & Clark 2003). We assume an ice limit to the south of the Armoy Moraine at this point in time, with occupation from the north occurring later (Knight 2004). This margin position is supported by nearby OSL ages from

Antrim (T7CAR; T7GLEN), which indicate that the ice margin must have been nearby to expose higher ground. For the rest of the ice sheet, we assume that monotonic retreat had occurred.

In the maximum reconstruction, there is no change to the margin position in the Minch or Otter Bank sectors. Retreat occurred west (JC123-073VC) and north (Ross 1996) of Shetland. The NCIS remained at the shelf break. For the purpose of this maximum reconstruction, the marine forams found in the southern North Sea (JC123-137VC) are treated as ice free ages only (e.g. their wider implications for opening up of the North Sea to marine conditions are treated as uncertain). Retreat occurred along the east coast of England (Sand13). The Welsh Ice Cap became independent in this maximum reconstruction, with ice retreat to the North Yorkshire Moors (Vincent *et al.* 2010), and is depicted to be as large as possible given the constraining data (Rowlands 1971; Phillips 1994; Hedges *et al.* 1996; T4ABER). Across the Irish Sea, the ice margin is constrained by ages from Cumbria (T3BC), the Isle of Man (Thrasher *et al.* 2009) and the Killkeel Steps (Clark, Gibbard *et al.* 2004, Clark, McCabe *et al.* b). Sites along the west coast of Ireland also limit the maximum ice extent (T4HOH; T4HOW; T4BRY; T4WIK; T4GREY; Ballantyne *et al.* 2006). There was no change in the maximum limit along the southern coast of Ireland. We assume a smaller Cork-Kerry Ice Cap (Barth *et al.* 2016). The limit in Galway Bay assumes a shallow lobe, with the Aran Islands as nunataks (T5IM). There is a small retreat of ice around Donegal Bay (McCabe 1986; McCabe *et al.* 2005; JC106-099VC). Ice reached the modern shoreline in the Malin Sea sector (Bowen *et al.* 2002; Ballantyne *et al.* 2007; T7FAWN). There is no change for the remainder of the ice sheet.

In the minimum reconstruction, the Minch Ice Stream had retreated, leading to a separate ice cap over Lewis, given ages nearby that indicate deglaciation in the following timeslice (Stone *et al.* 1998; T8ISL). We depict a smaller Orkney Ice Cap, with the interior yet to deglaciate (Phillips *et al.* 2008). The Shetland Ice Cap had also shrunk (JC123-092VC). The margin position of the Scottish-English Ice Sheet had retreated toward modern coastline in many locations, leaving a few tidewater glacier outlets (McCabe *et al.* 2007a, b; Phillips *et al.* 2008; Livingstone *et al.* 2015; Davies *et al.* 2019; Roberts *et al.* 2019; JC123-118VC; T7TMC). For the Irish Ice Sheet, retreat occurred to expose known sites on the east coast (McCabe & Clark 1998; McCabe *et al.* 2007a, b) and west coast (Ballantyne *et al.* 2008; Clark *et al.* 2009). However, the margin position is mainly fixed by sites yet to be deglaciated (McCabe & Haynes 1996; T5OU; Clark *et al.* 2009; T7PG).

19 ka. – In the optimum reconstruction, retreat occurred in northern Lewis (T8BRA), and we assume monotonic retreat across the Minch Ice Stream. Mono-

tonic retreat is also assumed across much of the Otter Bank and Shetland sectors. North of Shetland, TCN ages indicate ice retreat (Bradwell *et al.* 2021a). There was also ice retreat on the continental shelf east of Shetland, recorded at the Viking Bank site (Peacock 1995). We assume monotonic retreat across the east coasts of Scotland and England, apart from the North Sea Lobe along the east coast of England, where a re-advance occurred (JC132-144). Ice retreat continued across England (Telfer *et al.* 2009; Vincent *et al.* 2010; Davies *et al.* 2019). We assume monotonic retreat in the Irish Sea. On the east coast of Ireland, Cooley Point (McCabe & Haynes 1996) and Port were ice free (McCabe *et al.* 2007a, b) prior to a later re-advance. We assume monotonic retreat for the south and much of the west of Ireland. Near Donegal Bay, there was a withdrawal of ice from the Ox Mountains (Clark *et al.* 2009). Ice has also retreated from Corvish (McCabe & Clark 2003), Carey Valley (T7CAR) and Glenshesk Valley (T7GLEN), along the Malin Sea coast toward the North Channel. We assume that the reoccupation of the Armoy moraine from the north (Knight 2004) happened at around this time, but have no direct evidence for the timing of this event. We assume monotonic retreat across the Hebrides at this time. The Welsh Ice Cap is also depicted to have been smaller, consistent with TCN ages from the interior that indicate thinning (Glasser *et al.* 2012) and marginal ages (Glasser *et al.* 2018).

In the maximum reconstruction, OSL and TCN ages limit the extent of ice on Lewis (T8ABB; T8GAB). Ice had also retreated to the north of Scotland, toward Orkney (JC123-049VC). There was no change in margin position near Otter Bank and west of Shetland. Retreat is depicted to the north and northeast of Shetland, due to the deglacial ages of the Viking Bank (Peacock 1995). The NCIS has also retreated, with sea floor ages demarcating the margin (Morén *et al.* 2018). There is no change in the margin position across the southern North Sea, although in the Vale of York, ice retreat is required to satisfy data on the location of Glacial Lake Humber (Murton *et al.* 2009). No change in margin position is reconstructed across the Irish Sea, the south of Ireland, or for the Welsh Ice Cap. We assume the Cork-Kerry Ice Cap had deglaciated at this time (Barth *et al.* 2016). In Galway Bay, our margin position is consistent with the Bayesian age sequence modelling (Ó Cofaigh *et al.* 2021), but there is no change in margin position for the remainder of the west of Ireland. On the Malin Sea coast, Corvish was now ice free (McCabe & Clark 2003). Retreat in the Hebrides sector must also have occurred at this time (T7CAR; T7MIN).

In the minimum reconstruction, the Lewis Ice Cap had reduced in size (T7SGU). We also depict smaller Orkney and Shetland ice caps (T1DAL). Retreat occurred across Scotland (Stone *et al.* 1998; Everest & Kubik 2006; Phillips *et al.* 2006, 2008; Ballantyne *et al.* 2009), and England (Livingstone *et al.* 2015; Davies *et al.* 2019;

T3ALD), with the Lake District depicted as a separate ice cap at this time. In Ireland, retreat occurred at Cooley Point and Port (McCabe & Haynes 1996; McCabe *et al.* 2007a, b), but Linns and Rathcor Bay remained ice covered (McCabe *et al.* 2005). To reconstruct a plausible margin, much of the ice margin throughout midland Ireland remains similar to the previous times-lice. On the west coast, ice retreated from three locations in Galway (T5KK; T5OU; T5IE) and through Furnace Lough (Clark *et al.* 2009).

18 ka. – In the optimum reconstruction, ice had retreated across Lewis and the Minch (T8ISL; T8RAI). There was also retreat between Scotland and Orkney (Phillips *et al.* 2008), with our reconstruction showing ice still joined to Orkney at this time. We reconstruct the separation of the Shetland Ice Cap at this time, due to TCN ages in southern Shetland (T1DAL). Retreat occurred along the east coasts of Scotland and England (Hall & Jarvis 1989; JC123-118VC). This uncovered two sites that were difficult to reconcile with the broader data, even given the specified dating uncertainty (Lunan Bay, McCabe *et al.* 2007a, b; Momond Hill, Phillips *et al.* 2008). Retreat occurred through central England (Livingstone *et al.* 2015; Davies *et al.* 2019; T3ALD). At this time, we reconstruct contrasting behaviour in two adjacent outlets of the Irish Ice Sheet. A re-advance occurred over Cooley Point and Port sites (McCabe & Haynes 1996; McCabe *et al.* 2007a, b) whilst retreat occurred to uncover the Cranfield Point site (McCabe & Clark 1998). Furnace Lough in western Ireland deglaciated at this time (Clark *et al.* 2009). Nearby, we reconstruct a re-advance of ice into Donegal Bay from the south (Benetti *et al.* 2010), as this is the first time that there is space to accommodate this geomorphological imprint. Two sites in the Hebrides sector also become ice free in our reconstruction at this time (T7TMC; T7SGU). For the rest of the ice sheet we assume monotonic retreat occurred.

In the maximum reconstruction, ice had retreated on Lewis and in the Minch (T8BRA; T8RAI), but remained in the same location from Otter Bank to the north of Shetland. East of Shetland, and in the NCIS we depict ice retreat (JC123-092VC; Sejrup *et al.* 1994). Ice remained joined to the FIS, but there was retreat in the southern North Sea toward Scotland (JC123-111VC; JC123-118VC; Hall & Jarvis 1989). Retreat also occurred across the Stainmore Gap (Davies *et al.* 2019). We depict further ice retreat through the Irish Sea, due to deglacial ages on the Isle of Man (Thomas *et al.* 2004). Much of the eastern and southern Irish Ice Sheet margin remained the same. To the west, we now depict retreat behind the Aran Islands (T5IM) and in Donegal Bay (CE-08-004), which we assume leads to retreat across the rest of western Ireland. For the Malin and Hebrides Sector, the ice margin remained the same. We also depict retreat of the Welsh Ice Cap at this time, due to thinning ages in Snowdonia (Glasser *et al.* 2012).

In the minimum reconstruction, ice caps in the Lake District, Lewis (T8RUB) and the Orkneys (Phillips *et al.* 2008) were now absent. The Shetland Ice Cap is depicted to have retreated to the high ground of Shetland (T1GFIR; Bradwell *et al.* 2019). To explain offshore ages that produced consistent ages of 16 ka (Peacock & Long 1994; JC123-088VC; JC123-089VC), we are forced to invoke a separate Pobie Bank Ice Cap to the east of Shetland, which may have persisted longer, but is depicted here in the minimum reconstruction. For the Scottish-English Ice Sheet sector, ice had retreated in the northwest (T8CLA), but has yet to deglaciate the fjords (Ballantyne *et al.* 2009). Ice was also yet to deglaciate from the Moray Firth (Hedges *et al.* 1988) and reach the modern shoreline along parts of the east coast (JC123-128VC). The Tyne gap was mostly deglaciated (Livingstone *et al.* 2015) and ice remained in southwest Scotland (Ballantyne *et al.* 2013). We now depict a much reduced Irish Ice Sheet, with much of central Ireland becoming ice free (T5MOY01). Ice here is restricted to an ice cap that reached the northwest coast (Watson *et al.* 2010), had just deglaciated the east coast (McCabe *et al.* 2005), but covered high areas such as the Blue Stack Mountains (T6BSM).

17 ka. – In the optimum reconstruction, the retreat of ice in the Minch had left behind an ice cap over the higher ground of Lewis. Orkney also became an independent ice cap at this time (Phillips *et al.* 2008). In Shetland, we depict separation of ice into two separate ice caps, one on mainland Shetland and a hypothesized Pobie Bank Ice Cap to the east. This is due to retreat in east Shetland (T1OSW01) and sea floor ages of 16 ka to the east (Peacock & Long 1994; JC123-088VC; JC123-089VC). Ice was mostly constrained to outer portions of the fjords in northwest Scotland, with retreat from Clashnessie occurring at this time (T8CLA). We assume monotonic retreat of ice across the Northern Highlands, with retreat in northeast Scotland recorded at the Hill of Yarrows (Phillips *et al.* 2008). Along the east coast, the ice margin was mostly above the modern-day shoreline, with our reconstruction hinging on ages at Pitfichie (Phillips *et al.* 2008), Inchcoonans Claypit (Peacock & Browne 1998), Gallowflat (McCabe *et al.* 2007a, b) and offshore (JC123-128VC). At this point, we separate ice at the Lake District from the main ice sheet, following the reconstruction of Livingstone *et al.* (2015). This is also the time of the Scottish re-advance to the north of the Lake District (T3ALD) and across to Ireland (McCabe & Clark 1998), potentially reaching the Armoy Moraine (Knight 2004). At this time, we reconstruct a separate Irish Ice Sheet, with the margin constrained by ages at Rathcor Bay and Linns on the east coast (McCabe *et al.* 2005). At this time, we also reconstruct ice retreat from Rossaveel (T5OU), Kilkeiran (T5KK) and Claddaghuff (T5CL) in west Ireland. There is also retreat from the re-advance into Killala Bay (Benetti *et al.* 2010), at

Anaffrin (Ballantyne *et al.* 2008) and from the Ox Mountains (Clark *et al.* 2009). The margin position of the Welsh Ice Cap is constrained by ages from Glasser *et al.* (2018). We also reconstruct a margin position close to Poisoned Glen (T7PG). Elsewhere monotonic retreat is presumed.

In the maximum reconstruction, we reconstruct separate ice caps over Orkney and Shetland, due to TCN ages north of the Highlands (Phillips *et al.* 2008) and southern Shetland (T1DAL). The Shetland Ice Cap is also constrained by TCN dating to the north of Shetland (Bradwell *et al.* 2019). The Welsh Ice Cap is also reduced in size from the previous maximum timeslice. For the main ice sheet, retreat occurred along the east coast of mainland UK (Phillips *et al.* 2008; Roberts *et al.* 2019; JC123-128VC). Ice retreat occurred through the Tyne Gap (Livingstone *et al.* 2015) and north of the Lake District (T3ALD). We reconstruct a slight retreat over the Irish Sea, coinciding with limiting ages at Cooley Point (McCabe & Haynes 1996) and Port (McCabe *et al.* 2007a, b). Retreat also occurred to the west of Ireland, at Inner Galway Bay (JC106-180PC; JC106-184PC), Claddaghuff (T5CL), Lough Accorymore (Ballantyne *et al.* 2008), Furnace Lough (Clark *et al.* 2009) and the Ox Mountains (Clark *et al.* 2009). Elsewhere the ice margin remains the same as the previous timestep.

In the minimum reconstruction, we no longer reconstruct ice over Shetland, but a possible Pobie ice cap remains (Peacock & Long 1994; JC123-088VC; JC123-089VC). We reconstruct a separate ice cap in southern Scotland (Ballantyne *et al.* 2013), and a smaller ice cap covering higher ground in Ireland (T6BS). The Scottish Ice Sheet is also reduced in size, limited mostly to the Highlands. Ice free locations were at Slioch (Fabel *et al.* 2012), Rassay North (T8RAA), Strollamus (Small *et al.* 2012), Hawthornhill (Browne *et al.* 1983) and Gallowflat (McCabe *et al.* 2007a, b). Other areas toward the centre of the highlands were yet to become ice free.

16 ka. – In the optimum reconstruction, the Orkney (Phillips *et al.* 2008) and Pobie Bank (Peacock & Long 1994; JC123-088VC; JC123-089VC) ice caps are now absent, with only minimal ice remaining on mainland Shetland (T1PAP, T1HAM, T1GFIR). We also depict a smaller ice cap over Lewis, deglaciation of the Pennines, and a reduced Lake District Ice Cap (consistent with Wilson *et al.* 2018). We also reconstruct deglaciation of Wales at this time, due to cosmogenic nuclide dating of marginal moraines and thinning rates (Glasser *et al.* 2012, 2018). On the west coast of Scotland, the ice sheet is now reconstructed to be mostly confined to the fjords. From north to south, retreat is recorded by ages in the Inner Minch (JC123-013VC; JC123-015VC), on the Isle of Skye (Stone *et al.* 1998; T8RAB; T8RAA; Small *et al.* 2012), the inner Hebrides (Small *et al.* 2017a) and Arran (Finlayson *et al.* 2014). We assume monotonic retreat for the eastern margin of

the Scottish Ice Sheet at this time, with cosmogenic nuclide ages in the Moray Firth region taken to be loose constraints on retreat timing (Phillips *et al.* 2008). We reconstruct retreat of the Irish Ice Sheet to higher ground at this time, but with few dating constraints.

In the maximum reconstruction, Orkney had now deglaciated (Phillips *et al.* 2008), an independent ice cap had formed over the Lake District, and a Welsh Ice Cap persisted (Glasser *et al.* 2012, 2018). The main Scottish-Irish Ice Sheet is still conjoined in this maximum reconstruction. Ice retreat occurred in Lewis (T8ISL; T8RUB) and across the Minch to the northwest of Scotland (JC123-017VC; T8CLA; JC123-015VC; JC123-013VC). The eastern margin is constrained by two sets of radiocarbon ages in close agreement (Hedges *et al.* 1989; Peacock 2003; McCabe *et al.* 2007a, b). The Tyne Gap must have deglaciated at this time (Livingstone *et al.* 2015). We presume a small retreat in the Irish Sea and for the southern margin of the Irish Ice Sheet sector. In the west of Ireland, ice extent is limited by TCN ages in Galway (T5MOY). Poisoned Glen in the north also limits the maximum ice margin at this time (T7PG). The margin is constrained by two sites in the Hebrides (T7TMC; T7SGU).

In the minimum reconstruction, ice is now absent from Ireland, constrained by deglacial ages on the high ground of the Blue Stack Mountains (T6BSM). The Southern Uplands had also deglaciated (Ballantyne *et al.* 2013). A reduced Scottish Ice Cap is depicted, the position of which is mostly influenced by the distribution of high ground and a few dated sites. Limiting sites are centred around the Monadhliath Mountains (Sissons & Walker 1974; Gheorghiu *et al.* 2012) and the northwest of Scotland (T8LKAN; Stone *et al.* 1998; Bradwell *et al.* 2008a; Ballantyne *et al.* 2009). Ages from the interior and higher ground suggest that even in our minimum reconstruction, Scotland cannot be ice free at this time (Golledge *et al.* 2007; Fabel *et al.* 2012).

15 ka. – In the optimum reconstruction, we depict deglaciation of Lewis and the Lake District. A remnant ice cap is shown in the Southern Uplands, adjacent to the TCN ages of Ballantyne *et al.* (2013). Two small ice caps are depicted over high ground in Ireland, limited by TCN ages of 14.8 ka in the Blue Stack Mountains (T6BSM) and consistent with the reconstruction of Wilson *et al.* (2019). Ice in Scotland was now restricted to the high ground. The margin is limited by ages on the northwest coast, which show retreat in the Loanan Valley (Bradwell *et al.* 2008a), to the Achiltibuie Moraine (Bradwell *et al.* 2008a; Ballantyne *et al.* 2009), toward Sail Mhor (Bradwell *et al.* 2008a), to the Cnoc Breac Moraine (Everest *et al.* 2006), and to the Redpoint and Applecross moraines (Ballantyne *et al.* 2009). The southern margin is constrained by radiocarbon dating sites, the closest and most reliable of which are at Inchinnan (Browne *et al.* 1977), Wester Fulwood (Bishop & Dickson 1970) and Boquhapple (Holloway

et al. 2002). The ice margin in east Scotland is limited by TCN ages from the Monadhliath Mountains (Gheorghiu *et al.* 2012), radiocarbon dating of Loch Etteridge (Sissons & Walker 1974), and is in broad agreement with other nearby TCN ages (Everest & Kubik 2006; Ballantyne *et al.* 2009).

In the maximum reconstruction, Wales had been deglaciated (Glasser *et al.* 2012, 2018). We show the possibility of ice remaining in the Lake District (Wilson *et al.* 2018) and a large separate ice cap over the Southern Uplands (this does not contradict the range of ages from Ballantyne *et al.* 2013). This is separate from the main Scottish Ice Cap, to accommodate a suite of radiocarbon ages (Bishop & Dickson 1970; Peacock 1971; Browne *et al.* 1977; Browne & McMillan 1983; Holloway *et al.* 2002). Radiocarbon dating of Loch Etteridge (Sissons & Walker 1974) limits ice extent north of the Monadhliath Mountains, which we assume led to ice retreat across the eastern margin of the Scottish Ice Cap. To the west, we depict an independent Lewis Ice Cap, as Skye must have been ice free at this time (Stone *et al.* 1998; T8RAB; T8RAA; Small *et al.* 2012). Otherwise, the dating from northwest Scotland allows for an ice cap, which filled the fjords in this maximum reconstruction. Its extent is limited in the southwest by ages from the Inner Hebrides (Small *et al.* 2017a; Peacock 2008) and Arran (Finlayson *et al.* 2014). The Irish Ice Sheet also became separate at this time; the most pertinent site for limiting this is the radiocarbon ages on Rathlin Island (Carter 1993). Given the lack of dating from central Ireland, a large ice cap is still possible, with the margin constrained only by ages in County Clare (T5BH), the Ox Mountains (Clark *et al.* 2009), Donegal (Ballantyne *et al.* 2007) and radiocarbon ages from Lough Nadourcan (Watson *et al.* 2010). Ages of 15.3 ka BP in iceberg turbate from Galway Bay (Callard *et al.* 2020) suggest that at least for some outlet valleys that ice was still marine-terminating and discharging icebergs.

Given the difficulty in inferring the persistence of ice, as a minimum reconstruction at this time, we reconstruct only a small ice mass over the central Scottish Highlands. All other ice masses are assumed to have disappeared as a minimum constraint.

Model reconstruction of ice-sheet extent, flow geometry and thickness

Our preferred reconstruction of the ice sheet is shown in Fig. 6. We regard this as being the most physically realistic simulation of the ice sheet to date; it combines ice-sheet modelling and the empirical evidence in a single reconstruction. It does this by using physics of ice flow and mass balance, using the PISM ice-sheet model, nudged to fit the empirically defined ice margins (Fig. 5) and with an ice thickness optimized to match relative sea-level constraints (see Method of model reconstruction). Nudging of the model was aimed to get margins to approximately the positions of the optimum ice extents, thereby satisfying our dating constraints and geological soft knowledge, but where model physics required the margin was allowed to deviate from these positions as long as it remained within the minimum and maximum constraints from dating. The simulation satisfied these criteria for all timeslices apart from four (27, 26, 25 and 18 ka), where in some marine sectors it underran the empirically defined minimum extent (see later). For the other 13 timeslices we mostly achieved a near perfect match, or with modelled margins within 30 km of the optimum ice extents. The velocity distribution, ice divides, ice streams and ice shelves are not prescribed, and emerge from the modelling. Because nudging of the model specifically focused on matching the extent of the main ice sheet, any ice caps that emerged are useful predictions that naturally arose from the climate forcing required to generate the main ice sheet. For clarity in the model reconstruction (Fig. 6) we annotate those sectors where the simulation underran the minimum extent, a safe interpretation being that in these places we favour the empirical evidence and suggest that there might be processes or feedbacks missing in the modelling. section heading is called Mismatches in the empirical and model reconstructions. It should be remembered that our method of reconstructing ice extents at 1-ka timesteps means that although more granular oscillatory behaviour (e.g. centennial and millennial scale oscillations) might have existed, it is not reconstructed here. Even though such oscillations are known to exist in climate records from Greenland ice-cores, and which we used to drive our ice-sheet modelling (see Method of model reconstruction), such changes are not prominent in the modelled reconstruction, these are not prominent in the modelled changes. This is likely to be due to a combination of reasons: our method of nudging the model to fit the more granular (1 ka) timesteps likely dampened them out, or the climate may have been cold enough for brief warm episodes to have little effect. Different, more dynamic modelling approaches, free from empirical

---

Fig. 6. The BRITICE-CHRONO model reconstruction combining the physics of ice-sheet modelling with the geomorphological, geological and chronological data on ice limits and glacio-isostatic mass loading. The ice-sheet model was nudged to fit the empirical reconstruction presented in Fig. 5 and with ice thickness optimized to match ice loading history in relative sea level records. Contours record elevation of the ice-sheet surface (500-m contour interval). Ice shelves predicted by the model are shown in grey. The changes in palaeotopography and coastline position were reconstructed by glacio-isostatic adjustment modelling. At four timeslices (27, 26, 25 and 18 ka) the modelled ice margin, in places, underran the minimum ice extent identified in the empirical reconstruction. These places are annotated by a star and with a black line marking the minimum extent that should have been attained. A poster of this figure, a slideshow and a movie are available in Data S4 and on which it will be easier to visualize the detail. Evolution of palaeotopographies and coastline positions are also available in Data S5 for the period 14 to 6 ka.
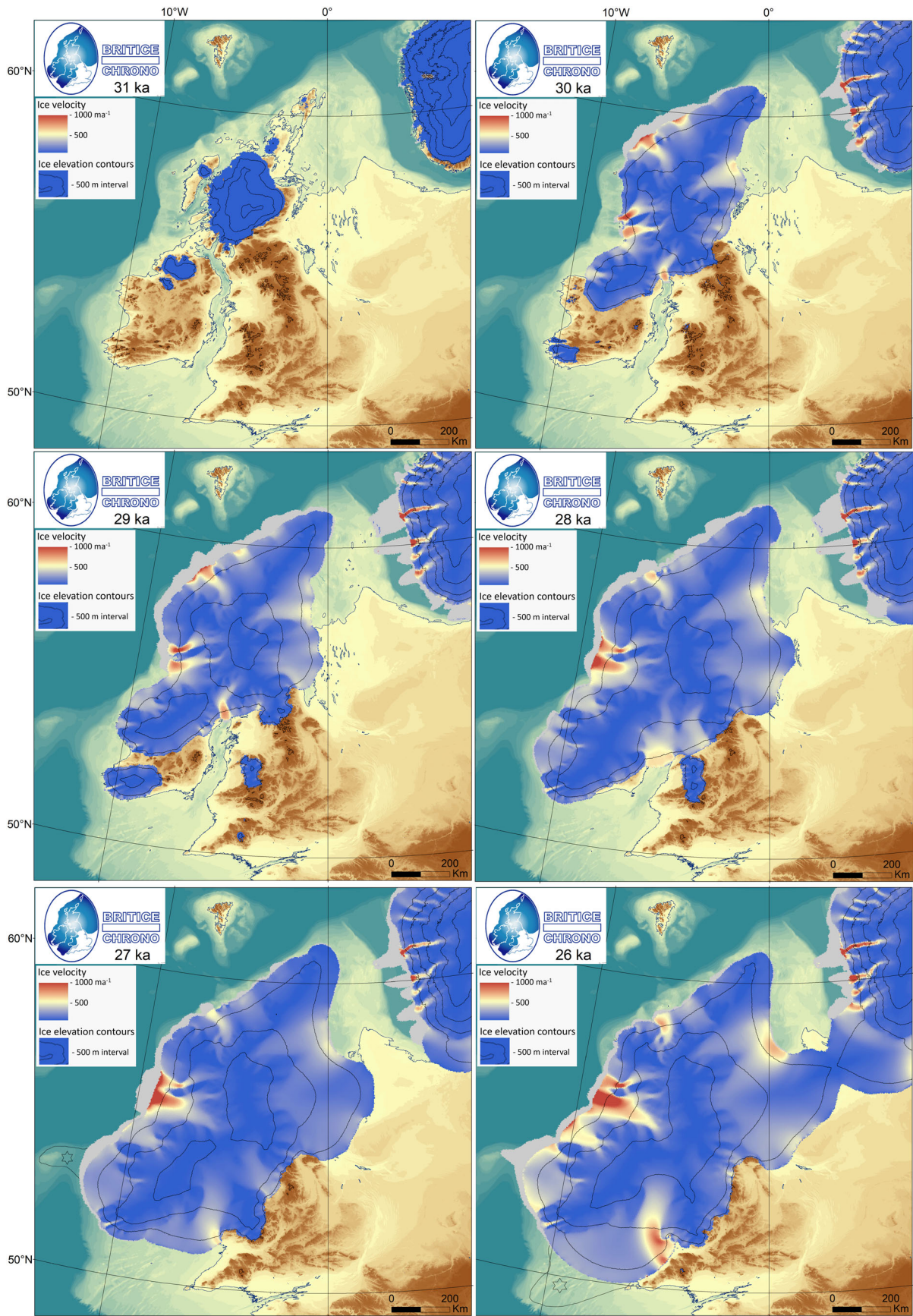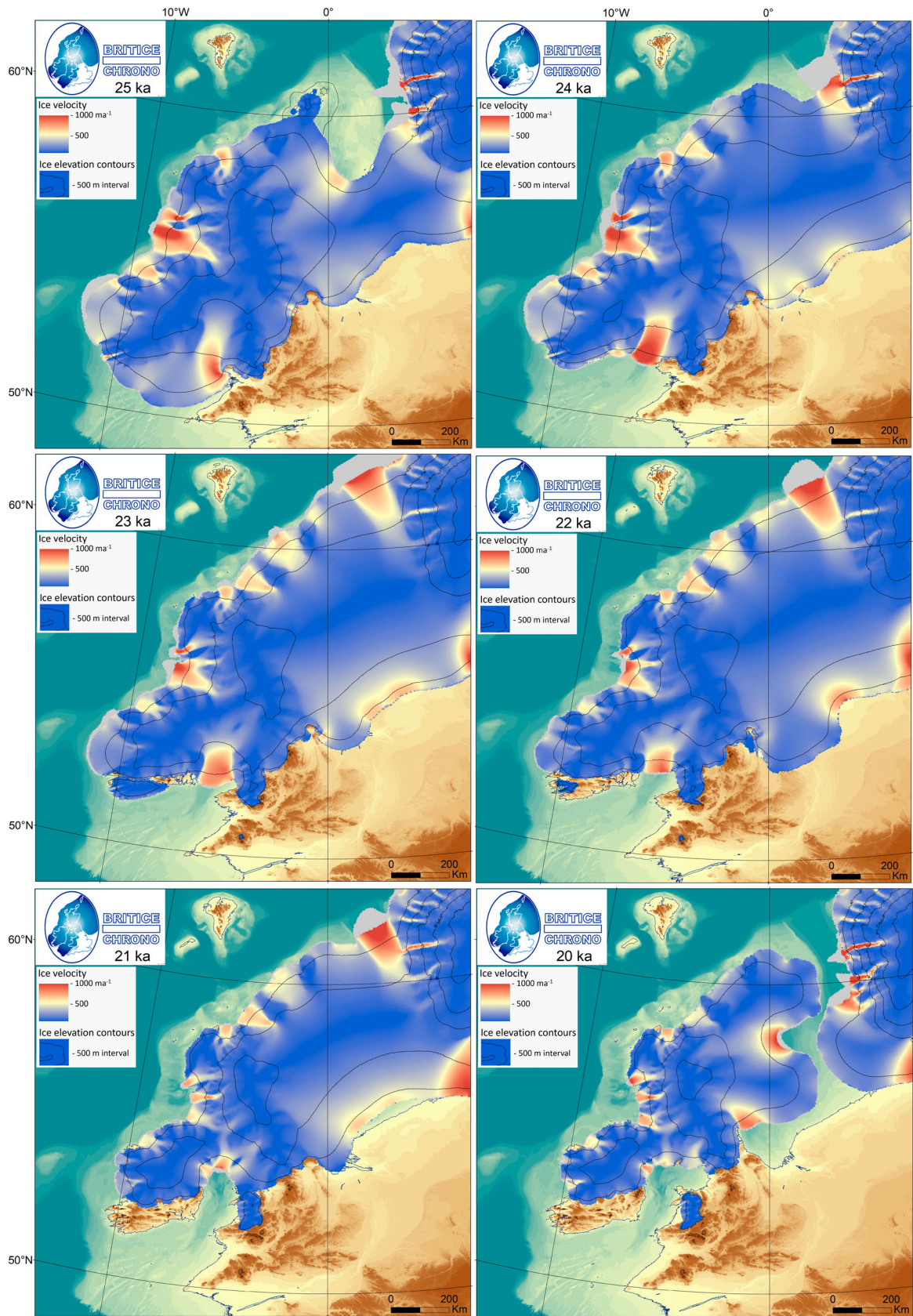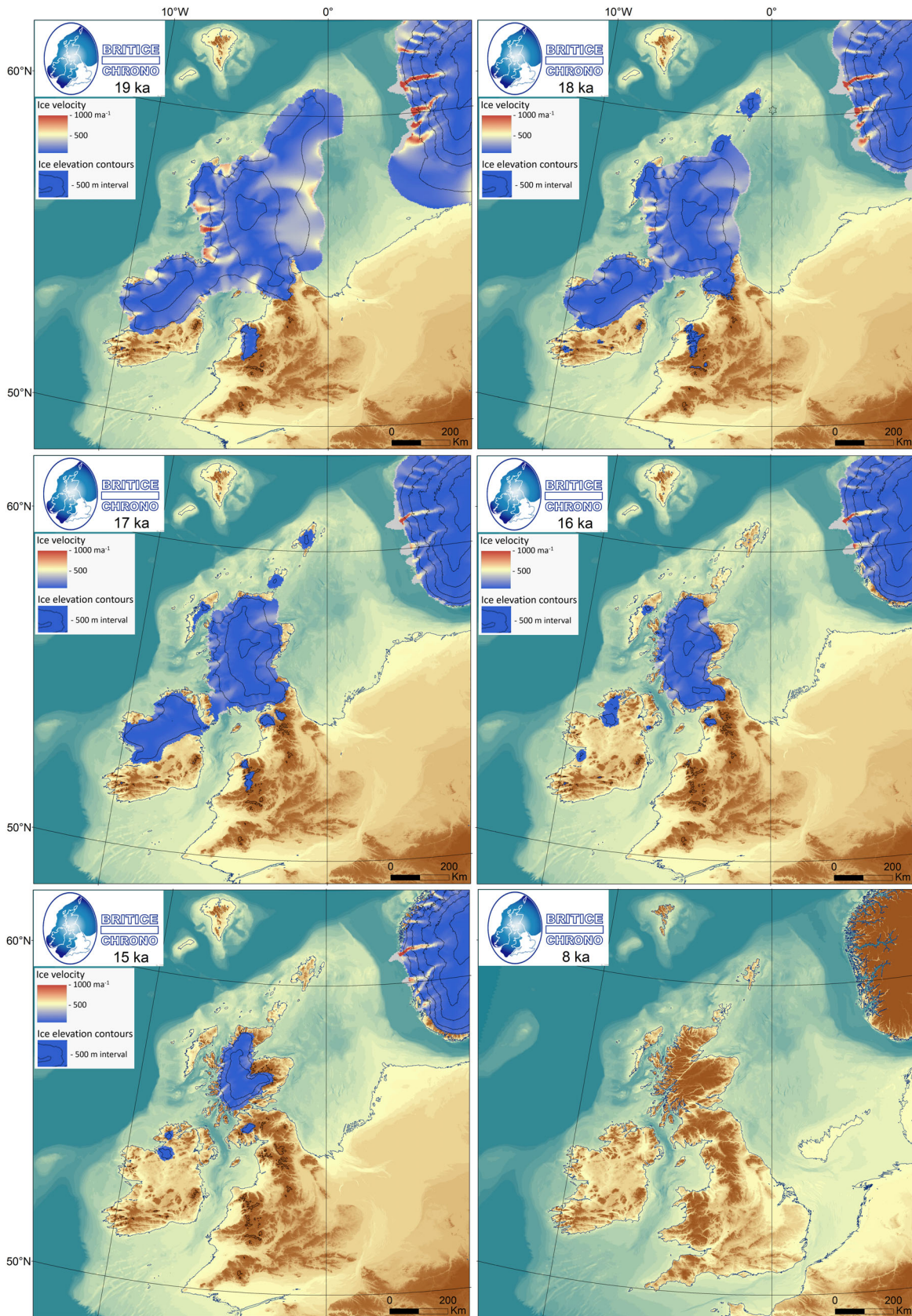
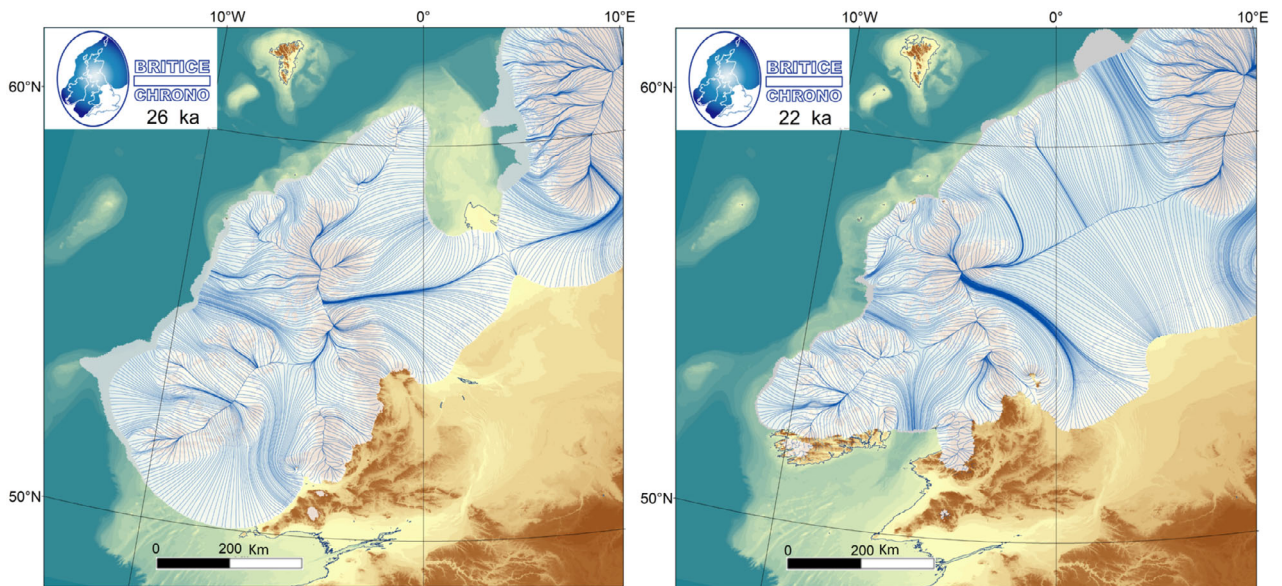*Fig. 6.* Continued.

Fig. 6. Continued.

Fig. 7. Ice-sheet extent and flow geometry (ice shelves in grey) at the maximum areal extent of the British–Irish Ice Sheet (left panel; 26 ka) and North Sea Ice Sheet (right panel; 22 ka). Build-up of ice over the North Sea occurred by head-on collision of British and Scandinavian ice lobes (left panel; 26 ka) resulting in an ice saddle that rapidly grew in elevation to build the major North Sea Ice Divide (1500 m thick) by 22 ka.

data, would be required to explore these effects more fully.

By 31 ka the Highlands of Scotland nourished a large ice cap reaching a kilometre thick and with a summit elevation of around 1500 m. It extended westwards to cover most of the Inner Hebridean islands. Ice caps grew at this time on Lewis, Arran, Orkney and Shetland. In the Southern Uplands of Scotland and in upland areas of England and Wales, ice fields and independent glaciers are predicted. These are found in the Cheviots, much of the North Pennines and the higher fells of the Lake District, on the hills of Snowdonia and the Berwyns, on Plynlimon, the Brecon Beacons and Black Mountains, and including areas as far south as Dartmoor (cf. Evans *et al.* 2012). In Ireland, a large ice cap existed reaching a summit elevation of 1000 m and spanning from the Derryveagh to the Sperrin Mountains. Ice fields and glaciers are predicted on the Wicklows, Iron and Dartry Mountains, the Mournes, and as far south as MacGillicuddy's Reeks and Knockmealdown Mountains. Apart from crossing small marine inlets in western Scotland, ice was entirely terrestrially based, with sea level much lower than today and with England part of the European landmass.

Rapid ice growth resulted in merging and fast expansion of most of the ice masses mentioned above, which by 30 ka gave rise to establishment of the combined BIIS. Major ice domes existed over the Grampian Mountains of Scotland (>1500 m ice elevation) and over Northern Ireland (>500 m). Shetland and Orkney were now part of the main ice sheet. In the south of Ireland a series of ice caps existed, reaching over 500 m in elevation and with ice margins nearly reaching the coastline in the south-

west. The main BIIS had thickened and advanced enough to spread out over the sea floor as grounded ice and it was now a truly marine influenced ice sheet, with over 80% of its margin terminating in seawater. Large ice streams had become established. The largest and fastest drained along the Minch in NW Scotland with its grounding line near the continental shelf edge, and which the model predicts to have terminated in an ice shelf. The ice stream is reconstructed as over 500 m in thickness and attaining velocities of 800 m a^{-1}. Other major ice streams existed in the Sea of Hebrides, south of Barra, and in the North Channel between Ireland and Scotland. By 29 ka the main ice sheet expanded further, notably eastwards into the North Sea and further south in Ireland. Upland ice masses in Wales had now coalesced to make a large autonomous Welsh Ice Cap, and ice had thickened over Dartmoor into an ice cap. Ice had reached beyond the coastline in SW Ireland yielding a long marine-terminating margin.

By 28 ka, Ireland was now almost completely covered by ice and a large Welsh Ice Cap was connected to the main ice sheet, soon to be subsumed in the next timestep. The largest ice stream was that draining west across the Malin Sea, discharging into an ice shelf. This 60-km-wide ice stream is reconstructed as reaching 800 m in thickness and attaining velocities exceeding 1000 m a^{-1}. Two major dynamic changes were initiated: the Irish Sea Ice Stream became established and commenced its rapid grounding line advance southwards; and a large ice lobe emanating from the Firth of Forth started a rapid advance eastwards across the North Sea, which was terrestrially exposed at this time. According to the modelling, fringing ice shelves existed along the entire

western and northern margins of the ice sheet. Grounded ice extending from Norway spread west as floating ice shelves across the trough of the Norwegian Channel, lightly grounding on its western bank. Ice shelves depicted here should be treated with caution because the modelling did not include tidal forcing, which in reality would have acted to limit the size of many ice shelves (cf. Scourse *et al.* 2018); additionally, the processes of ocean melt and calving remain uncertain and are highly parametrized in the modelling.

At the ice sheet's westernmost margin an ice shelf is predicted to have grown westwards from 27 to 26 ka, and as far west as the Porcupine Bank. In some model runs the shelf is thick enough to ground on the Bank leading to the growth of an autonomous Porcupine Ice Cap, perhaps better considered as an ice rise similar to those that occur when Antarctic ice shelves locally ground on the sea floor. Geological evidence for this happening is reported in Ó Cofaigh *et al.* (2021), but in our preferred model run presented here (Fig. 6, and see annotation at 27 ka) the Porcupine Ice Cap never quite emerges, even though it did in some model runs (Fig. 9).

The ice sheet continued increasing in overall size and by 26 ka confluence occurred between the British and Scandinavian ice sheets. This happened over the terrestrially exposed Great Fisher Bank, with ice margins north of here less able to advance because of ice losses by iceberg calving into marine waters. The maximum extent of the main BIIS, excluding ice over the North Sea, occurred at 26 ka (Fig. 7). The vertical extent of ice surface elevations exceeded all known trimlines, consistent with recent interpretations (Fabel *et al.* 2012) that they record thermal boundaries within the ice sheet, rather than its vertical extent. In spite of nudges to the model to try and force it such that all margins fell entirely within the minimum to maximum positions of the empirical reconstruction, we experienced problems with ice extent in the SW. Here, the modelled grounding line position of the Irish Sea Ice Stream falls some 150 km behind that indicated by the geological evidence (minimum reconstruction; Fig. 6; Scourse *et al.* 2021). We return to this issue in the Discussion and Conclusions. Note that modelled ice covers the island of Lundy and reaches as far as the north coast of Devon and Cornwall.

Between 26 and 22 ka the ice sheet underwent a major transition (Fig. 7), losing ice mass and extent over Ireland and Britain; deglaciation had started here even though the ice sheet simultaneously gained mass and extent over the North Sea. The North Sea ice dome or divide developed rapidly (4000 years) as a consequence of a head-on collision of British and Scandinavian ice lobes. This coalescence in the central North Sea resulted
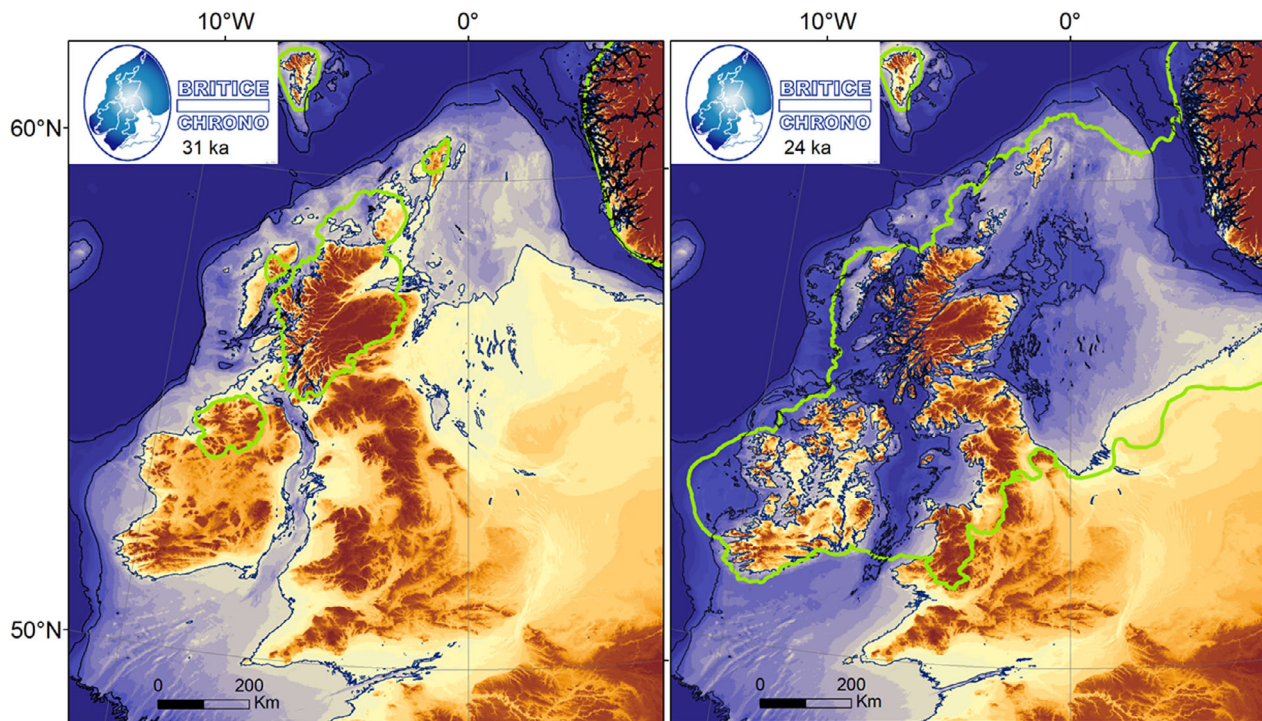

Fig. 8. Modelled palaeotopographies and shoreline position at the relative sea-level lowstand at 31 ka (left panel) and highstand at 24 ka (right panel), illustrating the extremes of shoreline position and palaeotopography in our studied time window (31–15 ka). Ice-sheet outlines are shown in green and bathymetric depth contours at 100 and 300 m. Note that by 24 ka, loading by the ice sheet had depressed over half of the bed below sea level making the ice sheet substantially marine-based. Data S5 Palaeotopographies and sea level 14–6 ka slideshow.

in an ice saddle that grew due to ice elevation feedback on mass balance. It became a major divide linking the British and Scandinavian ice sheets, attaining a thickness of around 1500 m. The maximum extent and volume of ice over the North Sea was at 22 ka. The maximum ice volume occurred after the maximum areal extent of the ice sheet because it was only once the BIIS and Scandinavian Ice Sheets had coalesced that widespread thickening over the North Sea occurred. Deglaciation of the BIIS was accelerated by large ice losses exported down the Malin Sea and Irish Sea ice streams, especially from 24 ka onwards. At 24 ka the Irish Sea Ice Stream was evacuating large ice fluxes with velocities exceeding 1000 m a^{-1}, an ice thickness reaching 1000 m and with its fast flowing trunk 100 km in width. Ice shelves simulated in the modelling were much less prominent in retreat than in advance.

Irish, British and North Sea ice masses were all retreating by 21 ka. Over the North Sea, a major ice collapse event occurred in a thousand years (20–19 ka) when ice discharge down the NCIS, along with accelerated wider melting losses, led to separation of British and Scandinavian ice. This was followed by a rapid collapse of marine-based ice by 18 ka. By this time, England was nearly deglaciated except in the far north, Ireland had lost much of its ice sheet and ice masses over Shetland and the main Welsh Mountains were now separate from the main ice sheet. Irish and British ice remained joined over the North Channel and around 75% of the ice sheet's perimeter was still marine-terminating such that ice losses were both by calving and by surface ablation.

The transition from largely marine-terminating ice margins to a smaller ice sheet, mostly terminating on land, occurred by 17 ka. Ice masses were characterized by separate Scottish and Irish ice sheets and outlying ice caps on the islands of Lewis, Shetland and Orkney, and over uplands of the Lake District, North Pennines, Snowdonia and Mid Wales. Contrary to simple expectations is that the separation of Irish and Scottish ice did not occur in the marine-based North Channel, rather the suture of separation was on land some 100 km to the west. This is a consequence of the greater ice thickness over Scotland. By 15 ka, continued deglaciation resulted in the loss of many of the outlying ice caps, but leaving a still substantial ice sheet over the Highlands of Scotland and remaining outlying ice caps in the Southern Uplands of Scotland and Blue Stack, Ox, Dartry and Iron mountains of Ireland. Although our modelling was directed at the ice-sheet scale, we note that glacial mass balance at 15 ka predicts the intersection of the equilibrium line altitude with many uplands (see black polygons without a blue fill in Fig. 6) including as far south as MacGillicuddy's Reeks, Dartmoor and Exmoor, the Brecon Beacons and the Peak District. We therefore expect that ice fields and glaciers likely existed in these locations at this time. Our reconstruction ends at 15 ka, although in Fig. 6 we also plot the modelled palaeoto-

pography and coastline at 8 ka, by which time Britain was now separated by the English Channel from mainland Europe. The Dogger Bank Island is predicted by glacio-isostatic modelling to have remained.

Model reconstruction of palaeotopography and sea level

Using glacio-isostatic modelling the loading of the lithosphere from the ice sheet was combined with far-field assessments of ice volume (e.g. Laurentide, Antarctic etc.) and their loading to predict palaeotopographies for our region. In our time window (31–15 ka) the lowest stand of sea level occurred at 31 ka, varying some 50–100 m below present-day sea level across the area (Fig. 8). This occurred when the ice sheet was small, mostly restricted to Scotland and part of Ireland so with only limited local ice loading, but with global sea levels drastically lowered due to the build-up of large ice sheets elsewhere at this time, such as in North America. By 24 ka the now much larger BIIS had locally depressed the lithosphere by some 60 m relative to today in central Ireland and 130 m in parts of Scotland, yielding a substantially lowered ice-sheet bed, much of it below sea level at this time (Fig. 8). With over half of the ice sheet resting below sea level this emphasizes its marine-based properties. Summed over growth and decay of the ice sheet, marine margins made up 49% of the perimeter.
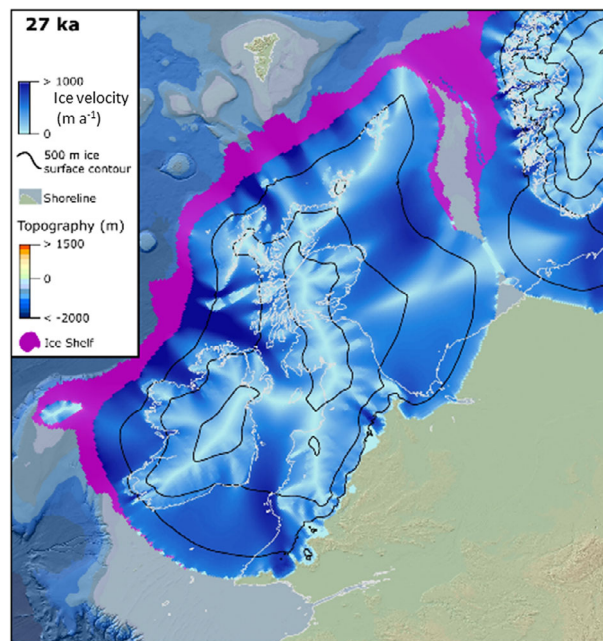

Fig. 9. In our preferred model reconstruction (Fig. 6) a thickening ice shelf on the west coast of Ireland failed to ground and so did not glaciate part of the Porcupine Bank (westernmost point of the ice sheet). In some model runs such as shown here, such grounding did occur, but with ice limits elsewhere that did not match the evidence, such as in the SW of England. Grounding on Porcupine Bank could have been a significant stabilizer of retreat by increasing the longevity of the ice shelf.

Palaeotopographies and sea level continued adjusting after the final disappearance of the ice sheets and with the southern North Sea being inundated by marine waters by 8 ka at which time our GIA model predicts an isolated Dogger Bank Island (Fig. 6).

Discussion

In the following discussion we first report on the mismatches between the empirical and model reconstructions, and then discuss key aspects of the growth and retreat history of the ice sheet regarding its rapid and early growth, its maximum extents and migration of its main ice divides. The earlier stated hypotheses, on the extent of synchroneity between sectors and on the pace of retreat across the marine to terrestrial transition, are tested using the new reconstruction. Changes in ice-sheet volume through the last glaciation are plotted and compared to potential drivers to explore and ascertain the main controls on ice-sheet demise. Finally, we plot the length of time for which land was exposed once the ice sheet withdrew as this is useful for biological, hydrogeological and archaeological investigations.

Mismatches in the empirical and model reconstructions

The empirical and model reconstructions of the ice sheet are by design, of course, similar, because the ice-sheet model was nudged to try to fit the optimum empirical ice limits, or failing that, to remain within the constraints of the maximum and minimum ice limits. The main systematic issue in our initial modelling experiments was that grounding lines along the western and northern margins of the ice sheet failed to retreat fast enough to keep up with the well-dated maximum empirical ice extents. This is most likely explained by local ocean warming effects that were not sufficiently included in the modelling, or perhaps from the effects of large tidal ranges (e.g. 4 m) that were forecast to exist (Scourse *et al*. 2018) but not applied in the modelling, and which might have destabilized any fringing ice shelves. Because of the large (50 km) and systematic misfit along these margins we chose to force the model reconstruction to the correct timing and pace by locally increasing ablation, and increasing ice shelf melting and calving rates across the whole domain at these times (see Method of model reconstruction).

On four of the 17 timeslices it was judged unreasonable to force the model to match the minimum limits in certain locations, without creating ('whack-a-mole') problems elsewhere. At 27 ka the ice shelf that expanded westwards from Ireland failed to thicken enough to ground on the Porcupine Bank, something that has been shown empirically to have occurred (Peters *et al*. 2016; Ó Cofaigh *et al*. 2021). We did not make adjustments to rectify this, but note that in some of our model simulations such grounding did occur (Fig. 9).

An egregious mismatch occurred at 26 ka, where the modelled grounding line position of the Irish Sea Ice Stream fell 150 km behind that indicated by the geological evidence (minimum reconstruction, Fig. 6; Scourse *et al*. 2021). We experimented with various nudges to the model to try and prevent this underrun but they resulted in significant overruns of other parts of the ice sheet, notably with the SW Peninsula of England (Cornwall and Devon) and much of the English Midlands becoming glaciated. The final choice of model run (Fig. 6) is therefore a compromise that mostly fits the wider empirical limits, but underruns in the Celtic Sea. The alternative choice of accepting a model run that reached the shelf edge in the Celtic Sea but also glaciated the SW Peninsula and parts of the English Midlands would have interesting implications for the long-standing hypothesis that some of the stones of Stonehenge may have been transported, at least partway as glacial erratics (e.g. Judd 1902; Scourse 1997; John 2018; Pearson *et al*. 2019). Although this may indeed be accommodated by earlier more extensive glaciations, we suggest however, that a process, forcing, or feedback is missing in the numerical modelling we present here and that once discovered would enable sufficient ice advance in the Celtic Sea without exceeding ice limits elsewhere. For example, Scourse *et al*. (2021) suggest that a non-steady oscillation (surge) arose as a release from the build-up of ice behind a topographic constriction in the Irish Sea. We further speculate that the drainage of lakes on the ice
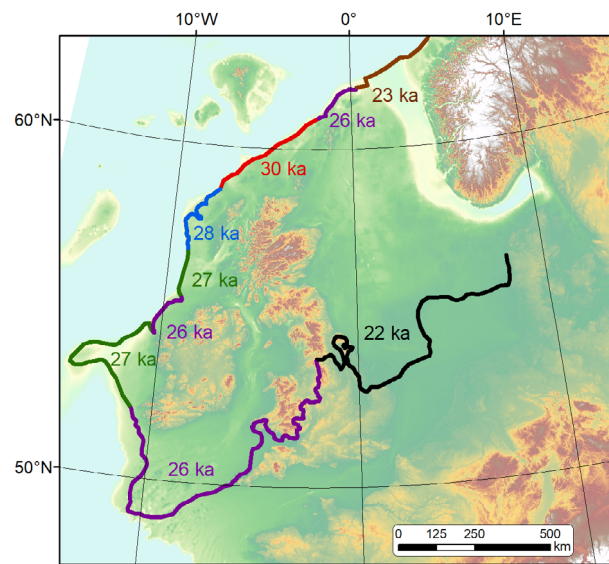

Fig. 10. Maximum extent attained by the Irish, British and North Sea Ice Sheet sectors, and timing of the onset of retreat for each sector. There is no single time at which the ice-sheet margins were everywhere at their maximum extent. The maximum areal extent was at 26 ka (see Fig. 7). Retreat commenced as early as 30 ka north of Scotland and as late as 22 ka in the southern North Sea. This asynchrony of retreat mirrors the asynchrony of build-up because the maximum limits were only briefly attained.

stream surface, or floods from subglacial lakes, may have temporarily facilitated faster ice flow and 'over-extension' of the ice margin by locally increasing basal lubrication. For the Irish Sea Ice Stream an important challenge remains, to develop new ingredients in process-based numerical modelling so that simulations can reconcile with the geological record.

Small mismatches (50 km) occur at 25 and 18 ka for marine-based ice surrounding Shetland. The modelled grounding lines underrun those defined empirically and we suggest that this may arise due to choices of marine-induced ice melt rates in the modelling. Model–data mismatches provide useful opportunities to improve ice-sheet modelling, and further work using hundreds of ensemble model runs quantitatively scored against the BRITICE-CHRONO ice margins is underway to address the mismatches identified here.

Rapid and 'early' ice-sheet growth

Constraints on growth of the ice sheet are much more uncertain than retreat because evidence is more difficult to find and most dating is deliberately focused on retreat phases. This is reflected in the wider levels of uncertainty expressed in the minimum and maximum extents in the empirical reconstruction (Fig. 5). In Scotland, little is known regarding the existence and extent of ice masses prior to our time focus of between 31 to 15 ka. On Transect 8 however, new luminescence ages on the island of Lewis led Bradwell *et al.* (2021b) to suggest a major Scottish Ice Sheet existed between ~44 and 38 ka, in MIS 3, nourished in the Highlands of mainland Scotland and with a functioning Minch Ice Stream. This ice sheet is interpreted to have retreated from Lewis and from much of the Minch during the 'Tolsta Interstadial' probably between 38 and 35 ka and prior to the main Late Devensian advance of the ice sheet.

By 31 ka, a Scottish Ice Sheet existed, with small satellite ice caps on uplands elsewhere. Subsequent growth was remarkably rapid, with the ice sheet expanding from a Scottish Highlands centred ice sheet to a fully coalesced BIIS (apart from the Welsh Ice Sheet) and reaching the continental shelf edge in places by 30 ka (Fig. 6). This fivefold expansion in size in only a thousand years demonstrates that ice advance can be nearly as rapid as retreat (see later) and that calving icebergs as the margin advanced across the shelf did little to slow down ice sheet growth. This growth is both earlier and faster than suggested in the Hughes *et al.* (2016) DATED reconstruction. The 'Late Devensian BIIS' has usually been ascribed to MIS 2, but as noted above our new ages demonstrate that the Scottish Ice Sheet started advancing in the latter parts of MIS 3, advancing through the north Minch at 32 to 31 ka and reaching as far as the continental shelf break by around 30 ka (Bradwell *et al.* 2021b).

Asynchrony of maximum ice extents and in the onset of deglaciation

The ice sheet is found to be larger than previously thought and extending as far west as the Porcupine Bank (Peters *et al.* 2016; Ó Cofaigh *et al.* 2021), and as far south as the continental shelf break in the Celtic Sea (Scourse *et al.* 2021). This southernmost limit reaches beyond 49°, the latitude of Paris! The maximum areal extent reaches 900 000 km^2, including Irish, British and North Sea ice up to the western edge of the Norwegian Channel. The maximum limits on the continental shelf are now based on robust evidence dated to the last glacial (MIS 2–3). This confirms earlier inferences about MIS 2–3 (Late Weichselian/Devensian) ice mostly reaching the continental shelf edge (e.g. Sejrup *et al.* 2005; Chiverrell & Thomas 2010; Clark *et al.* 2012) and rules out the possibility that these limits were only attained during more extensive prior glaciations such as in MIS 6 (Wolstonian) or MIS 12 (Anglian). There is no single time at which the ice sheet was everywhere at its maximum extent. As Fig. 10 demonstrates, maximum extents in the north and west were attained as early as 30 to 26 ka and as late as 22 ka along parts of the southern margin. This asynchrony in build-up is explained by simple geography in that the continental shelf west and northwest of the British Isles is relatively narrow (*c.* 100 km) and most of the snow-nourishing mountains lie close to these westernmost coasts. Ice masses grew from the mountains up to 31 ka and then rapidly became marine-based, advancing to the shelf break by 30–26 ka, beyond which the ice could grow no further due to excessive water depths that force flotation and calving. From a mass balance perspective, if the continental shelf was wider it would have taken longer for ice to expand across it and would have reached its maximum here much later. In contrast, the southern margin spent much longer advancing across England and the southern North Sea, reaching maximum limits here at 22 ka in response to the continued glacial cooling. It did not run out of ice0sheet bed on which to grow.

With no uplands to nourish ice caps, the North Sea depended on ice fed from adjacent source areas. Growth of British ice into the North Sea preceded that of Scandinavian ice and with lobes from each finally meeting around two thirds of the distance eastwards across the North Sea, at an area NE of Dogger Bank at around 27 ka. This led to the establishment of a distinct North Sea ice dome by 22 ka (see earlier and Fig. 7). At 22 ka North Sea ice was at its maximum, some 3000 years subsequent to the maximum of the Irish and British Ice Sheets. This is because the 200-m-deep Norwegian Channel steered much Scandinavian ice northwards, thus delaying ice confluence over the North Sea and delaying the timing of maximum extent here. We speculate that in earlier glaciations and prior to the existence of this important topographic channel, which
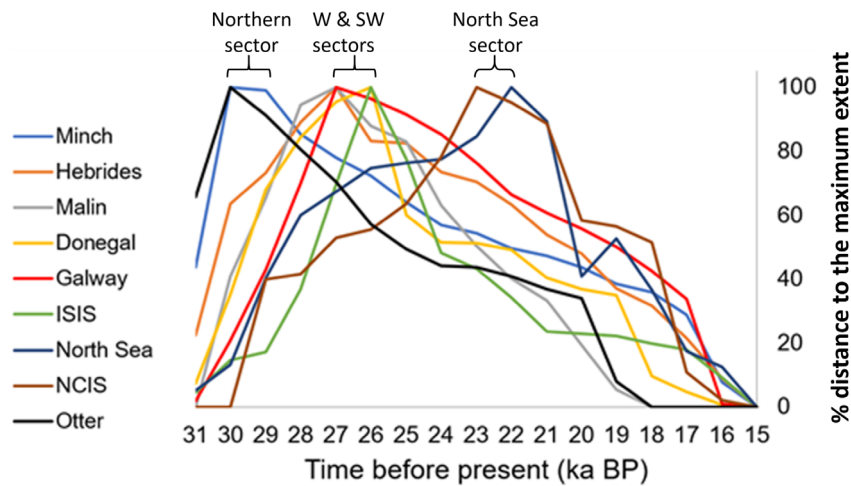
Fig. 11. Variation in ice margin behaviour across ice-sheet sectors demonstrating considerable asynchrony in the timing of maximum limits, and the onset of retreat. It is notable that maximum limits were only short-lived (1–3 thousand years) before the onset of retreat. To aid comparisons, margin position data are normalized to the percentage distance to the maximum extent per sector; ISIS is the Irish Sea Ice Stream and NCIS, the Norwegian Channel Ice Stream. Actual retreat rates in metres per year are discussed later and in Figs 12 and 13.

purged ice away, a North Sea ice dome would have been centred further west and with a much greater influence of Scandinavian ice over the North Sea. In the last glaciation the channel acted as a gutter diverting Norwegian ice northwards.

Clearly, a large ice sheet in steady state with long periods of neutral mass balance is not found in the reconstruction. Rather we have an always rapidly adjusting ice sheet, asynchronous in advance and retreat around

Fig. 12. Large changes occurred in the centres of ice mass over time, shown here in terms of modelled migrations of the main ice divides and flow geometry between 24 and 21 ka. Mainly as a consequence of ice drawdown through the Irish Sea Ice Stream, the divide across Ireland and southern Scotland migrated north by 70 km, and the North Sea divide moved northwards by 125 km during the later build-up of ice volume here, subsequent to the confluence between British and Scandinavian ice.

its perimeter and one that started recession in most places shortly after reaching its maximum. In Fig. 11 this asynchrony is illustrated by plots of ice margin advance and retreat for north, west and southwest, and North Sea sectors of the ice sheet. The northern sector of the ice sheet (Minch and Orkney–Shetland) experienced fast growth toward the continental shelf break reaching a maximum extent as early as 30 ka, followed by slow retreat relative to other sectors (Fig. 11). In general, western and southwestern sectors of the ice sheet experienced fast growth and slower retreat respectively, reaching maximum extents at 27 and 26 ka respectively. Exceptions to this were retreat of the Irish Sea Ice Stream and across Donegal Bay, both of which collapsed back rapidly. North Sea ice experienced the slowest growth of all sectors, because it had to wait for confluence to occur between British and Norwegian ice, finally reaching a maximum extent at 22 ka. Relative to other areas, the North Sea sector underwent the most rapid retreat phase of all comprising a dramatic collapse event that halved the ice-sheet area here in less than 1000 years.

Our reconstruction does not support Hypothesis 2, articulated in the Introduction, that the main ice catchments draining the ice sheet retreated synchronously in simple response to external climatic and sea level controls. This might be expected if external drivers (e.g. warming or sea level rise) outweigh the local controls on ice retreat. Rather we find that deglaciation is heavily influenced by local factors and especially the geography of the region, which preconditioned timing of coalescence and separation of ice masses emanating from uplands in Ireland, Scotland and Norway. Topographic complexity clearly exerts a large influence on the (a) synchrony of ice-sheet behaviour. A lesson here is that if one is seeking climate inferences from ice-sheet variations it might be best to choose ice sheets with simple
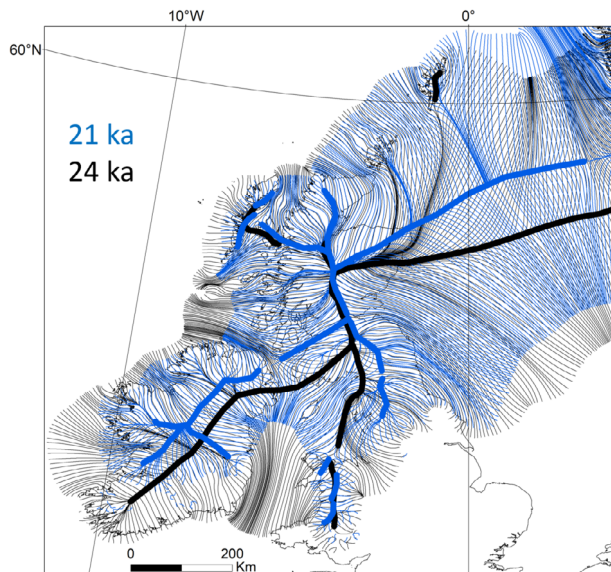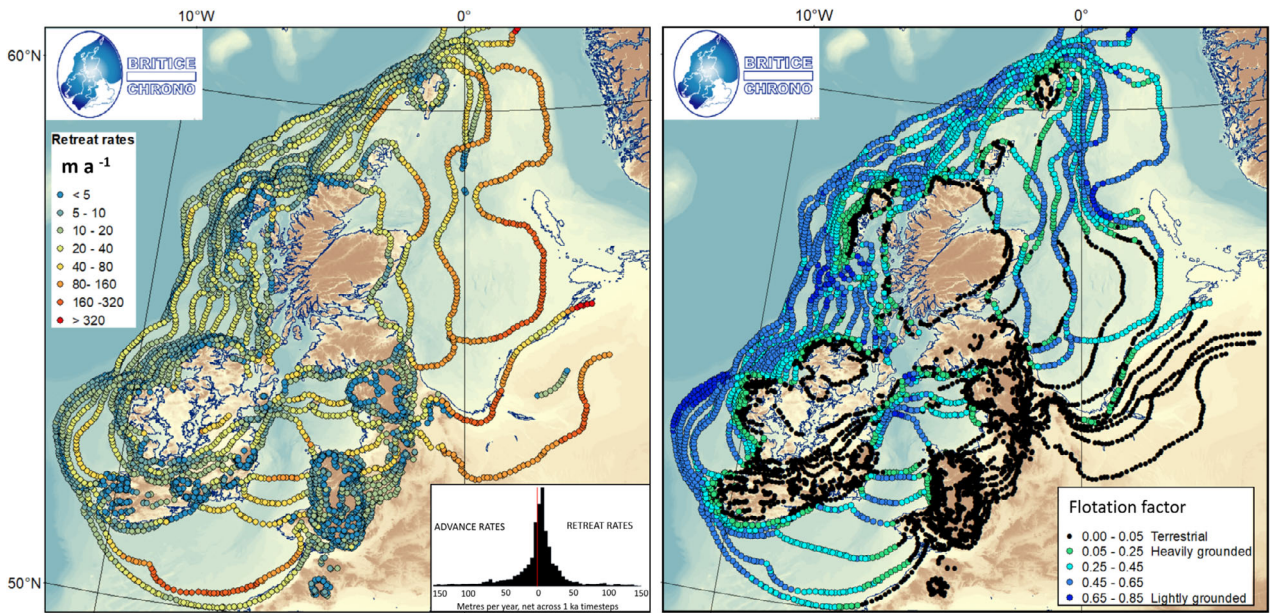
Fig. 13. Left panel: net rates of retreat calculated at 1-ka timesteps, demonstrating large variations between terrestrial (50 m a^{-1}) and marine sectors (>50 and up to 451 m a^{-1}). Note that these time-averaged values likely mask faster shorter-lived rates that are below our dating resolution. Inset panel shows frequency distribution of rates of retreat and advance. Right panel: flotation factor for marine-terminating margins (advancing and retreating) calculated using ice thickness behind grounding lines and water depths from the relative sea level modelling (black indicates terrestrial-terminating ice margins). Comparing both maps indicates a general correspondence between faster retreat for margins that were marine-based and for those that were more lightly grounded (high flotation factors).

radial structures and underlying topography, such as in Iceland. The surprise in the data for the BIIS is both the abundance of asynchronous variations, and that retreat in some sectors commenced prior to proxy records of warming. Why did ice retreat prior to the warming? Specific explanations for this 'early retreat', and stepped and oscillating margin retreat in relation to bed topographic and geological variations have been explored in the BRITICE-CHRONO transect papers (Benetti *et al.* 2021; Bradwell *et al.* 2021a, b; Chiverrell *et al.* 2021; Evans *et al.* 2021; Ó Cofaigh *et al.* 2021; Scourse *et al.* 2021). At the ice-sheet scale we return to these issues later.

Ice divide migrations

The spatial asymmetry of ice-sheet growth and decay shown by variations in ice extent over time (Fig. 6) is also reflected in migrations in the centres of mass, as defined by the main ice divides (Fig. 12). A notable example is that between 24 and 21 ka large changes in ice extent and flow geometry occurred, with ice volume reducing over Ireland and Britain but still expanding over the North Sea. During this time, ice drawdown from the Irish Sea Ice Stream helped drive the Irish-Scottish ice divide northwards by 70 km (Fig. 12) and the North Sea divide moved northwards by 125 km as a consequence of continued growth following confluence of British and Scandinavian ice. Changes in the flow geometry (e.g. streamlines in Figs 7 and 12) were less at the ice-sheet

periphery and with larger angular changes and increasing complexity inwards, especially near locations of divide migration. Some of the divide shifts we note here are consistent with those defined from an empirical reconstruction of the Irish Ice Sheet (Greenwood & Clark 2009) and which were built from flowsets of ice geometry from mapped drumlins and subglacial ribs. A fuller examination of how well the modelled flow geometric changes match with those defined by subglacial bedforms would be fruitful in terms of quantifying how well the model performs against observations of ice flow (e.g. Ely *et al.* 2021) and might also be useful for progressing knowledge about glaciological conditions required for drumlin formation.

Variations in pace of ice margin retreat

The pace of retreat (Fig. 13) varied between slow (<50 m a^{-1}) at mostly terrestrial margins, faster (up to 80 m a^{-1}) at marine-calving margins mostly on the west and northern continental shelves, and much faster (80–451 m a^{-1}) collapse events in the Celtic, Irish and North Seas. All really fast retreat rates (>200 m a^{-1}) were marine, but marine retreat can also be slow. Note that these time-averaged or net retreat rates at 1-ka timesteps likely mask faster short-lived (decadal) rates that are below our dating resolution. Retreat rates of up to 50 m a^{-1} were the most frequent (Fig. 13 inset panel), with 10 m a^{-1} as the modal value across the whole ice sheet. A notable exception to the generally slower
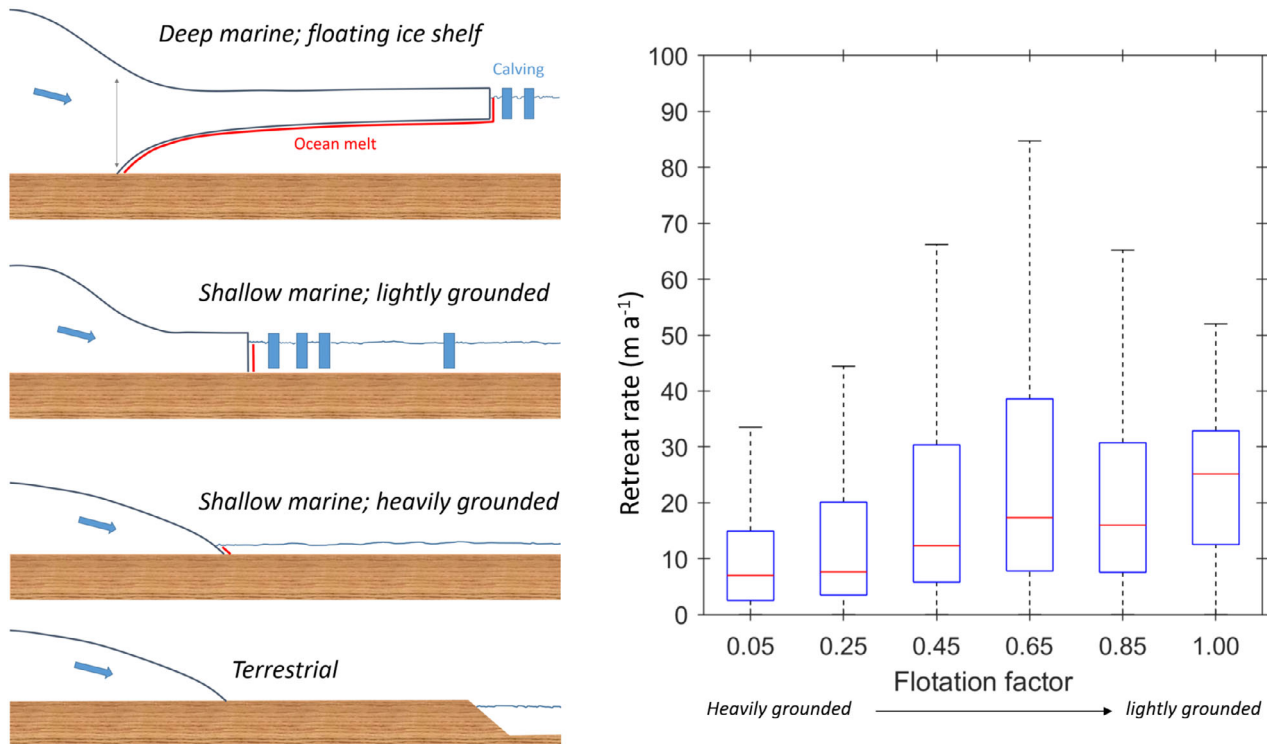
Fig. 14. Analysis of ice-marginal retreat rates (right panel) demonstrates faster retreat for margins with higher flotation factors. Zero flotation is fully grounded (terrestrial), and approaching 1.0 for buoyancy at the margin. Data are from 6954 measurements of flotation factor averaged from flowlines 0–5 km behind the ice margins from 31 to 15 ka. Median (red line), interquartile range (blue box) and 2.7 sigma (whiskers) are indicated. Modal flotation factor was 0.5. In the schematic cartoon (left panel) we suggest that retreat rate variation with flotation factor is not just a consequence of buoyancy-induced calving, but also arises from increased ice melting from contact with warm water (red annotation), noting that most (70%) of the marine margins were heavily grounded (<0.5 flotation) due to the mostly shallow seas.

terrestrial rates of retreat (<50 m a^{-1}) was in the southern North Sea, which was terrestrially exposed at this time (22–21 ka), and in places experienced retreat faster than 160 m a^{-1}. This might be a consequence of over-extension of this lobe by a flow instability or surge that increased the ablation area, promoting rapid surface melting and margin retreat (e.g. Evans & Thomson 2010). To explore the extent to which reverse-bed slopes hosted retreat rates faster than on normal slopes, in accordance with the marine ice-sheet instability theory (Schoof 2007), ice sheet-wide retreat rates were compared to the gradient of bed slope (averaged along 5-km flowlines) behind grounding lines. No relationship was found, and the fastest retreat rates in fact occurred across fairly flat parts of the sea floor, arising from a saddle collapse over the North Sea and retreat from over-extended ice lobes or ice streams. For some parts of the ice sheet however, notably in the Minch and in the Norwegian Channel (Gandy *et al.* 2018; Bradwell *et al.* 2021 b), which host reverse bed slopes in waters deeper than is typical across the domain, marine ice-sheet instability is predicted to have occurred using ice-sheet modelling experiments aimed at replicating the BRITICE-CHRONO glacial histories (Gandy *et al.* 2018, 2021). That the influence of marine ice-sheet instability was found to be largely absent across the ice-sheet domain

may indicate that its operation was the exception rather than the rule, consistent with some findings elsewhere (Greenwood *et al.* 2021), or in the case of the BIIS might simply arise from the relatively shallow waters (100–300 m) and heavily grounded margins that predominated. This contrasts with larger ice sheets such as in Antarctica where the ice mass is great enough to depress continental shelves to depths exceeding 500 m, thereby encouraging higher flotation factors and instability.

To examine the influence of ice-marginal buoyancy on retreat rates we calculated flotation factors (FF) along flowlines behind grounding lines using:

$$\text{Flotation Factor} = Pw \times g(D-1)/Pi \times g \times H \qquad 1$$

where *Pw* and *Pi* are the density of water and ice, respectively, g is gravitational acceleration, *D* is water depth and *H* is ice thickness at grounding line, averaged along the final 5-km flowline leading to the grounding line. The modal flotation factor was 0.5, with around 70% of marine margins heavily grounded (<0.5; thick ice in shallow water). Comparison of maps (Fig. 13) and graphs (Fig. 14) of retreat rates against flotation factor demonstrates that faster retreat is typical for marine margins compared with terrestrial (FF = 0) and that retreat was faster for more lightly grounded margins
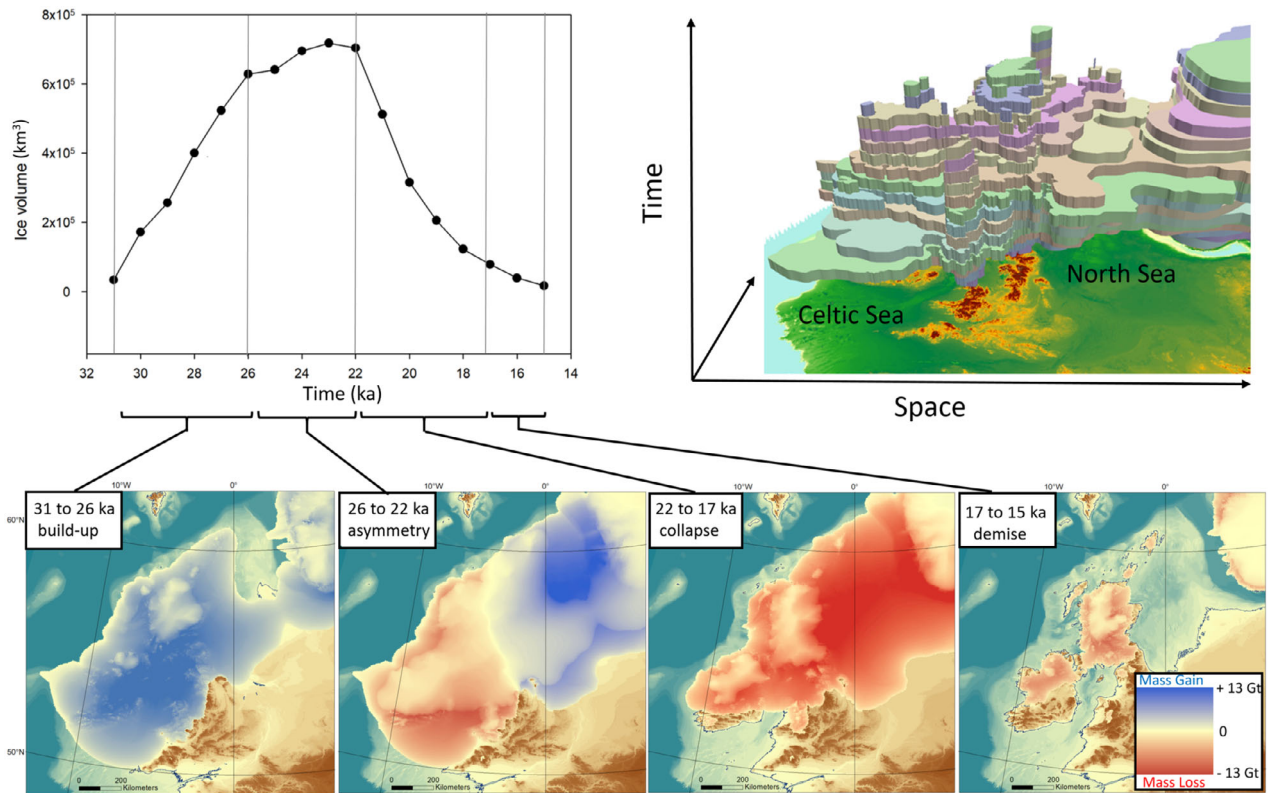
Fig. 15. Growth of the British–Irish Ice Sheet to its maximum volume of 717 112 km³ (1.8 m sea level equivalent) at 23 ka, and its rapid collapse starting at 22 ka, at rates of ice loss of up to 194 km³ a⁻¹. Four stages of development are shown in the lower panels, which plot the mass losses and gains computed by subtracting across these timesteps. Between 26 and 22 ka there was a dramatic west–east asymmetry in behaviour, the Irish and British sectors were losing mass at the same time as ice over the North Sea was gaining. The time–space plot of ice-sheet extents (top right panel) shows 1-ka 'time slabs' from the empirical reconstruction, illustrating the regional asymmetry in growth and decay and the large collapse events over the Celtic and North Seas.

(higher flotation factors). Variability in retreat rates is highest for mid-range flotation factors (0.45–0.65; Fig. 14), which might be explained by increased sensitivity to sea level perturbations in cases undampened by buttressing ice shelves. In addition to expected buoyancy effects, we suggest that margins with higher flotation factors will typically have greater surface areas of ice in contact with warm water (Fig. 14), increasing the loss by melting, and that submarine melting promotes calving by creating weak points (notches) for structural failure (Benn *et al*. 2007).

From our reconstruction of the ice sheet and analysis of retreat rates we therefore accept the earlier stated Hypothesis 1 (see Introduction), that the main marine-influenced sectors (e.g. North and Irish Seas) collapsed rapidly and that once onshore the ice sheet stabilized and retreated more slowly. The new data reject the alternative interpretation speculated in Clark *et al*. (2012), that widespread purging of ice by fast flow happened while marine-margins retreated slowly, dynamically thinning interior (land-based) ice, and preconditioning the ice sheet to more rapid retreat once it was terrestrially based. Activation of marine ice-sheet instability (MISI) was not found to be the primary cause for this marine–terrestrial

difference, because conditions where MISI arises are the exception across the area due to the mostly shallow seawater depths.

Ice volume changes

Changes in the volume of the ice sheet are plotted in Fig. 15, with values including all ice grounded over the North Sea up to the western edge of the Norwegian Channel. The maximum volume occurred at 23 ka with 717 112 km³ of grounded ice, with an estimated mass of 657 000 Giga tonnes, enough to raise sea level by 1.8 m once it all melted. This is about half the volume of the present-day West Antarctic Ice Sheet and a quarter of the Greenland Ice Sheet. A notable feature of the volume graph (Fig. 15) is the asymmetry in the peak, with faster rates of loss than for growth, and especially in the period 22–20 ka when the ice sheet collapsed at a rate of 194 km³ a⁻¹. That equates to a mass loss of 178 Gt a⁻¹ at this time, which proportionally is around twice as fast as the current rates of ice loss observed for the Greenland Ice Sheet (345 Gt a⁻¹ in 2011; IMBIE Team 2020) when scaled by the relative size of the ice sheets by volume. Four stages of development are evident from the plot of
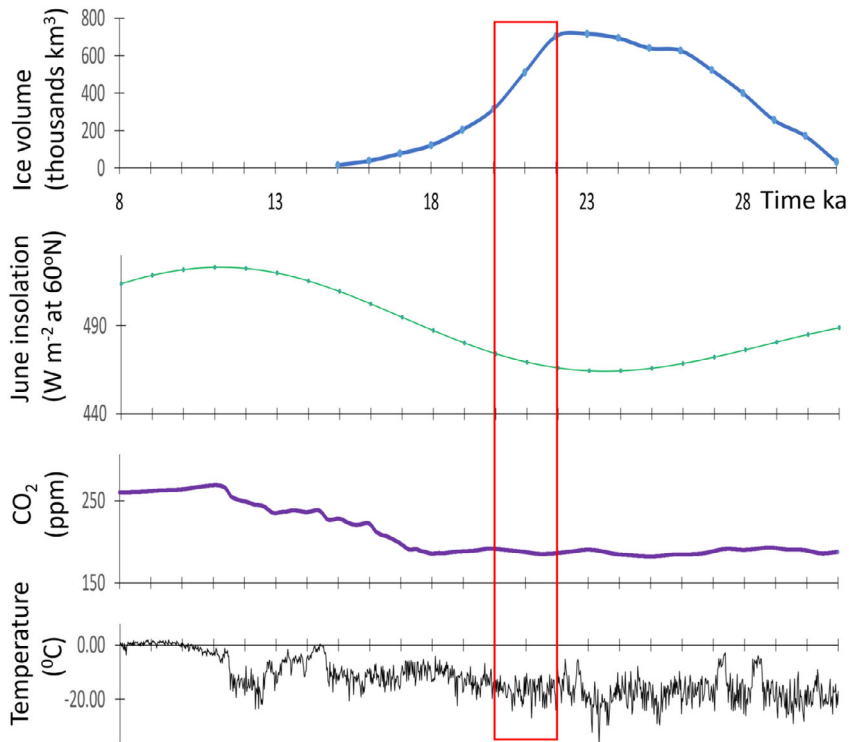
Fig. 16. Comparison of fluctuations in ice volume of the British–Irish Ice Sheet against potential climate-related drivers of change. Ice volume loss initiated at 22 ka and the ice sheet reduced to half of its maximum volume in just 2000 years (time interval marked by red rectangle). This collapse in ice volume and extent occurred thousands of years prior to deglacial warming and CO_2 rise (they are flat-lining in the 22–20 ka interval), but at a time when June insolation (W m^{-2} at 60°N) was rising from its minima. Ice volume graph (this study); insolation values from Berger & Loutre (1991) and Berger (1992); CO_2 values from Köhler *et al.* (2017) and the global temperature proxy from Helsen *et al.* (2012) and Bradley *et al.* (2018), which is a transfer of δ¹⁸O to temperature using the glacial index method.

volume. Steady growth (120 km^3 a^{-1}) from 31 to 26 ka occurred as ice built up over Ireland and Britain and extended out across the continental shelves. This was followed by a period (26–22 ka) of slower overall growth in ice volume (20 km^3 a^{-1}) but characterized by dramatic west to east asymmetry in behaviour (Fig. 15). Large losses from the Irish and British sectors were compensated and exceeded by gains over the North Sea as an ice divide grew following the confluence of British and Scandinavian ice. The third and most dramatic phase was from 22 to 17 ka when saddle-collapses occurred over the North and Irish Seas and the ice sheet lost its marine-based sectors (125 km^3 a^{-1}). The final demise of the much-reduced terrestrial ice sheet occurred more slowly (30 km^3 a^{-1}) from 17 ka onwards.

Controls on ice-sheet demise

The pace of ice margin retreat within each of the eight transects was analysed relative to atmospheric and ocean warming, and local sea level rise, and against topographical, geological factors and ice shelves as potential controls (Benetti *et al.* 2021; Bradwell *et al.* 2021a, b; Chiverrell *et al.* 2021; Evans *et al.* 2021; Ó Cofaigh *et al.* 2021; Scourse *et al.* 2021). Here we compare the change in volume of the whole ice sheet and reflect on

how well this fits with climate and sea level drivers (Fig. 16). Ice volume loss initiated at 22 ka and the ice sheet reduced to half of its maximum volume in just 2000 years. This collapse in volume and extent occurred thousands of years prior to deglacial warming and CO_2 rise; they can be seen 'flat-lining' in the 22–20 ka interval in Fig. 16, ruling out these as the primary triggers. The ice volume curve, however, closely mirrors the variation in June insolation (W m^{-2} at 60°N), with peak ice volume at 23 ka matching the insolation minimum and with volume decreasing as insolation rises (Fig. 16). This close relationship opens up the possibility that deglaciation might have been triggered by orbitally induced increasing levels of summer solar radiation producing more surface melting, and with associated positive feedbacks, for example on albedo (e.g. Roberts *et al.* 2013a, b; Ryan *et al.* 2019). Melt in ice-sheet modelling is usually computed via positive degree days of air temperature, with insolation not directly computed and so the hypothesized insolation trigger highlighted here may go undetected in modelling investigations. Interestingly, in modelling the Greenland Ice Sheet during the last interglacial (Eemian), Van de Berg *et al.* (2011) found that it was necessary to introduce an insolation term and that, along with its positive feedback effects, insolation contributed to 45% of the melt required to
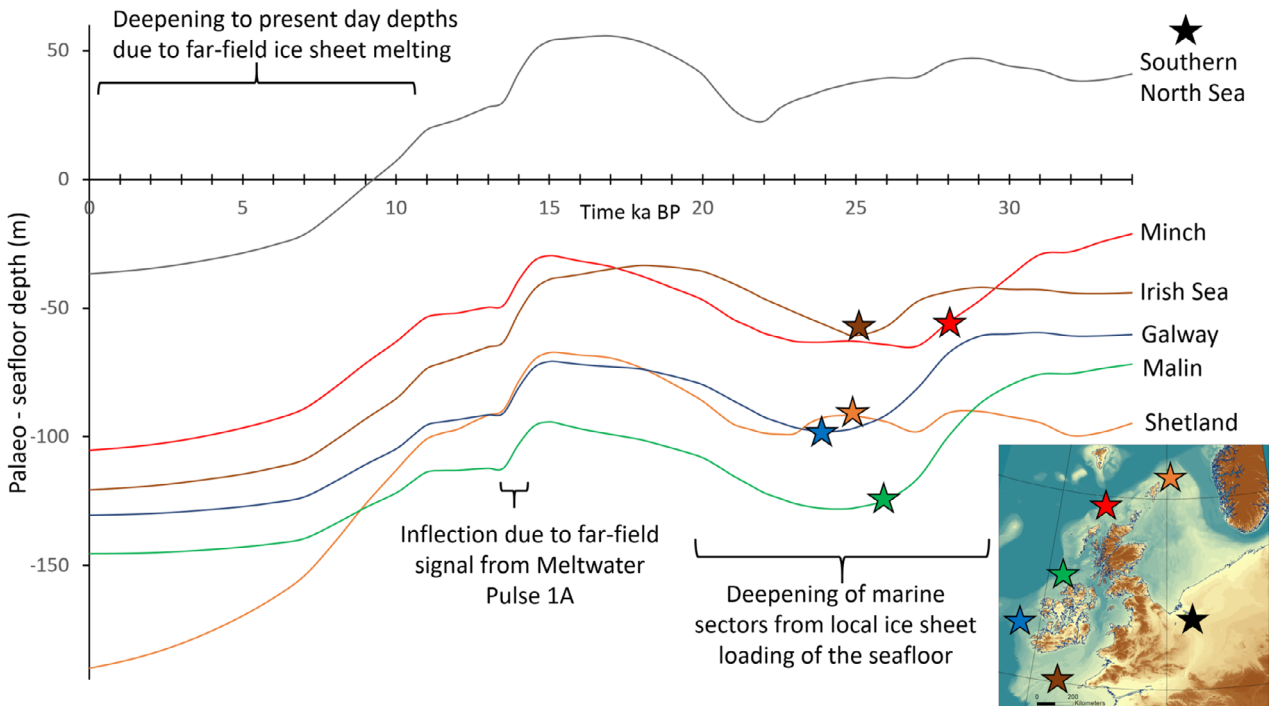
Fig. 17. Variation in sea floor depths (converted from modelled relative sea level computations) for marine sectors of the ice sheet, plotted for six locations close behind the maximal ice extents (stars on inset map of palaeotopography at 24 ka). In these places, water depths at the ice sheet's grounding line increased by around 50 m as a consequence of lithospheric downwarping by mass loading of the British–Irish Ice Sheet between around 30 and 25 ka. For most locations, the start of grounding line retreat (whose timing is marked by stars) occurred after deepening of the water column. We infer a causal link of glacio-isostatic deepening of the water column triggering deglaciation due to increased mass loss by iceberg calving. Glacio-isostatic adjustment modelling used BRITICE-CHRONO reconstructions of the mass of the British-Irish-Scandinavian-Barents ice sheets.

yield the smaller ice sheet at that time. The BRITICE-CHRONO reconstruction of the ice sheet along with the findings from Greenland therefore suggest that ice-sheet modelling investigations should assess the effects of insolation on surface melting directly in their computations.

The BIIS is now known to have had extensive marine margins (~50% of perimeter summed over growth and decay) and so ice loss by calving and submarine melting must have been a significant control on the ice sheet's mass balance. The rate of ice loss at marine margins by the calving of icebergs is known to increase with increasing water depths (e.g. Pelto & Warren 1991). Did increasing water depth trigger deglaciation? Figure 17 plots relative sea level calculations, converted to palaeo depths, from our glacio-isostatic adjustment modelling. This modelling includes loading of the lithosphere from local ice sheets from the BRITICE-CHRONO and DATED (Hughes *et al.* 2016) Scandinavian ice-sheet reconstructions (see Method of model reconstruction), and also accounts for the effect of far-field ice-sheet fluctuations on sea level. The results show that, superimposed upon sea level variations arising from ice-sheet fluctuations elsewhere in the world, the isostatic loading from the British–Irish Ice Sheet locally depressed the sea floor by over 140 m in interior regions where ice thickness was greatest (not illustrated) and in the order of

50 m close behind the ice sheet's maximum extents (Fig. 17). Using one of the most influential ice streams on mass balance as a case study, the ice stream draining through the Malin Sea, the present-day water depth on the continental shelf here is 145 m. At 30 ka the depth was only 75 m due to global lowering of sea level, but by 26 ka had increased to 130 m as a consequence of bed depression from the mass of the BIIS, which by now had advanced out across the shelf. Although calving rates are difficult to understand and model, a simple empirical relationship (Pelto & Warren 1991) suggests that this increase in depth, from local ice loading, increased the calving velocity by 66% to a value of 1153 m a^{-1}. For the marine sectors of the ice sheet, in four of the five cases the onset of retreat occurred following increases in water depths in the order of 50 m (plotted in Fig. 17). We infer a causal link between this lowering of the sea floor by ice mass loading and the onset of grounding line retreat across these sectors due to increased calving fluxes. This link is strengthened by the relationship reported earlier (Figs 13, 14) showing that more lightly grounded margins (in deeper water) experienced faster rates of retreat. The causal link is appealing because it can both explain why retreat commenced in the marine sectors thousands of years prior to rising temperatures, and why retreat in all sectors commenced shortly (1–2 ka) after reaching its maximum extent, this delay being the time-lag for
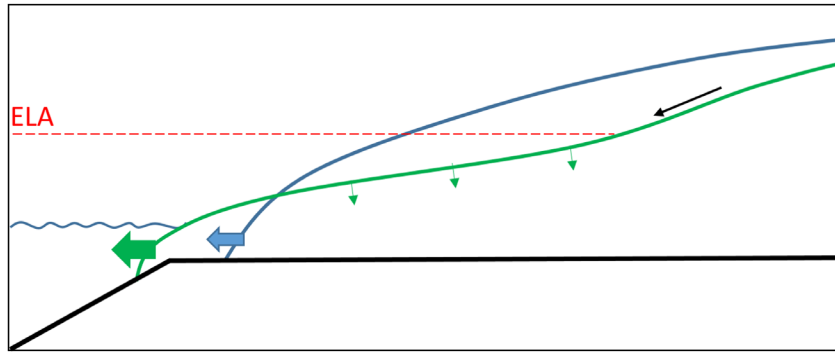
Fig. 18. Hypothesis of calving-induced ice stream–ELA feedback, and runaway retreat. In blue, an ice stream advancing across the continental shelf experiences an increase in ice flux (represented by size of arrows) once it reaches the deeper water at the shelf edge, which lowers interior ice surface elevations (green) increasing the area below the equilibrium line altitude (ELA in red) sufficient in some cases we suspect, to trigger widespread and irreversible ice-sheet retreat from the continental shelf edge. The ice surface lowering also steepens the surface slope at ice stream onset zones (black arrow), which locally increases ice velocity and enlarges ice stream networks (see text).

isostatic loading. The plots of palaeo-depth show that the seabed rebounded just a few thousand years after ice margin withdrawal.

Interactions between ice-sheet loading, ice fluxes and margin retreat have been previously suggested by Eyles & McCabe (1989) and in many of the BRITICE-CHRONO transect reconstructions (Callard *et al.* 2018; Ó Cofaigh *et al.* 2019, 2021, Benetti *et al.* 2021), and explored elsewhere in ice-sheet modelling, for example of the Antarctic Ice Sheet (Whitehouse *et al.* 2019). We note that Whitehouse *et al.* (2019) suggested that the unloading part of the cycle, when the sea floor rebounds upwards, might provide a stabilizing feedback on ongoing ice-sheet retreat by decreasing the water depth and ice flux. We speculate that such a stabilizing feedback might explain the slow rates of retreat on the continental shelf of Ireland (Benetti *et al.* 2021; Ó Cofaigh *et al.* 2021) and prominent reconstructed stillstands of the ice margin, such as at the mid-shelf grounding zone complex in Galway Bay (Roberts *et al.* 2020; Ó Cofaigh *et al.* 2021), and at large grounding zone wedges in the North Sea (Roberts *et al.* 2019). Specific GIA and ice-sheet modelling experiments could be usefully aimed at assessing these inferences and would need to account for strength of the lithosphere, because this value will determine the response time scale.

We explore two further possible reasons for why the ice sheet commenced deglaciation prior to the warming signal. The first stems from lack of knowledge of the actual NW European regional climate under which the ice sheet operated. Our comparisons of 'early retreat in relation to climate forcing' are in relation to global signals of air temperature and carbon dioxide. Perhaps the actual climate that developed over the region encompassed notable warming of air or ocean temperatures from 30 ka onwards, and the ice sheet simply responded to these. This could be investigated by developing regional climate model simulations for NW Europe (e.g. Strandberg *et al.* 2011) to drive ice-sheet

models rather than using climate-forcing from Greenland ice-cores that are over 2000 km distant and in a different regional climate system. We used an index approach to scale climate oscillations from the Greenland ice-core record to values more appropriate over NW Europe, the point being that it might not be just values that are different (e.g. Britain warmer than Greenland) but the timing of oscillations might vary. Furthermore, during the last glacial, the Atlantic Polar Front is known to have migrated from north of the British Isles to positions substantially to the south (e.g. Ruddiman & McIntyre 1981; Lowe *et al.* 1994; Scourse *et al.* 2009; Hall *et al.* 2011) profoundly affecting the ice sheet's upwind air and sea temperature, and the incidence of sea ice and moisture availability, all of which would have affected the mass balance of the ice sheet. Despite apparent synchrony between sea surface temperatures and millennial-scale flux of ice rafted debris from the ice sheet (Scourse *et al.* 2009) it is likely that north–south shifts in the locus of snow accumulation and melting would have influenced mass balance across different ice drainage basins that might help explain the asynchrony of ice advance and retreat, as discussed earlier and in Fig. 11. Establishing if such ice-sheet asymmetric response arose from the Polar Front migrations is not easy, and ideally would require regional climate model simulations that encapsulate the effect of the Polar Front on spatial fields of temperature and precipitation.

The ice sheet did not stay at its maximum extent for long; shortly after (1 or 2 ka) reaching the continental shelf edge it commenced retreat, with different sectors doing this at different times, which rules out a simple climate explanation. Earlier we suggested that this was because such maximum extents were not sustainable (not enough ice being fed by outflow from the ice sheet) once glacio-isostatic loading increased water depths and iceberg calving, thereby flipping the drainage basin into negative mass balance. Although this explanation appears reasonable in that the time delay of a few
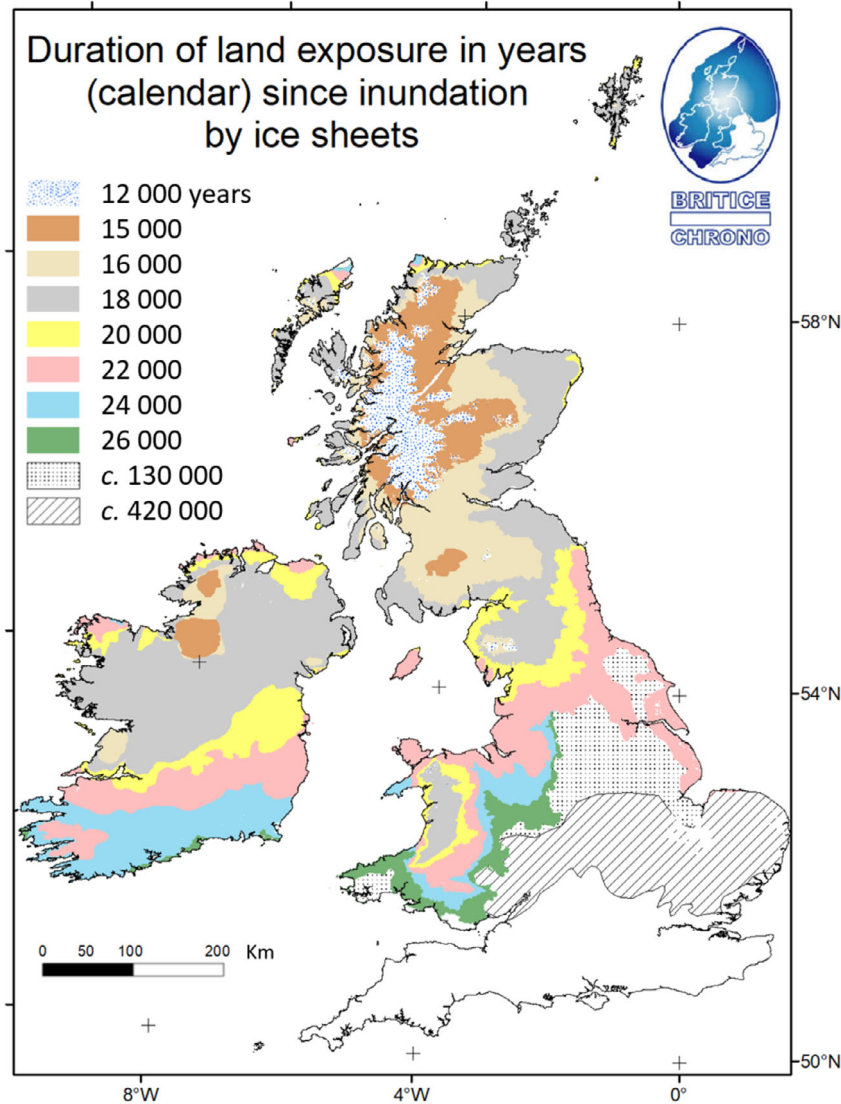
Fig. 19. The duration of time that has elapsed since land has been exposed from beneath ice sheets. Relevant for biological, hydrogeological and archaeological investigations this is based on the BRITICE-CHRONO reconstruction presented earlier, along with younger (Loch Lomond and Nahanagan Stadial) and older (Wolstonian and Anglian) ice cover estimates from Bickerdike *et al.* (2016), and Gibbard & Clark (2011), respectively.

thousand years matches the GIA-modelled time-lag for lithospheric down-warping, we here propose an alternative based on ice stream dynamics. In Fig. 18 we consider an ice stream advancing out across the continental shelf in a cool climate, its grounding line advancing because ice flux from the accumulation area exceeds mass losses by surface melting and by iceberg discharge, which is controlled by water depth at the grounding line. Once the ice margin reaches the continental shelf edge, ice flux dramatically increases because of the much deeper waters encountered, halting further advance and producing upstream ice thinning. For an ice margin in a climate cold enough that surface melting is not happening (e.g. pre-Anthropocene Antarctica) then the grounding line would simply adjust position to balance the

incoming and outgoing fluxes. But for ice margins in more marginal conditions of glaciation, such as a mid-latitude ice sheet advancing into elevations low enough for surface melting (i.e. below the equilibrium line altitude, ELA) then we propose that an important negative feedback occurs in ice dynamics. Upon reaching the continental shelf edge, the increased calving flux produces upstream thinning of the ice stream surface, lowering elevations below the ELA and yielding more widespread surface melting, sufficient in some cases we suspect to trigger widespread and irreversible ice-sheet retreat from the continental shelf edge. For a network of ice streams whose surface elevations are now below the ELA then negative mass balance will force grounding line retreat, noting that earlier on, advance across this

area was only possible because the advancing ice streams had thicker surface profiles prior to reaching the continental shelf edge. This calving-induced ice stream–ELA feedback that we sketch out here requires investigation by modelling because of the large number of coupled factors that are involved. Is there a 'sweet spot' that exists for marine sectors of ice sheets and their ELAs such that this feedback or instability occurs?

A version of this destabilizing feedback has already been physically demonstrated in numerical ice-sheet modelling (Robel & Tziperman 2016; Gandy *et al.* 2019) but in cases not from increased calving on reaching the continental shelf edge, but from a lowering of the ELA (warming) during deglaciation. An additional accelerant to the feedback, first identified in Robel & Tziperman (2016) and then in Gandy *et al.* (2019), is that the increase in surface slopes in ice stream onset zones (Fig. 18) increases ice velocity here and promotes upstream growth of ice streaming and expansion of fast flow networks. Further feedbacks could also arise from increased surface meltwater reaching the bed and increasing basal lubrication (Zwally *et al.* 2002). We therefore speculate that for the BIIS its anomalous 'early retreat' from marine sectors might have occurred through a cascade of effects primarily driven by calving-induced ice stream–ELA feedback and runaway retreat. In this argument the ice sheet was sensitive to this feedback because it was already close to its climatically controlled maximum extent when it ran out of continental shelf to advance across. It explains why the grounding line did not persist at the continental shelf edge for long and why it retreated prior to climate warming. Much of our understanding about the mechanics and dynamics of ice streams comes from observations and modelling of Antarctic examples, which are not typical of mid-latitude ice sheets (or future Polar ice sheets) in that they (currently) experience little to no surface melting to influence their dynamics, and yet important instabilities between melt, ELA and dynamics might exist.

Duration of land exposure from beneath ice

The presence of a kilometre thick ice sheet flowing over the landscape resulted in erosion of bedrock and a widespread redistribution of sediment as glacial deposits. After deglaciation these freshly exposed surfaces became available for the production of soil and a recolonization by biota, including humans, and with a refreshed and renewed hydrological and groundwater system. To help in biological and archaeological studies we plot the duration of time that has elapsed since land has been exposed from beneath ice, based on our reconstruction of the last glacial period and those of earlier glacials (Fig. 19). Reintroductions of biota from distant refugia were affected by pathways available for inward migration and our reconstructed maps of sea level change and ice cover at various times (Figs 5, 6)

might also help in these studies. The length of time that the seabed has been exposed from beneath ice can visualized in Fig. 5 and in Data S3 and S4.

Palaeoglaciological lessons for the interpretation and modelling of existing and future ice sheets

The main lesson for interpreting short-term (10–100 years) ice-marginal fluctuations of existing ice sheets is that such retreat rate measurements may not be representative of longer term trends. The markedly stepped retreat of the British–Irish Ice Sheet and the characteristic that individual margins were often not acting in concert with their neighbours highlight the perils of such thinking. Rather, specific topographical, geographical and geological factors of a region can lead to ice-marginal changes out of synchrony with climate or sea level forcing, and out of synchrony with nearby catchments due to ice piracy and wider flow adjustments. We propose that such stepped and knock-on ice geometrical readjustments are widespread in the behaviour of palaeo-, existing and future ice sheets and yet are difficult to diagnose, are easily ignored, or relegated in significance in favour of more newsworthy interpretations of (over) simplified climate teleconnections or instabilities. Our quantification of retreat rates and how these varied across the marine to terrestrial transition and across different topographical and geographical settings might provide useful contexts for framing and interpreting retreat rates from modern ice sheets.

We show that glacio-isostatic depression of the bed of the ice sheet triggered retreat, and suggest that bed relaxation upwards during the course of deglaciation likely also influenced rates of ice loss, with possible stabilizing effects on the mid continental shelf. These interactions highlight the importance of improved knowledge of glacio-isostasy for the modelling of future ice sheets and sea level rise.

In addition to glacio-isostatic and warming controls on deglaciation, our reconstruction underlines the importance of second order regional bed topographic and bed strength controls on modulating the rate of retreat of marine-based sectors of ice sheets. The lessons from this are firstly that we should not over-interpret or extrapolate from observed grounding line changes, say in Antarctica, without good knowledge of subglacial topography and bed properties, and secondly, that efforts to improve the resolution and accuracy of subglacial topography (e.g. Fretwell *et al.* 2013) will be vital for improving predictions of ice mass loss and seal level rise.

Are ice streams merely slaves to mass balance (arising from, and governed as part of, a wider self-adjusting network), or do individual ice streams profoundly alter the course of deglaciation by key activations? For the Laurentide Ice Sheet, Stokes *et al.* (2016) found that ice stream activity simply scaled with ice-sheet volume during deglaciation, pointing to the former interpreta-

tion. For the BIIS however, we suspect that its smaller size and increased sensitivity to change meant that whilst most ice streams likely operated in a regulating role, some underwent changes large enough to significantly alter the pace of whole ice-sheet deglaciation (tipping points), notably those that triggered knock-on ice geometric effects, such as the collapse of North Sea ice. The question could be usefully addressed by a series of ice-sheet modelling experiments that try to elucidate the extent to which individual ice streams and their knock-on effects control whole ice-sheet volume change, rather than just a regional redistribution of ice loss that other ice streams then balance out.

Although the early loss of marine sectors of the ice sheet was primarily concluded to be due to ice loading, which increased water depths and therefore ice calving, we suggested two alternatives that might have acted in concert or have been dominant factors. These deserve further exploration, namely the calving-induced ice stream–ELA feedback, and whether the close relationship found between timing of early deglaciation and orbitally induced increase in summer insolation, producing more surface melting, is causative or coincidental. Does the direct inclusion of these in ice-sheet models improve their predictability, and hence reliability for making forecasts?

We note that the time resolution of our analysis is of the order of 100–1000 years (due mostly to dating precision) and that satellite observations of modern ice sheets are of the order of 10 years, but we suggest that the 100s-year time scale is of most relevance to society and might actually be the most important glaciological time scale for dynamics. We suggest that improvements in the precision of dating are therefore worthwhile and that palaeo-records of deglaciation at 100-year scales should be sought.

Although we nudged the PISM model reconstruction of the ice sheet to the empirically defined limits, we found that for four timeslices (Fig. 6) we were unable to reasonably get the modelled ice extent close enough to the empirical limits (see Discussion). From this we infer that there are ingredients missing in the ice-sheet modelling and deserving of further attention to improve model formulation. That we initially struggled to get the model to retreat from the shelf edge fast enough along the western and northern margins is most likely explained by local ocean warming effects that were not sufficiently included in the modelling, or perhaps from flexure of ice shelves from the large tidal ranges forecast to exist but not applied in the modelling. The 150-km model underrun in the Celtic Sea points to a process, forcing, or feedback that is likely missing in the numerical modelling. We suggest that a thermal or basal water instability might be required to produce a non-steady oscillation (surge), or as an alternative we speculate that the drainage of lakes on, or under the ice stream, may have temporarily facilitated faster ice flow by locally increasing basal

lubrication. In common with our own efforts, no numerical model has been able to simulate the full extension of the Irish Sea Ice Stream and so an important challenge remains; to develop new ingredients in process-based numerical modelling so that simulations can reconcile with the geological record.

Given the BIIS's small size and topographic complexity, along with its well-constrained history of retreat and relative sea level variations, we suggest that it is an excellent and data-rich target for future exploration, testing and improving of ice-sheet modelling formulations. Specific examples so far that use BRITICE-CHRONO reconstructions include ice-sheet modelling simulations using BICICLES (Cornford *et al.* 2013) on exploring the role of marine ice-sheet instability and ice shelves in the retreat of the Minch Ice Stream (Gandy *et al.* 2018), deciphering the model ingredients required to correctly predict ice streaming within the ice sheet (Gandy *et al.* 2019) and on understanding the role of ice saddle collapse and marine ice-sheet instabilities in deglaciating the North Sea (Gandy *et al.* 2021). The development of tools for assessing model simulations against empirical data have been reported in Ely *et al.* (2021) and have been used with BRITICE-CHRONO data to assess (quantitatively score) the performance of ensemble runs of the evolution of the ice sheet, using the PISM (Winkelmann *et al.* 2011). Our reconstructions have also been used in GIA modelling and sea level investigations, such as on fingerprinting of Meltwater Pulse 1A (Lin *et al.* 2021), forecasting 21st century sea levels around Britain and NW Europe, the UKCP18 Marine Report (Palmer *et al.* 2018), and the finding of marine ice-sheet instability (Gandy *et al.* 2018; Bradwell *et al.* 2019) used in consideration of ice-sheet instabilities in relation to sea level rise in the 6th Assessment Report of the Intergovernmental Panel on Climate Change (IPCC) (Fox-Kemper *et al.* 2021). The glaciological meaning of records of ice rafted debris has been investigated using ice flux data from the model reconstruction; to what extent do variations in IRD flux match with changes in ice-sheet mass balance? Wilton *et al.* (2021) explored this comparing by results from an iceberg–ocean model tracking the trajectory of icebergs discharged from the ice sheet (using fluxes from the ice-sheet modelling), and computing the likely fluxes of debris delivered to nearby observations of ice rafted debris.

Conclusions

The BRITICE-CHRONO project has tripled the number of dated sites for constraining the timing of ice-sheet retreat and has extended the spatial footprint of information on timing to the marine sectors. Samples were deliberately positioned orthogonal to the known pattern of ice retreat and within a transect scheme at an ice sheet-wide scale (Fig. 2) in order to maximize the constraining

value of each age. The BIIS is now the world's most well-constrained retreating ice sheet, contemporary or palaeo, at time scales of 10^{-2} to 10^{-4} years, and with ages well spread across its former extent.

In summary, the BRITICE-CHRONO project (logistics and participants described in Clark *et al.* 2021) sampled material for dating at 914 sites, on- and offshore, producing 690 new age assessments (338 radiocarbon; 162 luminescence and 190 cosmogenic) related to the advance or retreat of the ice sheet. A quality control exercise (Small *et al.* 2017b) reported 1189 legacy ages, reducing those deemed useful to 221. Together, these legacy and new age constraints have been reported along with their stratigraphical and glaciological contexts to build local and regional reconstructions of ice advance and retreat in a series of 23 publications (Peters *et al.* 2016; Sejrup *et al.* 2016; Evans *et al.* 2017; Small *et al.* 2017a, 2018; Smedley *et al.* 2017a, b; Arosio *et al.* 2018; Bateman *et al.* 2018; Callard *et al.* 2018, 2020; Chiverrell *et al.* 2018; Evans *et al.* 2018a, b; Lockhart *et al.* 2018; Roberts *et al.* 2018, 2019, 2020; Bradwell *et al.* 2019; Ó Cofaigh *et al.* 2019; Scourse *et al.* 2019; Wilson *et al.* 2019; Tarlati *et al.* 2020). These findings were then synthesized into coherent map-based reconstructions of ice advance and retreat across the marine to terrestrial transition for each of the eight transects investigated. This was achieved with the help of Bayesian age sequence modelling to deal with age outliers and uncertainties regarding marine reservoir correction, and to improve dating precision. These benchmark reconstructions are reported in a special issue of the *Journal of Quaternary Science* (BRITICE-CHRONO reconstructions of the last British-Irish Ice Sheet, 2021; Benetti *et al.* 2021; Bradwell *et al.* 2021a, b; Chiverrell *et al.* 2021; Evans *et al.* 2021; Ó Cofaigh *et al.* 2021; Scourse *et al.* 2021) and include assessments of the hierarchical controls on ice-sheet retreat, including climatic, sea level, topographical, geological, ice shelf buttressing and ice streaming, and with some findings of unforced oscillations (glaciological instabilities) including ice-marginal re-advances.

Here we used all assembled information on the timing constraints to make whole ice-sheet reconstructions from 31 ka, including from the eight transects and for all areas in between, and from the continental shelf edge until the final remaining small ice caps at 15 ka. An empirical reconstruction (lines drawn on maps that best fit the evidence) was presented as a series of palaeogeographical maps at 1-ka intervals, and which include error assessment on margin positions. Using a novel method of climate forcing and glacio-isostatic adjustment, a numerical ice-sheet model (PISM; Winkelmann *et al.* 2011) was nudged to fit within the error bounds of the empirical reconstruction to produce a model reconstruction that includes ice thickness, velocity, flow geometry and basal thermal regime. We consider this as our preferred reconstruction and it constitutes the main conclusion

of this paper. It is presented as a series of palaeoglaciological and palaeotopographical maps and data (including relative sea level change) at 1-ka intervals between 31 and 15 ka. This reconstruction of the evolution of the ice sheet through time has been analysed and described earlier and yields the following headline findings:

- Initiation and rapid early growth of the ice sheet pre-dates its previously assumed timing (i.e. Late Devensian, MIS 2), with the Scottish Ice Sheet advancing in the later parts of MIS 3 through the North Minch at 32–31 ka and reaching as far as the continental shelf break by around 30 ka (Bradwell *et al.* 2021b). Growth was remarkably rapid with the ice sheet expanding from a Scottish Highlands Ice Sheet, to a fully coalesced BIIS, although not yet joined with the Welsh Ice Sheet. This fivefold expansion in size in 1000 years demonstrates that ice advance can be rapid and that calving icebergs along an ice margin advancing across the shelf did little to slow down ice-sheet growth.
- Robust confirmation is made of earlier inferences that ice reached the continental shelf edge during the last glacial around most of its perimeter, rather than solely during previous glacial stages, and that confluence between British and Scandinavian ice led to establishment of a thick (>1 km) North Sea ice divide.
- The ice sheet is found to be larger than previously thought and extending as far west as the Porcupine Bank (Peters *et al.* 2016; Ó Cofaigh *et al.* 2021), and as far south as the continental shelf break in the Celtic Sea (Scourse *et al.* 2019). This southernmost limit reaches beyond 49°, the latitude of Paris. The maximum areal extent reached 900 000 km^2 at 26 ka, and the maximum volume occurred at 23 ka with 717 112 km^3 of grounded ice and an estimated mass of 657 377 Giga tonnes, enough to raise sea level by 1.8 m once it melted. This is about half the volume of the present-day West Antarctic Ice Sheet and a quarter of the Greenland Ice Sheet.
- At 24 ka over half of the ice sheet rested below sea level, which emphasizes its marine-based properties. The lithosphere was depressed by some 60 m relative to today in central Ireland and 130 m in parts of Scotland. The ice sheet had marine margins of around 50% summed over the whole cycle of growth and decay, and so ice loss by calving and submarine melting was a significant control on the ice sheet's mass balance.
- The existence of fringing ice shelves in some locations such as the Minch and west of Ireland (Bradwell *et al.* 2019; Ó Cofaigh *et al.* 2021) has been established through interpretation of submarine glacial landforms and sediments and we indicate their widespread occurrence in simulations by ice-sheet/shelf modelling. Ice shelves are shown to influence retreat rates through the effects on buttressing upstream ice flow (Gandy *et al.* 2018, 2021).

- Maximum ice extents were asynchronous between sectors and there is no single time at which the ice-sheet margins were everywhere at their maximum extent. Overall, the maximum areal extent of the ice sheet was at 26 ka. In the north and west, maximum limits were attained as early as 30–26 ka, and as late as 22 ka along parts of the southern margin. This asynchrony is explained by simple geography in that the continental shelf west of the British Isles is narrow (~100 km) and most of the snow-nourishing mountains lay close to the western coasts, such that ice growth here rapidly reached the limit imposed by the shelf width. In contrast, the southern margin spent longer advancing across England in response to continued glacial cooling, and the southern North Sea reached its maximum limit as late as 22 ka, arising from the later coalescence with Scandinavian ice, delayed because much Scandinavian ice was lost down the NCIS. The Channel acted as an overspill of Scandinavian ice with its western margin being an important suture between the ice-sheet complexes, permitting them to behave quasi-independently, for example with British ice around Shetland retreating at a time that the NCIS was still advancing.
- Given the above-mentioned asynchrony, then the concept of a Local LGM for the ice sheet breaks down, or at least does not exist in the sense of a narrowly defined window of time. An ice sheet in steady state (neutral mass balance) is not found in the reconstruction; rather we have a constantly rapidly adjusting ice sheet.
- The hypothesis that margins of the main ice catchments retreated synchronously in simple response to external climate forcing is rejected because we find asynchrony in the onset of retreat across the sectors, ranging between 30 and 22 ka. This rules out a simple climate explanation for the onset of retreat, especially as retreat was occurring thousands of years prior to climate warming.
- From analyses of retreat rates we accept the hypothesis that the marine-influenced sectors collapsed rapidly (<1000 years) and that once onshore the ice sheet stabilized and retreated more slowly. The pace of retreat was found to vary between slow (<50 m a^{-1}) at mostly terrestrial margins, faster (up to 80 m a^{-1}) at marine-calving margins mostly on the west and northern continental shelves, and with much faster (80–451 m a^{-1}) collapse events in the Celtic, Irish and North Seas. All very fast retreat rates (>200 m a^{-1}) were marine, but marine retreat can also be slow. Retreat rates of up to 50 m a^{-1} were the most frequent with 10 m a^{-1} as the modal value across the whole ice sheet. Note that these time-averaged or net retreat rates at 1-ka timesteps likely mask faster short-lived (decadal) rates that are below our dating resolution.

- Quantitative comparison of rates of grounding line retreat against their computed flotation factors demonstrate that retreat was faster for more lightly grounded margins (higher flotation factors) than heavily grounded cases.
- Marine ice-sheet instability (MISI) was not found to be the primary driver of deglaciation, because MISI was the exception rather than the rule across the region due to the mostly shallow seawater depths. It very likely occurred, however, in the Minch and Norwegian Channel Ice Steams (Gandy *et al.* 2018, 2021; Bradwell *et al.* 2019), which have greater water depths than is typical across the domain. This is a crucial discovery because in the case of the Minch Ice Stream, rapid retreat occurred across reverse bed slopes when the climate was cooling, thereby providing rare and valuable empirical demonstration that an instability occurred, rather than grounding line retreat simply accompanying climate-forced retreat.
- A major finding is that we reject our Hypothesis 2 (see Introduction) because the ice sheet responded differently to climate and sea level forcing across sectors and scales. Controls on ice-sheet demise are a mixture of forcings that are best considered in a scale hierarchy from ice-sheet scale, down through outlet scale (transect), and then more locally, as described in the following.

The first order controls on deglaciation were threefold: glacio-isostatic loading of continental shelves, increased water depths and ice calving, all of which triggered retreat in marine-based areas ahead of climate warming. This was staggered between sectors according to their loading history, with Scotland first (30 ka) and then Ireland (27 ka). Then the collapse of North Sea ice (21–19 ka) was a consequence of retreat of the NCIS (see below), which unzipped British and Scandinavian ice permitting widespread ingress of marine waters and expansion of calving margins. Final deglaciation was by climate warming from around 19 ka, which increased surface melting, leading to fairly even ice margin retreat of the remaining, terrestrially grounded ice sheet. A further complicating factor was collapse events, where margin retreat was a consequence of glaciological instabilities that had over-extended the margin (i.e. went further than predicted by modelling of mass balance), such as in the Irish Sea Ice Stream (Celtic–Irish Sea) and in the southern North Sea. More simply, the first order controls on demise were that glacio-isostatic loading killed the marine sectors aided by glaciological instabilities, and then climate warming finished off the smaller, now terrestrial ice sheet.

Operating at smaller spatial and temporal scales, the second order controls are explored and documented in our transect and modelling papers (Gandy *et al.* 2018, 2021; Benetti *et al.* 2021; Bradwell *et al.* 2021a, b; Chiverrell *et al.* 2021; Evans *et al.* 2021; Ó Cofaigh

et al. 2021; Scourse *et al.* 2021). They include large fluctuations in rates of retreat arising from marine ice-sheet instability and from the loss of ice shelf buttressing, on for example the Minch Ice Stream (Bradwell *et al.* 2019; Gandy *et al.* 2019). The trigger for retreat of the NCIS, suggested by modelling simulations that broadly fit the empirical data (Gandy *et al.* 2020), was by calving-induced ice stream–ELA feedback (Fig. 18) along with episodes of MISI. Topography has been shown to modulate rates of retreat due to variations in trough geometry, with pinning points (shallowings and narrowings) producing stillstands of ice margins, overdeepenings accelerating retreat, and with variations in the width of calving margins influencing the rate of grounding line retreat (Smedley *et al.* 2017a; Callard *et al.* 2018; Chiverrell *et al.* 2018; Small *et al.* 2018; Bradwell *et al.* 2019). Such variations in trough geometry were often found to have a greater influence in regulating retreat than climate–ocean forcing on time scales of thousands of years. Relief development of large grounding zone wedges may also have stabilized retreat in places (Batchelor & Dowdeswell 2015). Ice dammed lakes were found to frequently accompany ice-marginal retreat in some sectors (Roberts *et al.* 2019; Chiverrell *et al.* 2021) and for the larger examples, such as Dogger Lake, their effect on ice advance, flow dynamics and retreat might have been substantial. Such influences of ice dammed lakes deserve future ice-sheet modelling experiments which include water ponding and ice calving on mass balance and flow speeds.

Related to bed topography, the wider geography was also found to exert a strong influence on ice dynamics and retreat rates. Large (10–100 km) adjustments to ice margins were frequently encountered across the transect reconstructions as direct consequences of nearby changes in ice mass geometry due to the disposition and pattern of, for example, coastal shape, and relative positioning of uplands, large troughs and marine embayments. Examples include interaction between retreat of the Malin Sea Ice Stream and ice flowing from adjacent uplands in Ireland (Wilson *et al.* 2019; Benetti *et al.* 2021), flow and ice-marginal readjustments, including re-advances, of Shetland ice as it felt changes in North Sea ice masses (Bradwell *et al.* 2021 a), an East Minch re-advance in the aftermath of ice shelf loss (Bradwell *et al.* 2021b), and expansion of Welsh ice into the accommodation space made available as Irish Sea ice withdrew from the Cheshire-Shropshire Plain (Chiverrell *et al.* 2021). Additionally, oscillations were found to arise from ice piracy, for example with increased outflow from the Irish Sea Ice Stream capturing ice accumulation away from its adjacent catchment and affecting retreat there and leading to widespread flow stagnation (Scourse *et al.* 2021). Together these geographical effects can be thought of as knock-on ice geometric readjustments, again seemingly independent of direct climate forcings.

In summary, retreat of the BIIS had first order controls on its demise by glacio-isostatic loading triggering retreat of the marine sectors and aided by glaciological instabilities (marine ice-sheet instability, calving-induced ice steam–ELA feedback, and saddle-collapse); climate warming then finished off the smaller, terrestrial ice sheet. Rapid ice-sheet collapse was initiated (22 ka) by ice stream retreat and saddle-collapse over the North Sea and at rates of ice loss of up to 194 km^3 a^{-1}. However, overprinted on the ice sheet-scale signal were second order controls exerting large (10–100 s km, over 1–4 thousands years) changes in the pace of retreat modulated by topographic variations of key troughs and with sector-scale ice geometrical readjustments arising from variations in the geography of the landscape. These second order controls produced a strongly stepped nature to deglaciation in specific sectors.

shore were conducted by most of the authors including MB, SLC, MS, DS, DD, SLL, D. Praeg, KJJVL, CB and PW. Scientific guidance and varied inputs on modelling, data compilation and interpretation were provided by LG, NG, EG, ALCH, GRB, SMC, D. Pollard and HPS.

Data availability statement. – GIS shapefiles of the empirical reconstruction, the master spreadsheet of chronology v2.1, modelling files of ice thickness and velocity and the GIA-modelled palaeotopographies and coastline position are available for download in Clark *et al.* (2022).

References

Arosio, R., Crocket, K. C., Nowell, G. M., Callard, S. L., Howe, J. A., Benetti, S., Fabel, D., Moreton, S. & Clark, C. D. 2018: Weathering fluxes and sediment provenance on the SW Scottish shelf during the last deglaciation. *Marine Geology 402*, 81–98.

Ascough, P., Cook, G. & Dugmore, A. 2005: Methodological approaches to determining the marine radiocarbon reservoir effect. *Progress in Physical Geography: Earth and Environment 29*, 532–547.

Austin, W. E. N., Bard, E., Hunt, J. B., Kroon, D. & Peacock, J. D. 1995: The ¹⁴C age of the Icelandic Vedde Ash: implications for Younger Dryas marine reservoir age corrections. *Radiocarbon 37*, 53–62.

Bailey, R. M., Bray, H. & Stokes, S. 2003: Inductively-coupled plasma mass spectrometry (ICP-MS) for dose rate determination: some guidelines for sample preparation and analysis. *Ancient TL 21*, 11–14.

Balco, G., Stone, J. O., Lifton, N. A. & Dunai, T. J. 2008: A complete and easily accessible means of calculating surface exposure ages or erosion rates from ¹⁰Be and ²⁶Al measurements. *Quaternary Geochronology 3*, 174–195.

Ballantyne, C. K. & Stone, J. O. 2015: Trimlines, blockfields and the vertical extent of the last ice sheet in southern Ireland. *Boreas 44*, 277–287.

Ballantyne, C. K., Fabel, D., Gheorghiu, D., Rodés, Á., Shanks, R. & Xu, S. 2017: Late Quaternary glaciation in the Hebrides sector of the continental shelf: cosmogenic nuclide dating of glacial events on the St Kilda archipelago. *Boreas 46*, 605–621.

Ballantyne, C. K., McCarroll, D. & Stone, J. O. 2006: Vertical dimensions and age of the Wicklow Mountains ice dome, Eastern Ireland, and implications for the extent of the last Irish Ice Sheet. *Quaternary Science Reviews 25*, 2048–2058.

Ballantyne, C. K., McCarroll, D. & Stone, J. O. 2007: The Donegal ice dome, northwest Ireland: dimensions and chronology. *Journal of Quaternary Science 22*, 773–783.

Ballantyne, C. K., Rinterknecht, V. & Gheorghiu, D. M. 2013: Deglaciation chronology of the Galloway Hills Ice Centre, southwest Scotland. *Journal of Quaternary Science 28*, 412–420.

Ballantyne, C. K., Schnabel, C. & Xu, S. 2009: Readvance of the last British–Irish Ice Sheet during Greenland Interstade 1 (GI-1): the Wester Ross Readvance, NW Scotland. *Quaternary Science Reviews 28*, 783–789.

Ballantyne, C. K., Stone, J. O. & McCarroll, D. 2008: Dimensions and chronology of the last ice sheet in Western Ireland. *Quaternary Science Reviews 27*, 185–200.

Barr, I. D., Ely, J. C., Spagnolo, M., Clark, C. D. & Evans, I. S. 2017: Climate patterns during former periods of mountain glaciation in Britain and Ireland: inferences from the cirque record. *Palaeogeography, Palaeoclimatology, Palaeoecology 485*, 466–475.

Barth, A. M., Clark, P. U., Clark, J., McCabe, A. M. & Caffee, M. 2016: Last Glacial Maximum cirque glaciation in Ireland and implications for reconstructions of the Irish Ice Sheet. *Quaternary Science Reviews 141*, 85–93.

Batchelor, C. & Dowdeswell, J. 2015: Ice-sheet grounding-zone wedges (GZWs) on high-latitude continental margins. *Marine Geology 363*, 65–92.

Bateman, M. D., Evans, D. J. A., Roberts, D. H., Medialdea, A., Ely, J. & Clark, C. D. 2018: The timing and consequences of the blockage of the Humber Gap by the last British–Irish Ice Sheet. *Boreas 47*, 41–61.

Becker, L. W. M., Sejrup, H. P., Hjelstuen, B. O., Haflidason, H. & Dokken, T. M. 2018: Ocean-ice sheet interaction along the SE Nordic Seas margin from 35 to 15 ka BP. *Marine Geology 402*, 99–117.

Benetti, S., Chiverrell, R. C., Ó Cofaigh, C., Burke, M., Medialdea, A., Small, D., Ballantyne, C., Bateman, M. D., Callard, S. L., Wilson, P., Fabel, D., Clark, C. D., Arosio, R., Bradley, S., Dunlop, P., Ely, J. C., Gales, J., Livingstone, S. J., Moreton, S. G., Purcell, C., Saher, M., Schiele, K., Van Landeghem, K. & Weilbach, K. 2021: Exploring controls of the early and stepped deglaciation on the western margin of the British Irish Ice Sheet. *Journal of Quaternary Science 36*, 833–870.

Benetti, S., Dunlop, P. & Ó Cofaigh, C. 2010: Glacial and glacially-related features on the continental margin of northwest Ireland mapped from marine geophysical data. *Journal of Maps 6*, 14–29.

Benn, D. I., Warren, C. R. & Mottram, R. H. 2007: Calving processes and the dynamics of calving glaciers. *Earth Science Reviews 82*, 143–179.

Berger, A. 1992: *Orbital Variations and Insolation Database*. IGBP PAGES/World Data Center for Paleoclimatology. *Data Contribution Series #92-007*. NOAA/NGDC Paleoclimatology Program, Boulder CO, USA.

Berger, A. & Loutre, M. F. 1991: Insolation values for the climate of the last 10 million years. *Quaternary Science Reviews 10*, 297–317.

Bickerdike, H. L., Evans, D. J. A., Ó Cofaigh, C. & Stokes, C. R. 2016: The glacial geomorphology of the Loch Lomond Stadial in Britain: a map and geographic information system resource of published evidence. *Journal of Maps 12*, 1178–1186.

Bishop, W. W. & Dickson, J. H. 1970: Radiocarbon dates related to the Scottish Late-Glacial Sea in the Firth of Clyde. *Nature 227*, 480–482.

Borchers, B., Marrero, S., Balco, G., Caffee, M., Goehring, B., Lifton, N., Nishiizumi, K., Phillips, F., Schaefer, J. & Stone, J. 2016: Geological calibration of spallation production rates in the CRONUS-Earth project. *Quaternary Geochronology 31*, 188–198.

Boulton, G. & Hagdorn, M. 2006: Glaciology of the British Isles Ice Sheet during the last glacial cycle: form, flow, streams and lobes. *Quaternary Science Reviews 25*, 3359–3390.

Bowen, D. Q., Phillips, F. M., McCabe, A. M., Knutz, P. C. & Sykes, G. A. 2002: New data for the Last Glacial Maximum in Great Britain and Ireland. *Quaternary Science Reviews 21*, 89–101.

Bowen, D. Q., Rose, J., McCabe, A. M. & Sutherland, D. G. 1986: Correlation of Quaternary glaciations in England, Ireland, Scotland and Wales. *Quaternary Science Reviews 5*, 299–340.

Braconnot, P., Harrison, S. P., Otto-Liesner, B., Abe-Ouchi, A., Jungclaus, J. & Peterschmitt, J. 2011: The paleoclimate modeling intercomparison project contribution to CMIP5. *CLIVAR Exchanges 56*, 15–18.

Bradley, S. L., Milne, G. A., Shennan, I. & Edwards, R. 2011: An improved glacial isostatic adjustment model for the British Isles. *Journal of Quaternary Science 26*, 541–552.

Bradley, S. L., Reerink, T. J., Wal, R. S. W. & van de Helsen, M. M. 2018: Simulation of the Greenland Ice Sheet over two glacial–interglacial cycles: investigating a sub-ice-shelf melt parameterization and relative sea level forcing in an ice-sheet–ice-shelf model. *Climate of the Past 14*, 619–635.

Bradwell, T., Fabel, D., Stoker, M., Mathers, H., McHargue, L. & Howe, J. 2008a: Ice caps existed throughout the Lateglacial Interstadial in northern Scotland. *Journal of Quaternary Science 23*, 401–407.

Bradwell, T., Stoker, M. S., Golledge, N. R., Wilson, C. K., Merritt, J. W., Long, D., Everest, J. D., Hestvik, O. B., Stevenson, A. G., Hubbard, A. L., Finlayson, A. G. & Mathers, H. E. 2008b: The northern sector of the last British Ice Sheet: maximum extent and demise. *Earth Science Reviews 88*, 207–226.

Bradwell, T., Small, D., Fabel, D., Smedley, R. K., Clark, C. D., Saher, M. H., Callard, S. L., Chiverrell, R. C., Dove, D., Moreton, S. G., Roberts, D. H., Duller, G. A. T. & Ó Cofaigh, C. 2019: Ice-stream demise dynamically conditioned by trough shape and bed strength. *Science Advances 4*, eaau1380, https://doi.org/10.1126/sciadv.aau1380.

Bradwell, T., Small, D., Fabel, D., Clark, C. D., Chiverrell, R. C., Saher, M. H., Dove, D., Callard, S. L., Burke, M. J., Moreton, S. G., Medialdea, A., Bateman, M. D., Roberts, D. H., Golledge, N. R., Finlayson, A., Morgan, S. & Ó Cofaigh, C. 2021a: Pattern, style and timing of British–Irish Ice Sheet retreat: Shetland and northern North Sea sector. *Journal of Quaternary Science 36*, 681–722.

Bradwell, T., Fabel, D., Clark, C. D., Chiverrell, R. C., Small, D., Smedley, R. K., Saher, M. H., Moreton, S. G., Dove, D., Callard, S. L., Duller, G. A. T., Medialdea, A., Bateman, M. D., Burke, M. J., McDonald, N., Gilgannon, S., Morgan, S., Roberts, D. H. & Ó Cofaigh, C. 2021b: Pattern, style and timing of British–Irish Ice Sheet advance and retreat over the last 45 000 years: evidence from NW Scotland and the adjacent continental shelf. *Journal of Quaternary Science 36*, 871–933.

BRITICE-CHRONO reconstructions of the last British-Irish Ice Sheet. 2021: Special Issue of *Journal of Quaternary Science 26*, 673–960.

Bronk Ramsey, C. 2009: Bayesian analysis of radiocarbon dates. *Radiocarbon 51*, 337–360.

Brown, E. J., Rose, J., Coope, R. G. & Lowe, J. J. 2007: An MIS 3 age organic deposit from Balglass Burn, central Scotland: palaeoenvironmental significance and implications for the timing of the onset of the LGM ice sheet in the vicinity of the British Isles. *Journal of Quaternary Science 22*, 295–308.

Browne, M. A. E. & McMillan, A. A. 1983: A late-Devensian marine and non-marine sequence near Dumbarton, Strathclyde. *Scottish Journal of Geology 19*, 229–234.

Browne, M. A. E., McMillan, A. A. & Hall, I. H. S. 1983: Blocks of marine clay in till near Helensburgh, Strathclyde. *Scottish Journal of Geology 19*, 321–325.

Browne, M. A. E., Harkness, D. D., Peacock, J. D. & Ward, R. G. 1977: The date of deglaciation of the Paisley-Renfrew area. *Scottish Journal of Geology 13*, 301–303.

Bueler, E. & Brown, J. 2009: Shallow shelf approximation as a "sliding law" in a thermomechanically coupled ice sheet model. *Journal of Geophysical Research 114* (Issue F3), https://doi.org/10.1029/2008jf001179.

Callard, S. L., Ó Cofaigh, C., Benetti, S., Chiverrell, R. C., Van Landeghem, K. J. J., Saher, M. H., Gales, J. A., Small, D., Clark, C. D., Livingstone, S. J., Fabel, D. & Moreton, S. G. 2018: Extent and retreat history of the Barra Fan Ice Stream offshore western Scotland and Northern Ireland during the last glaciation. *Quaternary Science Reviews 201*, 280–302.

Callard, S. L., Ó Cofaigh, C., Benetti, S., Chiverrell, R. C., Van Landeghem, K. J. J., Saher, M. H., Livingstone, S. J., Clark, C. D., Small, D., Fabel, D. & Moreton, S. G. 2020: Oscillating retreat of the last British-Irish Ice Sheet on the continental shelf offshore Galway Bay, western Ireland. *Marine Geology 420*, 106087, https://doi.org/10.1016/j.margeo.2019.106087.

Calov, R. & Greve, R. 2005: Correspondence: a semi-analytical solution for the positive degree-day model with stochastic temperature variations. *Journal of Glaciology 51*, 173–175.

Carr, S. J., Hiemstra, J. F. & Owen, G. 2017: Landscape evolution of Lundy Island: challenging the proposed MIS 3 glaciation of SW Britain. *Proceedings of the Geologists Association 128*, 722–741.

Carter, R. W. G. 1993: Age, origin and significance of the raised gravel barrier at Church Bay, Rathlin Island, County Antrim. *Irish Geography 26*, 141–146.

Chiverrell, R. C. & Thomas, G. S. P. 2010: Extent and timing of the Last Glacial Maximum (LGM) in Britain and Ireland: a review. *Journal of Quaternary Science 25*, 535–549.

Chiverrell, R. C., Burke, M. J. & Thomas, G. S. P. 2016: Morphological and sedimentary responses to ice mass interaction during the last deglaciation. *Journal of Quaternary Science 31*, 265–280.

Chiverrell, R. C., Smedley, R. K., Small, D., Ballantyne, C. K., Burke, M. J., Callard, S. L., Clark, C. D., Duller, G. A. T., Evans, D. J. A., Fabel, D., van Landeghem, K., Livingstone, S., Ó Cofaigh, C., Thomas, G. S. P., Roberts, D. H., Saher, M., Scourse, J. D. & Wilson, P. 2018: Ice margin oscillations during deglaciation of the northern Irish Sea Basin. *Journal of Quaternary Science 33*, 739–762.

Chiverrell, R. C., Thomas, G. S. P., Burke, M., Medialdea, A., Smedley, R., Bateman, M., Clark, C., Duller, G. A. T., Fabel, D., Jenkins, G., Ou, X., Roberts, H. M. & Scourse, J. D. 2021: The evolution of the terrestrial-terminating Irish Sea glacier during the last glaciation. *Journal of Quaternary Science 36*, 752–779.

Chiverrell, R. C., Thrasher, I. M., Thomas, G. S. P., Lang, A., Scourse, J. D., Van Landeghem, K. J. J., McCarroll, D., Clark, C. D., Ó Cofaigh, C., Evans, D. J. A. & Ballantyne, C. K. 2013: Bayesian modelling the retreat of the Irish Sea Ice Stream. *Journal of Quaternary Science 28*, 200–209.

Choi, Y., Morlighem, M., Rignot, E. & Wood, M. 2021: Ice dynamics will remain a primary driver of Greenland ice sheet mass loss over the next century. *Communications Earth & Environment 2*, 1–9.

Clark, C. D., Chiverrell, R. C., Fabel, D., Hindmarsh, R. C. A., Ó Cofaigh, C. & Scourse, J. D. 2021: Timing, pace and controls on ice sheet retreat: an introduction to the BRITICE-CHRONO transect reconstructions of the British–Irish Ice Sheet. *Journal of Quaternary Science 36*, 673–680.

Clark, C. D., Ely, J. C., Fabel, D. & Bradley, S. 2022: BRITICE-CHRONO maps and GIS data of the last British-Irish Ice Sheet 31 to 15 ka, including model reconstruction, geochronometric age spreadsheet, palaeotopographies and coastline positions. *Pangaea*. https://doi.org/10.1594/PANGAEA.945729.

Clark, C. D., Ely, J. C., Greenwood, S. L., Hughes, A. L. C., Meehan, R., Barr, I. D., Bateman, M. D., Bradwell, T., Doole, J., Evans, D. J. A., Jordan, C. J., Monteys, X., Pellicer, X. M. & Sheehy, M. 2018: BRITICE Glacial Map, version 2: a map and GIS database of glacial landforms of the last British–Irish Ice Sheet. *Boreas 47*, 11–27.

Clark, C. D., Gibbard, P. L. & Rose, J. 2004: Pleistocene glacial limits in England, Scotland and Wales. *Developments in Quaternary Science 2* (Part 1), 47–82.

Clark, C. D., Hughes, A. L. C., Greenwood, S. L., Jordan, C. J. & Sejrup, H. P. 2012: Pattern and timing of retreat of the last British-Irish Ice Sheet. *Quaternary Science Reviews 44*, 112–146.

Clark, P. U., McCabe, A. M., Mix, A. C. & Weaver, A. J. 2004: Rapid rise of sea level 19,000 years ago and its global implications. *Science 304*, 1141–1144.

Clark, J., McCabe, A. M., Schnabel, C., Clark, P. U., McCarron, S., Freeman, S. P. H. T., Maden, C. & Xu, S. 2009: Cosmogenic ^{10}Be chronology of the last deglaciation of western Ireland, and implications for sensitivity of the Irish Ice Sheet to climate change. *Geological Society of America Bulletin 121*, 3–16.

Colarossi, D., Duller, G. A. T., Roberts, H. M., Tooth, S. & Lyons, R. 2015: Comparison of paired quartz OSL and feldspar post-IR IRSL dose distributions in poorly bleached fluvial sediments from South Africa. *Quaternary Geochronology 30*, 233–238.

Cornford, S. L., Martin, D. F., Graves, D. T., Ranken, D. F., Le Brocq, A. M., Gladstone, R. M., Payne, A. J., Ng, E. G. & Lipscomb, W. H. 2013: Adaptive mesh, finite volume modeling of marine ice sheets. *Journal of Computational Physics 232*, 529–549.

Dansgaard, W., Johnsen, S. J., Clausen, H. B., Dahl-Jensen, D., Gundestrup, N. S., Hammer, C. U., Hvidberg, C. S., Steffensen, J. P., Sveinbjörnsdottir, A. E., Jouzel, J. & Bond, G. 1993: Evidence for general instability of past climate from a 250-kyr ice-core record. *Nature 364*, 218–220.

Davies, B. J., Livingstone, S. J., Roberts, D. H., Evans, D. J. A., Gheorghiu, D. M. & Ó Cofaigh, C. 2019: Dynamic ice stream retreat in the central sector of the last British-Irish Ice Sheet. *Quaternary Science Reviews 225*, 105989, https://doi.org/10.1016/j.quascirev.2019.105989.

Davies, B. J., Roberts, D. H., Bridgland, D. R. & Ó Cofaigh, C. 2012: Dynamic Devensian ice flow in NE England: a sedimentological reconstruction. *Boreas 41*, 337–336.

Dove, D., Evans, D. J. A., Lee, J. R., Roberts, D. H., Tappin, D. R., Mellett, C. L., Long, D. & Callard, S. L. 2017: Phased occupation and retreat of the last British–Irish Ice Sheet in the southern North Sea; geomorphic and seismostratigraphic evidence of a dynamic ice lobe. *Quaternary Science Reviews 163*, 114–134.

Duller, G. A. T. 2006: Single grain optical dating of glacigenic sediments. *Quaternary Geochronology 1*, 296–304.

Duller, G. A. T. 2008a: Single grain optical dating of Quaternary sediments: why aliquot size matters in luminescence dating. *Boreas 37*, 589–612.

Duller, G. A. T. 2008b: *Luminescence Dating: Guidelines on Using Luminescence Dating in Archaeology.* 44 pp. English Heritage Publishing, Swindon.

Dunne, J., Elmore, D. & Muzikar, P. 1999: Scaling factors for the rates of production of cosmogenic nuclides for geometric shielding and attenuation at depth on sloped surfaces. *Geomorphology 27*, 3–11.

Durcan, J. A., King, G. E. & Duller, G. A. T. 2015: DRAC: Dose Rate and Age Calculator for trapped charge dating. *Quaternary Geochronology 28*, 54–61.

Dyke, A. S. & Prest, V. K. 1987: Late Wisconsinan and Holocene history of the Laurentide Ice Sheet. *Géographie Physique et Quaternaire 41*, 237–263.

Ely, J. C., Clark, C. D., Hindmarsh, R. C. A., Hughes, A. L. C., Greenwood, S. L., Bradley, S. L., Gasson, E., Gregoire, L., Gandy, N., Stokes, C. R. & Small, D. 2021: Recent progress on combining geomorphological and geochronological data with ice sheet modelling, demonstrated using the last British–Irish Ice Sheet. *Journal of Quaternary Science 36*, 946–960.

Ely, J. C., Clark, C. D., Small, D. & Hindmarsh, R. C. A. 2019: ATAT 1.1, an Automated Timing Accordance Tool for comparing ice-sheet model output with geochronological data. *Geoscientific Model Development 12*, 933–953.

Evans, D. J. A. & Thomson, S. A. 2010: Glacial sediments and landforms of Holderness, eastern England: a glacial depositional model for the North Sea lobe of the British–Irish Ice Sheet. *Earth-Science Reviews 101*, 147–189.

Evans, D. J. A., Bateman, M. D., Roberts, D. H., Medialdea, A., Hayes, L., Duller, G. A. T., Fabel, D. & Clark, C. D. 2017: Glacial Lake Pickering: stratigraphy and chronology of a proglacial lake dammed by the North Sea Lobe of the British-Irish Ice Sheet. *Journal of Quaternary Science 32*, 295–310.

Evans, D. J. A., Harrison, S., Vieli, A. & Anderson, E. 2012: The glaciation of Dartmoor: the southernmost independent Pleistocene ice cap in the British Isles. *Quaternary Science Reviews 45*, 31–53.

Evans, D. J. A., Roberts, D. H., Bateman, M. D., Ely, J., Medialdea, A., Burke, M. J., Chiverrell, R. C., Clark, C. D. & Fabel, D. 2018a: A chronology for North Sea Lobe advance and recession on the Lincolnshire and Norfolk coasts during MIS 2 and 6. *Proceedings of the Geologist's Association 130*, 523–540.

Evans, D. J. A., Roberts, D. H., Bateman, M. D., Medialdea, A., Ely, J., Moreton, S. G., Clark, C. D. & Fabel, D. 2018b: Sedimentation during Marine Isotope Stage 3 at the eastern margins of the Glacial Lake Humber basin, England. *Journal of Quaternary Science 33*, 871–891.

Evans, D. J. A., Roberts, D. H., Bateman, M. D., Clark, C. D., Medialdea, A., Callard, L., Grimoldi, E., Chiverrell, R. C., Ely, J., Dove, D., Ó Cofaigh, C., Saher, M., Bradwell, T., Moreton, S. G., Fabel, D. & Bradley, S. L. 2021: Retreat dynamics of the eastern sector of the British–Irish Ice Sheet during the last glaciation. *Journal of Quaternary Science 36*, 723–751.

Everest, J. & Kubik, P. 2006: The deglaciation of eastern Scotland: cosmogenic [10]Be evidence for a Lateglacial stillstand. *Journal of Quaternary Science 21*, 95–104.

Everest, J. D., Bradwell, T., Fogwill, C. J. & Kubik, P. W. 2006: Cosmogenic [10]Be age constraints for the wester ross readvance moraine: insights into British ice-sheet behaviour. *Geografiska Annaler Series A Physical Geography 88*, 9–17.

Everest, J. D., Bradwell, T., Stoker, M. & Dewey, S. 2013: New age constraints for the maximum extent of the last British–Irish Ice Sheet (NW sector). *Journal of Quaternary Science 28*, 2–7.

Eyles, N. & McCabe, A. M. 1989: The Late Devensian Irish Sea Basin: the sedimentary record of a collapsed ice sheet margin. *Quaternary Science Reviews 8*, 307–351.

Fabel, D., Ballantyne, C. K. & Xu, S. 2012: Trimlines, blockfields, mountain-top erratics and the vertical dimensions of the last British–Irish Ice Sheet in NW Scotland. *Quaternary Science Reviews 55*, 91–102.

Finlayson, A., Fabel, D., Bradwell, T. & Sugden, D. 2014: Growth and decay of a marine terminating sector of the last British–Irish Ice Sheet: a geomorphological reconstruction. *Quaternary Science Reviews 83*, 28–45.

Fisher, D., Reeh, N. & Langley, K. 1985: Objective reconstructions of the Late Wisconsinan Laurentide Ice Sheet and the significance of deformable beds. *Geographie Physique et Quaternaire 39*, 229–238.

Fox-Kemper, B., Hewitt, H. T., Xiao, C., Aðalgeirsdóttir, G., Drijfhout, S. S., Edwards, T. L., Golledge, N. R., Hemer, M., Kopp, R. E., Krinner, G., Mix, A., Notz, D., Nowicki, S., Nurhati, I. S., Ruiz, L., Sallée, J.-B., Slangen, A. B. A. & Yu, Y. 2021: Ocean, cryosphere and sea level change. *In Climate Change 2021: The Physical Science Basis – Contribution of Working Group I to the Sixth Assessment Report of the Intergovernmental Panel on Climate Change.* Geneva: Intergovernmental Panel on Climate Change 2021.

Fretwell, P. and 59 others 2013: Bedmap2: improved ice bed, surface and thickness datasets for Antarctica. *The Cryosphere 7*, 375–393.

Fuchs, M. & Owen, L. A. 2008: Luminescence dating of glacial and associated sediments: review, recommendations and future directions. *Boreas 37*, 636–659.

Gandy, N., Gregoire, L. J., Ely, J. C., Clark, C. D., Hodgson, D. M., Lee, V., Bradwell, T. & Ivanovic, R. F. 2018: Marine ice sheet instability and ice shelf buttressing of the Minch Ice Stream, northwest Scotland. *The Cryosphere 12*, 3635–3651.

Gandy, N., Gregoire, L. J., Ely, J. C., Cornford, S. L., Clark, C. D. & Hodgson, D. M. 2019: Exploring the ingredients required to successfully model the placement, generation, and evolution of ice streams in the British-Irish Ice Sheet. *Quaternary Science Reviews 223*, 105915, https://doi.org/10.1016/j.quascirev.2019.105915.

Gandy, N., Gregoire, L. J., Ely, J. C., Cornford, S. L., Clark, C. D. & Hodgson, D. M. 2021: Collapse of the last Eurasian Ice Sheet in the North Sea modulated by combined processes of ice flow, surface melt, and marine ice sheet instabilities. *Journal of Geophysical Research, Earth Surface 126*, e2020JF005755. https://doi.org/10.1029/2020jf005755.

Gemmell, A., Murray, A. S. & Connell, E. R. 2007: Devensian glacial events in Buchan (NE Scotland): a progress report on new OSL dates and their implications. *Quaternary Geochronology 2*, 237–242.

Gibbard, P. L. & Clark, C. D. 2011: Pleistocene glaciation limits in Great Britain. *Developments in Quaternary Sciences 15*, 75–93.

Gibbard, P. L., Hughes, P. D. & Rolfe, C. J. 2017: New insights into the Quaternary evolution of the Bristol Channel, UK. *Journal of Quaternary Science 32*, 564–578.

Gladstone, R. M., Payne, A. J. & Cornford, S. L. 2010: Parameterising the grounding line in flow-line ice sheet models. *The Cryosphere 4*, 605–619.

Golledge, N. R. 2020: Long-term projections of sea-level rise from ice sheets. *Wiley Interdisciplinary Review of Climate Change 11*, e634, https://doi.org/10.1002/wcc.634.

Golledge, N. R., Fabel, D., Everest, J. D., Freeman, S. & Binnie, S. 2007: First cosmogenic [10]Be age constraint on the timing of Younger Dryas glaciation and ice cap thickness, western Scottish Highlands. *Journal of Quaternary Science 22*, 785–791.

Gheorghiu, D. M., Fabel, D., Hansom, J. D. & Xu, S. 2012: Lateglacial surface exposure dating in the Monadhliath Mountains, Central Highlands, Scotland. *Quaternary Science Reviews 41*, 132–146.

Glasser, N. F., Hughes, P. D., Fenton, C., Schnabel, C. & Rother, H. 2012: [10]Be and [26]Al exposure-age dating of bedrock surfaces on the Aran ridge, Wales: evidence for a thick Welsh Ice Cap at the Last Glacial Maximum. *Journal of Quaternary Science 27*, 97–104.

Glasser, N. F., Davies, J. R., Hambrey, M. J., Davies, B. J., Gheorghiu, D. M., Balfour, J., Smedley, R. K. & Duller, G. A. T. 2018: Late Devensian deglaciation of south-west Wales from luminescence and cosmogenic isotope dating. *Journal of Quaternary Science 33*, 804–818.

Gowan, E. J., Tregoning, P., Purcell, A., Lea, J., Fransner, O. J., Noormets, R. & Dowdeswell, J. A. 2016: ICESHEET 1.0: a program to produce paleo-ice sheet reconstructions with minimal assumptions. *Geoscientific Model Development 9*, 1673–1682.

Graham, A. G. C., Lonergan, L. & Stoker, M. S. 2010: Depositional environments and chronology of Late Weichselian glaciation and deglaciation in the central North Sea. *Boreas 39*, 471–492.

Greenwood, S. L. & Clark, C. D. 2009: Reconstructing the last Irish Ice Sheet 2: a geomorphologically-driven model of ice sheet growth, retreat and dynamics. *Quaternary Science Reviews 28*, 3101–3123.

Greenwood, S. L., Simkins, L. M., Winsborrow, M. C. M. & Bjarnadóttir, L. R. 2021: Exceptions to bed-controlled ice sheet flow and retreat from glaciated continental margins worldwide. *Science Advances 7*, eabb6291, https://doi.org/10.1126/sciadv.abb6291.

Guérin, G., Mercier, N. & Adamiec, G. 2011: Dose-rate conversion factors: update. *Ancient TL 29*, 5–8.

Hall, A. M. & Jarvis, J. 1989: A preliminary report on the late Devensian glaciomarine deposits around St. Fergus, Grampian Region. *Quaternary Newsletter 59*, 7.

Hall, I. R., Colmenero-Hidalgo, E., Zahn, R., Peck, V. L. & Hemming, S. R. 2011: Centennial- to millennial-scale ice-ocean interactions in the subpolar northeast Atlantic 18-41 kyr ago. *Palaeoceanography 26*, PA2224, https://doi.org/10.1029/2010PA002084.

Hansen, V., Murray, A., Buylaert, J.-P., Yeo, E.-Y. & Thomsen, K. 2015: A new irradiated quartz for beta source calibration. *Radiation Measurements 81*, 123–127.

Heaton, T. J., Köhler, P., Butzin, M., Bard, E., Reimer, R. W., Austin, W. E. N., Ramsey, C. B., Grootes, P. M., Hughen, K. A., Kromer, B., Reimer, P. J., Adkins, J., Burke, A., Cook, M. S., Olsen, J. & Skinner, L. C. 2020: Marine20 - The marine radiocarbon age calibration curve (0–55,000 cal BP). *Radiocarbon 62*, 779–820.

Hedges, R. E. M., Housley, R. A., Law, I. A. & Perry, C. 1988: Radiocarbon-dates from the Oxford Ams system - Archaeometry Datelist-7. *Archaeometry 30*, 155–164.

Hedges, R. E. M., Housley, R. A., Law, I. A. & Bronk, C. R. 1989: Radiocarbon dates from the Oxford AMS system: archaeometry datelist 9. *Archaeometry 31*, 207–234.

Hedges, R. E. M., Housley, R. A., Ramsey, C. B. & Van Klinken, G. J. 1994: Radiocarbon dates from the Oxford ams system: archaeometry datelist 18. *Archaeometry 36*, 337–374.

Hedges, R. E. M., Pettitt, P. B., Ramsey, C. B. & Klinken, G. J. V. 1996: Radiocarbon dates from the Oxford Ams system - Archaeometry Datelist-22. *Archaeometry 38*, 391–415.

Helsen, M. M., van de Berg, W. J., van de Wal, R. S. W., van den Broeke, M. R. & Oerlemans, J. 2012: Coupled regional climate–ice-sheet simulation shows limited Greenland ice loss during the Eemian. *Climate of the Past 9*, 1773–1788.

Hill, A. R. & Prior, D. B. 1968: Directions of ice movement in North-East Ireland. *Proceedings of the Royal Irish Academy B66*, 71–84.

Hjelstuen, B. O., Sejrup, H. P., Valvik, E. & Becker, L. W. M. 2017: Evidence of an ice-dammed lake outburst in the North Sea during the last deglaciation. *Marine Geology 402*, 118–130.

Holloway, L. K., Peacock, J. D. & Smith, D. E. 2002: A Windermere Interstadial marine sequence: environmental and relative sea level interpretations for the western Forth Valley, Scotland. *Scottish Journal of Geology 38*, 41–54.

Hubbard, A., Bradwell, T., Golledge, N., Hall, A., Patton, H., Sugden, D., Cooper, R. & Stoker, M. 2009: Dynamic cycles, ice streams and their impact on the extent, chronology and deglaciation of the British–Irish ice sheet. *Quaternary Science Reviews 28*, 758–776.

Hughes, A. L. C., Greenwood, S. L. & Clark, C. D. 2011: Dating constraints on the last British-Irish Ice Sheet: a map and database. *Journal of Maps 7*, 156–184.

Hughes, A. L. C., Gyllencreutz, R., Lohne, Ä. S., Mangerud, J. & Svendsen, J. I. 2016: The last Eurasian ice sheets–a chronological database and time-slice reconstruction, DATED-1. *Boreas 45*, 1–45.

Huybrechts, P. 2002: Sea-level changes at the LGM from ice-dynamic reconstructions of the Greenland and Antarctic ice sheets during the glacial cycles. *Quaternary Science Reviews 21*, 203–231.

IMBIE Team 2020: Mass balance of the Greenland Ice Sheet from 1992 to 2018. *Nature 579*, 233–239.

IPCC 2010: *Workshop Report of the Intergovernmental Panel on Climate Change Workshop on Sea Level Rise and Ice Sheet Instabilities*, 227 pp. IPCC Working Group I Technical Support Unit, University of Bern, Bern, Switzerland.

Jacobi, R. M., Rose, J., MacLeod, A. & Higham, T. F. G. 2009: Revised radiocarbon ages on woolly rhinoceros (Coelodonta antiquitatis) from western central Scotland: significance for timing the extinction of woolly rhinoceros in Britain and the onset of the LGM in central Scotland. *Quaternary Science Reviews 28*, 2551–2556.

Jardine, W. G., Dickson, J. H., Haughton, P. D. W., Harkness, D. D., Bowen, D. Q. & Sykes, G. A. 1988: A late Middle Devensian interstadial site at Sourlie, near Irvine, Strathclyde. *Scottish Journal of Geology 24*, 288–295.

Jenkins, G. T. H., Duller, G. A. T., Roberts, H. M., Chiverrell, R. C. & Glasser, N. F. 2018: A new approach for luminescence dating glaciofluvial deposits - High precision optical dating of cobbles. *Quaternary Science Reviews 192*, 263–273.

John, B. 2018: *The Stonehenge Bluestones*. 256 pp. Greencroft Books, Newport.

Judd, J. W. 1902: Note on the nature and origin of the rock-fragments found in the excavations made at Stonehenge by Mr Gowland in 1901. *Archaeologia 58*, 106–118.

Knight, J. 2004: Sedimentary evidence for the formation mechanism of the Armoy moraine and late Devensian glacial events in the north of Ireland. *Geological Journal 39*, 403–417.

Köhler, P., Nehrbass-Ahles, C., Schmitt, J., Stocker, T. F. & Fishcer, H. 2017: Continuous record of the atmospheric greenhouse gas carbon dioxide (CO_2), final spline-smoothed data of calculated radiative forcing (Version 1). *PANGAEA*, https://doi.org/10.1594/PANGAEA.871271.

Lal, D., Barg, E. & Pavich, M. 1991: Development of cosmogenic nuclear methods for the study of soil erosion and formation rates. *Current Science 61*, 636–640.

Lawson, T. J. 1984: Reindeer in the Scottish Quaternary. *Quaternary Newsletter 42*, 7.

Lin, Y., Hibbert, F. D., Whitehouse, P. L., Woodroffe, S. A., Purcell, A., Shennan, I. & Bradley, S. L. 2021: A reconciled solution of Meltwater Pulse 1A sources using sea-level fingerprinting. *Nature Communications 12*, 2015, https://doi.org/10.1038/s41467-021-21990-y.

Livingstone, S. J., Roberts, D. H., Davies, B. J., Evans, D. J. A., Ó Cofaigh, C. & Gheorghiu, D. M. 2015: Late Devensian deglaciation of the Tyne gap palaeo-ice stream, northern England. *Journal of Quaternary Science 30*, 790–804.

Lockhart, E. A., Scourse, J. D., Praeg, D., Van Landeghem, K. J. J., Mellett, C., Saher, M., Callard, L., Chiverrell, R. C., Benetti, S., Ó Cofaigh, C. & Clark, C. D. 2018: A stratigraphic investigation of the Celtic Sea megaridges based on seismic and core data from the Irish-UK sectors. *Quaternary Science Reviews 198*, 156–170.

Lowe, J. J., Ammann, B., Birks, H. H., Björck, S., Coope, G. R., Cwynar, L., de Beaulieu, J.-L., Mott, R., Peteet, D. M. & Walker, M. J. C. 1994: Climatic changes in areas adjacent to the North Atlantic during the last glacial-interglacial transition (14-9 ka BP): a contribution to IGCP-253. *Journal of Quaternary Science 9*, 185–198.

Marrero, S. M., Phillips, F. M., Borchers, B., Lifton, N., Aumer, R. & Balco, G. 2016: Cosmogenic nuclide systematics and the CRONUS-calc program. *Quaternary Geochronology 31*, 160–187.

Martin, L. C. P., Blard, P. H., Balco, G. & Lavé, J. 2017: The CREp program and the ICE-D production rate calibration database: a fully parameterizable and updated online tool to compute cosmic-ray exposure ages. *Quaternary Geochronology 38*, 25–49.

Martin, M. A., Winkelmann, R., Haseloff, M., Albrecht, T., Bueler, E., Khroulev, C. & Levermann, A. 2011: The Potsdam parallel ice sheet model (PISM-PIK)–Part 2: dynamic equilibrium simulation of the Antarctic ice sheet. *The Cryosphere 5*, 727–740.

McCabe, A. M. 1986: Glaciomarine facies deposited by retreating tidewater glaciers; an example from the late Pleistocene of Northern Ireland. *Journal of Sedimentary Research 56*, 880–894.

McCabe, A. M. & Clark, P. U. 1998: Ice-sheet variability around the North Atlantic Ocean during the last deglaciation. *Nature 392*, 373–377.

McCabe, A. M. & Clark, P. U. 2003: Deglacial chronology from County Donegal, Ireland: implications for deglaciation of the British–Irish ice sheet. *Journal of the Geological Society of London 160*, 847–855.

McCabe, A. M. & Haynes, J. R. 1996: A late Pleistocene intertidal boulder pavement from an isostatically emergent coast, Dundalk bay, eastern Ireland. *Earth Surface Processes and Landforms 21*, 555–572.

McCabe, A. M., Clark, P. U. & Clark, J. 2005: AMS ^{14}C dating of deglacial events in the Irish Sea Basin and other sectors of the British–Irish ice sheet. *Quaternary Science Reviews 24*, 1673–1690.

McCabe, A. M., Clark, P. U. & Clark, J. 2007a: Radiocarbon constraints on the history of the western Irish ice sheet prior to the Last Glacial Maximum. *Geology 35*, 147–150.

McCabe, A. M., Cooper, J. A. G. & Kelley, J. T. 2007b: Relative sea-level changes from NE Ireland during the last glacial termination. *Journal of the Geological Society of London 164*, 1059–1063.

McCarroll, D., Stone, J. O., Ballantyne, C. K., Scourse, J. D., Fifield, L. K., Evans, D. J. A. & Hiemstra, J. F. 2010: Exposure-age constraints on the extent, timing and rate of retreat of the last Irish Sea ice stream. *Quaternary Science Reviews 29*, 1844–1852.

Morén, B. M., Sejrup, H. P., Hjelstuen, B. O., Borge, M. V. & Schäuble, C. 2018: The last deglaciation of the Norwegian Channel - geomorphology, stratigraphy and radiocarbon dating. *Boreas 47*, 347–366.

Murton, D. K., Pawley, S. M. & Murton, J. B. 2009: Sedimentology and luminescence ages of Glacial Lake Humber deposits in the central Vale of York. *Proceedings of the Geologists' Association 120*, 209–222.

Murray, A., Buylaert, J.-P. & Thiel, C. 2015: A luminescence dating intercomparison based on a Danish beach-ridge sand. *Radiation Measurements 81*, 32–38.

Nadeau, M.-J., Grootes, P. M., Voelker, A., Bruhn, F., Duhr, A. & Oriwall, A. 2001: Carbonate ^{14}C background: does it have multiple personalities? *Radiocarbon 43*, 169–176.

Nishiizumi, K., Imamura, M., Caffee, M. W., Southon, J. R., Finkel, R. C. & McAninch, J. 2007: Absolute calibration of ^{10}Be AMS standards. *Nuclear Instrumental Methods in Physics Research B258*, 403–413.

Niu, L., Lohmann, G., Hinck, S. & Gowan, E. J. 2017: Sensitivity of atmospheric forcing on Northern Hemisphere ice sheets during the last glacial-interglacial cycle using output from PMIP3. *Climate of the Past, Discussion* [preprint], https://doi.org/10.5194/cp-2017-105.

Nye, J. F. 1952: The mechanics of glacier flow. *Journal of Glaciology 2*, 82–93.

Ó Cofaigh, C. & Evans, D. J. A. 2007: Radiocarbon constraints on the age of the maximum advance of the British–Irish Ice Sheet in the Celtic Sea. *Quaternary Science Reviews 26*, 1197–1203.

Ó Cofaigh, C., Telfer, M. W., Bailey, R. M. & Evans, D. J. A. 2012: Late Pleistocene chronostratigraphy and ice sheet limits, southern Ireland. *Quaternary Science Reviews 44*, 160–179.

Ó Cofaigh, C., Weilbach, K., Lloyd, J. M., Benetti, S., Callard, S. L., Purcell, C., Chiverrell, R. C., Dunlop, P., Saher, M., Livingstone, S. J., Van Landeghem, K. J. J., Moreton, S. G., Clark, C. D. & Fabel, D. 2019: Early deglaciation of the British-Irish Ice Sheet on the Atlantic shelf northwest of Ireland driven by glacioisostatic depression and high relative sea level. *Quaternary Science Reviews 208*, 76–96.

Ó Cofaigh, C., Callard, S. L., Roberts, D. H., Chiverrell, R. C., Ballantyne, C. K., Evans, D. J. A., Saher, M., Van Landeghem, K. J. J., Smedley, R., Benetti, S., Burke, M., Clark, C. D., Duller, G. A. T., Fabel, D., Livingstone, S. J., McCarron, S., Medialdea, A., Moreton, S. G. & Sacchetti, F. 2021: Timing and pace of ice-sheet withdrawal across the marine–terrestrial transition west of Ireland during the last glaciation. *Journal of Quaternary Science 36*, 805–832.

Palmer, M., Howard T, Tinker, J., Lowe, J., Bricheno. L., Calvert, D., Edwards, T., Gregory, J., Harris, G., Krijnen, J., Pickering, M., Roberts, C. & Wolf, J. 2018: *UKCP18 Marine Report*. Available at https://www.metoffice.gov.uk/pub/data/weather/uk/ukcp18/science-reports/UKCP18-Marine-report.pdf.

Patton, H., Hubbard, A., Bradwell, T., Glasser, N. F., Hambrey, M. J. & Clark, C. D. 2013a: Rapid marine deglaciation: asynchronous retreat dynamics between the Irish Sea Ice Stream and terrestrial outlet glaciers. *Earth Surface Dynamics 1*, 53–65.

Patton, H., Hubbard, A., Glasser, N. F., Bradwell, T. & Golledge, N. R. 2013b: The last Welsh Ice Cap: part 1–modelling its evolution, sensitivity and associated climate. *Boreas 42*, 471–490.

Patton, H., Hubbard, A., Andreassen, K., Auriac, A., Whitehouse, P. L., Stroeven, A. P., Shackleton, C., Winsborrow, M., Heyman, J. & Hall, A. M. 2017: Deglaciation of the Eurasian ice sheet complex. *Quaternary Science Reviews 169*, 148–172.

Pawley, S. M., Bailey, R. M., Rose, J., Moorlock, B. S. P., Hamblin, R. J. O., Booth, S. J. & Lee, J. R. 2008: Age limits on Middle Pleistocene glacial sediments from OSL dating, north Norfolk, UK. *Quaternary Science Reviews 27*, 1363–1377.

Peacock, J. D. 1971: Marine shell radiocarbon dates and chronology of deglaciation in western Scotland. *Nature Physical Science 230*, 43–45.

Peacock, J. D. 1995: Late Devensian to early Holocene palaeoenvironmental changes in the Viking Bank area, northern North Sea. *Quaternary Science Reviews 14*, 1029–1042.

Peacock, J. D. 2003: Late Devensian marine deposits (Errol Clay Formation) at the Gallowflat Claypit, eastern Scotland: new evidence for the timing of ice recession in the Tay Estuary. *Scottish Journal of Geology 39*, 1–10.

Peacock, J. D. 2008: Late Devensian palaeoenvironmental changes in the sea area adjacent to Islay, SW Scotland: implications for the deglacial history of the Island. *Scottish Journal of Geology 44*, 183–190.

Peacock, J. D. & Browne, M. A. E. 1998: Radiocarbon dates from the Errol Beds (pre-Windermere Interstadial raised marine deposits) in eastern Scotland. *Quaternary Newsletter 86*, 1–7.

Peacock, J. D. & Long, D. 1994: Late Devensian glaciation and deglaciation of Shetland. *Quaternary Newsletter 74*, 16–21.

Peacock, J. D., Austin, W. E. N., Selby, I., Graham, D. K., Harland, R. & Wilkinson, I. P. 1992: Late Devensian and Flandrian palaeoenvironmental changes on the Scottish continental shelf west of the Outer Hebrides. *Journal of Quaternary Science 7*, 145–161.

Pearson, M. P., Pollard, J., Richards, C., Welham, K., Casswell, C., French, C., Schlee, D., Shaw, D., Simmons, E., Stanford, A., Bevins, R. & Ixer, R. 2019: Megalith quarries for Stonehenge's bluestones. *Antiquity 93*, 45–62.

Peck, V. L., Hall, I. R., Zahn, R., Elderfield, H., Grousset, F., Hemming, S. R. & Scourse, J. D. 2006: High resolution evidence for linkages between NW European ice sheet instability and Atlantic meridional overturning circulation. *Earth and Planetary Science Letters 243*, 476–488.

Pelto, M. S. & Warren, C. R. 1991: Relationship between tidewater glacier calving velocity and water depth at the calving front. *Annals of Glaciology 15*, 115–118.

Penck, A. & Bruckner, E. 1909: *Die Alpen im Eiszeitalter, vol. 3*, 1199 pp. Tauchnitz, Leipzig.

Penny, L. F., Coope, G. R. & Catt, J. A. 1969: Age and insect fauna of the Dimlington Silts, East Yorkshire. *Nature 224*, 65–67.

Peters, J. L., Benetti, S., Dunlop, P., Ó Cofaigh, C., Moreton, S. G., Wheeler, A. J. & Clark, C. D. 2016: Sedimentology and chronology of the advance and retreat of the last British-Irish Ice Sheet on the continental shelf west of Ireland. *Quaternary Science Reviews 140*, 101–124.

Phillips, F. M., Bowen, D. Q. & Elmore, D. 1994: Surface exposure dating of glacial features in Great Britain using cosmogenic chlorine-36: preliminary results. *Mineralogical Magazine 58A*, 722–723.

Phillips, W. M., Hall, A. M., Mottram, R., Fifield, L. K. & Sugden, D. E. 2006: Cosmogenic ^{10}Be and ^{26}Al exposure ages of tors and erratics, Cairngorm Mountains, Scotland: timescales for the development of a classic landscape of selective linear glacial erosion. *Geomorphology 73*, 222–245.

Phillips, W. M., Hall, A. M., Ballantyne, C. K., Binnie, S., Kubik, P. W. & Freeman, S. 2008: Extent of the last ice sheet in northern Scotland tested with cosmogenic ^{10}Be exposure ages. *Journal of Quaternary Science 23*, 101–107.

Praeg, D., McCarron, S., Dove, D., Ó Cofaigh, C., Scott, G., Monteys, X., Facchin, L., Romeo, R. & Coxon, P. 2015: Ice sheet extension to the Celtic Sea shelf edge at the Last Glacial Maximum. *Quaternary Science Reviews 111*, 107–112.

Reeh, N. 1982: A plasticity theory approach to the steady-state shape of a three-dimensional ice sheet. *Journal of Glaciology 28*, 431–455.

Reimer, P. J., Bard, E., Bayliss, A., Warren Beck, J., Blackwell, P. G., Ramsey, C. B., Buck, C. E., Cheng, H., Lawrence Edwards, R., Friedrich, M., Grootes, P. M., Guilderson, T. P., Haflidason, H., Hajdas, I., Hatté, C., Heaton, T. J., Hoffmann, D. L., Hogg, A. G., Hughen, K. A., Felix Kaiser, K., Kromer, B., Manning, S. W., Niu, M., Reimer, R. W., Richards, D. A., Marian Scott, E., Southon, J. R., Staff, R. A., Turney, C. S. M. & van der Plicht, J. 2013: IntCal13 and Marine13 radiocarbon age calibration curves 0–50,000 years cal BP. *Radiocarbon 55*, 1869–1887.

Reimer, P. J. and 41 others 2020: The IntCal20 Northern Hemisphere radiocarbon age calibration curve (0–55 cal kBP). *Radiocarbon 62*, 725–757.

Rhodes, E. J. 2011: Optically stimulated luminescence dating of sediments over the past 200,000 years. *Annual Review of Earth and Planetary Sciences 39*, 461–488.

Rhodes, E. J., Bronk Ramsey, C., Outram, Z., Batt, C., Willis, L., Dockrill, S. & Bond, J. 2003: Bayesian methods applied to the interpretation of multiple OSL dates: high precision sediment ages from Old Scatness Broch excavations, Shetland Isles. *Quaternary Science Reviews 22*, 1231–1244.

Robel, A. A. & Tziperman, E. 2016: The role of ice stream dynamics in deglaciation. *Journal of Geophysical Research, Earth Surface 121*, 1540–1554, https://doi.org/10.1002/2016JF003937.

Roberts, D. H., Evans, D. J. A., Callard, S. L., Clark, C. D., Bateman, M. D., Medialdea, A., Dove, D., Cotterill, C. J., Saher, M., Ó Cofaigh, C., Chiverrell, R. C., Moreton, S. G., Fabel, D. & Bradwell, T. 2018: Ice marginal dynamics of the last British-Irish Ice Sheet in the southern North Sea: ice limits, timing and the influence of the Dogger Bank. *Quaternary Science Reviews 198*, 181–207.

Roberts, D. H., Evans, D. J. A., Lodwick, J & Cox, N. J. 2013a: The subglacial and ice-marginal signature of the North Sea Lobe of the British–Irish Ice Sheet during the Last Glacial Maximum at Upgang, North Yorkshire, UK. *Proceedings of the Geologists' Association 124*, 503–519.

Roberts, D. H., Grimoldi, E., Callard, L., Evans, D. J A., Clark, C. D., Stewart, H. A., Dove, D., Saher, M., Ó Cofaigh, C., Chiverrell, R. C., Bateman, M. D., Moreton, S. G., Bradwell, T., Fabel, D. & Medialdea, A. 2019: The mixed-bed glacial landform imprint of the North Sea Lobe in the western North Sea. *Earth Surface Processes and Landforms 44*, 1233–1258.

Roberts, D. H., Ó Cofaigh, C., Ballantyne, C. K., Burke, M., Chiverrell, R. C., Evans, D. J. A., Clark, C. D., Duller, G. A. T., Ely, J., Fabel, D., Small, D., Smedley, R. K. & Callard, S. L. 2020: The deglaciation of the western sector of the Irish Ice Sheet from the inner continental shelf to its terrestrial margin. *Boreas 49*, 438–460.

Roberts, D. H., Rea, B. R., Lane, T. P., Schnabel, C. & Rodés, A. 2013b: New constraints on Greenland ice sheet dynamics during the last glacial cycle: evidence from the Uummannaq ice stream system. *Journal of Geophysical Research, Earth Surface 118*, 519–541.

Robinson, M. & Ballantyne, C. K. 1979: Evidence for a glacial readvance pre-dating the Loch Lomond Advance in Wester Ross. *Scottish Journal of Geology 15*, 271–277.

Rokoengen, K., Løfaldli, M., Rise, L., Løken, T. & Carlsen, R. 1982: Description and dating of a submerged beach in the northern North Sea. *Marine Geology 50*, 21–28.

Rolfe, C. J., Hughes, P. D., Fenton, C. R., Schnabel, C., Xu, S. & Brown, A. G. 2012: Paired 26Al and 10Be exposure ages from Lundy: new evidence for the extent and timing of Devensian glaciation in the southern British Isles. *Quaternary Science Reviews 43*, 61–73.

Rose, J. 2008: The Dimlington Stadial/Dimlington Chronozone: a proposal for naming the main glacial episode of the Late Devensian in Britain. *Boreas 14*, 225–230.

Ross, H. 1997: *The last glaciation of Shetland*. Ph.D. thesis, University of St Andrews, 53 pp.

Rowlands, B. M. 1971: Radiocarbon evidence of the age of an Irish Sea Glaciation in the Vale of Clwyd. *Nature Physical Science 230*, 9–11.

Ruddiman, F. W. & McIntyre, A. 1981: The North Atlantic Ocean during the last deglaciation. *Palaeogeography Palaeoclimatology Palaeoecology 35*, 145–214.

Ryan, J. C., Smith, L. C., van As, D., Cooley, S. W., Cooper, M. G., Pitcher, L. H. & Hubbard, A. 2019: Greenland Ice Sheet surface melt amplified by snowline migration and bare ice exposure. *Science Advances 5*, eaav3738, https://doi.org/10.1126/sciadv.aav3738.

Schoof, C. 2006: Variational methods for glacier flow over plastic till. *Journal of Fluid Mechanics 555*, 299–320.

Schoof, C. 2007: Ice sheet grounding line dynamics: steady states, stability, and hysteresis. *Journal of Geophysical Research: Earth Surface 112*, F3, https://doi.org/10.1029/2006JF000664.

Scourse, J. D. 1997: Transport of the Stonehenge Bluestones: testing the glacial hypothesis. *Proceedings of the British Academy 92*, 271–314.

Scourse, J. D., Chiverrell, R. C., Smedley, R. K., Small, D., Burke, M. J., Saher, M., Van Landeghem, K. J. J., Duller, G. A. T., Ó Cofaigh, C., Bateman, M. D., Benetti, S., Bradley, S., Callard, L., Evans, D. J. A., Fabel, D., Jenkins, G. T. H., McCarron, S., Medialdea, A., Moreton, S., Ou, X., Praeg, D., Roberts, D. H., Roberts, H. M. & Clark, C. D. 2021: Maximum extent and readvance dynamics of the Irish Sea Ice Stream and Irish Sea Glacier since the Last Glacial Maximum. *Journal Quaternary Science 36*, 780–804.

Scourse, J. D., Haapaniemi, A. I., Colmenero-Hidalgo, E., Peck, V. L., Hall, I. R., Austin, W. E. N., Knutz, P. C. & Zahn, R. 2009: Growth, dynamics and deglaciation of the last British-Irish ice sheet: the deep-sea ice-rafted detritis record. *Quaternary Science Reviews 28*, 3066e3084, https://doi.org/10.1016/j.quascirev.2009.08.009.

Scourse, J. D., Ward, S. L., Wainwright, A., Uehara, K. & Bradley, S. 2018: The role of megatides and relative sea level in controlling the deglaciation of the British-Irish and Fennoscandian Ice Sheets. *Journal of Quaternary Science 33*, 139–149.

Scourse, J., Saher, M., Van Landeghem, K. J. J., Lockhart, E., Purcell, C., Callard, L., Roseby, Z., Allinson, B., Pieńkowski, A. J., Ó Cofaigh, C., Praeg, D., Ward, S., Chiverrell, R., Moreton, S., Fabel, D. & Clark, C. D. 2019: Advance and retreat of the marine-terminating Irish Sea Ice Stream into the Celtic Sea during the Last Glacial: timing and maximum extent. *Marine Geology 412*, 53–68.

Seguinot, J., Ivy-Ochs, S., Jouvet, G., Huss, M., Funk, M. & Preusser, F. 2018: Modelling last glacial cycle ice dynamics in the Alps. *The Cryosphere 12*, 3265–3285.

Sejrup, H. P., Clark, C. D. & Hjelstuen, B. O. 2016: Rapid ice sheet retreat triggered by ice stream debuttressing: evidence from the North Sea. *Geology 44*, 355–358.

Sejrup, H. P., Haflidason, H., Aarseth, I., King, E., Forsberg, C. F., Long, D. & Rokoengen, K. 1994: Late Weichselian glaciation history of the northern North Sea. *Boreas 23*, 1–13.

Sejrup, H. P., Haflidason, H., Aarseth, I., King, E., Forsberg, C. F., Long, D. & Rokoengen, K. 2008: Late Weichselian glaciation history of the northern North Sea. *Boreas 23*, 1–13.

Sejrup, H. P., Hjelstuen, B. O., Torbjørn Dahlgren, K. I., Haflidason, H., Kuijpers, A., Nygård, A., Praeg, D., Stoker, M. S. & Vorren, T. O. 2005: Pleistocene glacial history of the NW European continental margin. *Marine and Petroleum Geology 22*, 1111–1119.

Singarayer, J. S., Richards, D. A., Ridgwell, A., Valdes, P. J., Austin, W. E. N. & Beck, J. W. 2008: An oceanic origin for the increase of atmospheric radiocarbon during the Younger Dryas. *Geophysical Research Letters 35*, L14707, https://doi.org/10.1029/2008GL034074.

Sissons, J. B. & Walker, M. J. C. 1974: Late glacial site in the central Grampian Highlands. *Nature 249*, 822–824.

Small, D., Benetti, S., Dove, D., Ballantyne, C. K., Fabel, D., Clark, C. D., Gheorghiu, D. M., Newall, J. & Xu, S. 2017a: Cosmogenic exposure age constraints on deglaciation and flow behaviour of a marine-based ice stream in western Scotland, 21–16 ka. *Quaternary Science Reviews 167*, 30–46.

Small, D., Clark, C. D., Chiverrell, R. C., Smedley, R. K., Bateman, M. D., Duller, G. A. T., Ely, J. C., Fabel, D., Medialdea, A. & Moreton, S. G. 2017b: Devising quality assurance procedures for assessment of legacy geochronological data relating to deglaciation of the last British-Irish Ice Sheet. *Earth-Science Reviews 164*, 232–250.

Small, D., Rinterknecht, V. & Austin, W. 2012: In situ cosmogenic exposure ages from the Isle of Skye, northwest Scotland: implications for the timing of deglaciation and readvance from 15 to 11 ka. *Journal of Quaternary Science 27*, 150–158.

Small, D., Smedley, R. K., Chiverrell, R. C., Scourse, J. D., Ó Cofaigh, C., Duller, G. A. T., McCarron, S., Burke, M. J., Evans, D. J. A., Fabel, D., Gheorghiu, D. M., Thomas, G. S. P., Xu, S. & Clark, C. D. 2018: Trough geometry was a greater influence than climate-ocean forcing in regulating retreat of the marine-based Irish-Sea Ice Stream. *Geological Society of America Bulletin 130*, 1981–1999.

Smedley, R. K., Buylaert, J. P. & Ujvari, G. 2019: Comparing the accuracy and precision of luminescence ages for partially-bleached sediments using single grains of K-feldspar and quartz. *Quaternary Geochronology 53*, p101007, https://doi.org/10.1016/j.quageo.2019.101007.

Smedley, R. K., Chiverrell, R. C., Ballantyne, C. K., Burke, M. J., Clark, C. D., Duller, G. A. T., Fabel, D., McCarroll, D., Scourse, J. D., Small, D. & Thomas, G. S. P. 2017a: Internal dynamics condition centennial-scale oscillations in smarine-based ice-stream retreat. *Geology 45*, 787–790.

Smedley, R. K., Scourse, J. D., Small, D., Hiemstra, J. F., Duller, G. A. T., Bateman, M. D., Burke, M. J., Chiverrell, R. C., Clark, C. D., Davies, S. M., Fabel, D., Gheorghiu, D. M., McCarroll, D., Medialdea, A. & Xu, S. 2017b: New age constraints for the limit of the British–Irish Ice Sheet on the Isles of Scilly. *Journal of Quaternary Science 32*, 48–62.

Stokes, C. R., Margold, M., Clark, C. D. & Tarasov, L. 2016: Ice stream activity scaled to ice sheet volume during Laurentide Ice Sheet deglaciation. *Nature 530*, 322–326.

Stokes, C. R., Tarasov, L., Blomdin, R., Cronin, T. M., Fisher, T. G., Gyllencreutz, R., Hättestrand, C., Heyman, J., Hindmarsh, R. C. A., Hughes, A. L. C., Jakobsson, M., Kirchner, N., Livingstone, S. J., Margold, M., Murton, J. B., Noormets, R., Peltier, W. R., Peteet, D. M., Piper, D. J. W., Preusser, F., Renssen, H., Roberts, D. H., Roche, D. M., Saint-Ange, F., Stroeven, A. P. & Teller, J. T. 2015: On the reconstruction of palaeo-ice sheets: recent advances and future challenges. *Quaternary Science Reviews 125*, 15–49.

Stone, J. O. 2000: Air pressure and cosmogenic isotope production. *Journal of Geophysical Research 105*, 23753–23759.

Stone, J. O., Ballantyne, C. K. & Keith Fifield, L. 1998: Exposure dating and validation of periglacial weathering limits, northwest Scotland. *Geology 26*, 587–590.

Strandberg, G., Brandefelt, J., Kjellström, E. & Smith, B. 2011: High-resolution regional simulation of last glacial maximum climate in Europe. *Tellus A 63*, 107–125.

Straw, A. 1979: The Devensian glaciation. *In* Straw, A. & Clayton, K. M. (eds.): *The Geomorphology of the British Isles: Eastern and Central England*, 21–45. Methuen, London.

Stroeven, A. P., Hättestrand, C., Kleman, J., Fabel, D., Fredin, O., Bradley, W. G., Harbor, J. M., Jansen, J. D., Olsen, L., Caffee, M. W., Fink, D., Lundqvist, J., Rosqvist, G. C., Strömberg, B. & Jansson, K. N. 2016: Deglaciation of Fennoscandia. *Quaternary Science Reviews 147*, 91–121.

Sutherland, D. G. & Walker, M. J. C. 1984: A late Devensian ice-free area and possible interglacial site on the Isle of Lewis, Scotland. *Nature 309*, 701–703.

Synge, F. M. 1952: Retreat stages of the last ice sheet in the British Isles. *Bulletin of the Geographical Society of Ireland 2*, 168–171.

Tarasov, L., Dyke, A. S., Neal, R. M. & Peltier, W. R. 2012: A data-calibrated distribution of deglacial chronologies for the North American ice complex from glaciological modeling. *Earth and Planetary Science Letters 315-316*, 30–40.

Tarlati, S., Benetti, S., Callard, S. L., Ó Cofaigh, C., Dunlop, P., Georgiopoulou, A., Edwards, R., Van Landeghem, K., Saher, M., Chiverrell, R., Fabel, D., Moreton, S., Morgan, S. & Clark, C. D. 2020: Final deglaciation of the Malin Sea through meltwater release and calving events. *Scottish Journal of Geology 56*, 117–130.

Telfer, M. W., Wilson, P., Lord, T. C. & Vincent, P. J. 2009: New constraints on the age of the last ice sheet glaciation in NW England using optically stimulated luminescence dating. *Journal of Quaternary Science 24*, 906–915.

Thomas, G. S. P., Chiverrell, R. C. & Huddart, D. 2004: Ice-marginal depositional responses to readvance episodes in the Late Devensian deglaciation of the Isle of Man. *Quaternary Science Reviews 23*, 85–106.

Thrasher, I. M., Mauz, B., Chiverrell, R. C., Lang, A. & Thomas, G. S. P. 2009: Testing an approach to OSL dating of Late Devensian glaciofluvial sediments of the British Isles. *Journal of Quaternary Science 24*, 785–801.

Van de Berg, W. J., van den Broeke, M., Ettema, J., van Meijgaard, E. & Kaspar, F. 2011: Significant contribution of insolation to Eemian melting of the Greenland ice sheet. *Nature Geoscience 4*, 679–683.

Van Landeghem, K. J. J. & Chiverrell, R. C. C. 2020: Bed erosion during fast ice streaming regulated the retreat dynamics of the Irish Sea Ice Stream. *Quaternary Science Reviews 245*, 106526, https://doi.org/10.1016/j.quascirev.2020.106526.

Van Landeghem, K. J. J., Wheeler, A. J. & Mitchell, N. C. 2009: Seafloor evidence for palaeo-ice streaming and calving of the grounded Irish Sea Ice Stream: implications for the interpretation of its final deglaciation phase. *Boreas 38*, 119–131.

Vincent, P. J., Wilson, P., Lord, T. C., Schnabel, C. & Wilcken, K. M. 2010: Cosmogenic isotope (^{36}Cl) surface exposure dating of the Norber erratics, Yorkshire Dales: further constraints on the timing of the LGM deglaciation in Britain. *Proceedings of the Geologists' Association 121*, 24–31.

Voelker, A., Grootes, P. M., Nadeau, M. J. & Sarnthein, M. 2000: Radiocarbon levels in the Iceland Sea from 25–53 kyr and their link to the earth's magnetic field intensity. *Radiocarbon 42*, 437–452.

Von Weymarn, J. & Edwards, K. J. 1973: Interstadial site on the Island of Lewis, Scotland. *Nature 246*, 473–474.

Waelbroeck, C., Duplessy, J. C., Michel, E., Labeyrie, L., Paillard, D. & Duprat, J. 2001: The timing of the last deglaciation in the North Atlantic climate records. *Nature 412*, 724–727.

Wanamaker, A. D., Jr., Butler, P. G., Scourse, J. D., Heinemeier, J., Eiríksson, J., Knudsen, K. L. & Richardson, C. A. 2012: Surface changes in the North Atlantic meridional overturning circulation during the last millennium. *Nature Communications 3*, 899, https://doi.org/10.1038/ncomms1901.

Watson, J. E., Brooks, S. J., Whitehouse, N. J., Reimer, P. J., Birks, H. J. B. & Turney, C. 2010: Chironomid-inferred late-glacial summer air temperatures from Lough Nadourcan, Co. Donegal, Ireland. *Journal of Quaternary Science 25*, 1200–1210.

Whitehouse, P. L., Gomez, N., King, M. A. & Wiens, D. A. 2019: Solid Earth change and the evolution of the Antarctic Ice Sheet. *Nature Communications 10*, 503, https://doi.org/10.1038/s41467-018-08068-y.

Whittington, G. & Hall, A. M. 2002: The Tolsta Interstadial, Scotland: correlation with D–O cycles GI-8 to GI-5? *Quaternary Science Reviews 21*, 901–915.

Wilson, P., Rodes, A. & Smith, A. 2018: Valley glaciers persisted in the Lake District, north-west England, until 16-15 ka as revealed by terrestrial cosmogenic nuclide (^{10}Be) dating: a response to Heinrich event 1? *Journal of Quaternary Science 33*, 518–526.

Wilson, P., Ballantyne, C. K., Benetti, S., Small, D., Fabel, D. & Clark, C. D. 2019: Deglaciation chronology of the Donegal Ice Centre, north-west Ireland. *Journal of Quaternary Science 34*, 16–28.

Wilton, D. J., Bigg, G. R., Scourse, J. D., Ely, J. C. & Clark, C. D. 2021: Exploring the extent to which fluctuations in ice-rafted debris reflect mass changes in the source ice sheet: a model–observation comparison using the last British–Irish Ice Sheet. *Journal of Quaternary Science 36*, 934–945.

Winkelmann, R., Martin, M. A., Haseloff, M., Albrecht, T., Bueler, E., Khroulev, C. & Levermann, A. 2011: The Potsdam parallel ice sheet model (PISM-PIK)-part 1: model description. *The Cryosphere 5*, 715–726.

Woodman, P., McCarthy, M. & Monaghan, N. 1997: The Irish Quaternary fauna project. *Quaternary Science Reviews 16*, 129–159.

Xu, S., Dougans, A. B., Freeman, S. & Schnabel, C. 2010: Improved ^{10}Be and ^{26}Al-AMS with a 5 MV spectrometer. *Nuclear Instruments and Methods in Physics Research Section B: Beam Interactions with Materials and Atoms 268*, 736–738.

Zwally, H., Abdalati, W., Herring, T., Larson, K., Saba, J. & Steffen, K. 2002: Surface melt-induced acceleration of Greenland ice sheet flow. *Science 297*, 218–222.

Supporting Information

Additional Supporting Information to this article is available at http://www.boreas.dk.

Data S1. Luminescence dating laboratory inter-comparison results.

Data S2. BRITICE-CHRONO master spreadsheet of chronology v2.1.

Data S3. BRITICE-CHRONO empirical reconstruction (poster and slideshow).

Data S4. BRITICE-CHRONO model reconstruction (poster, slideshow, and movie).

Data S5. Palaeotopographies and sea level 14–6 ka slideshow.